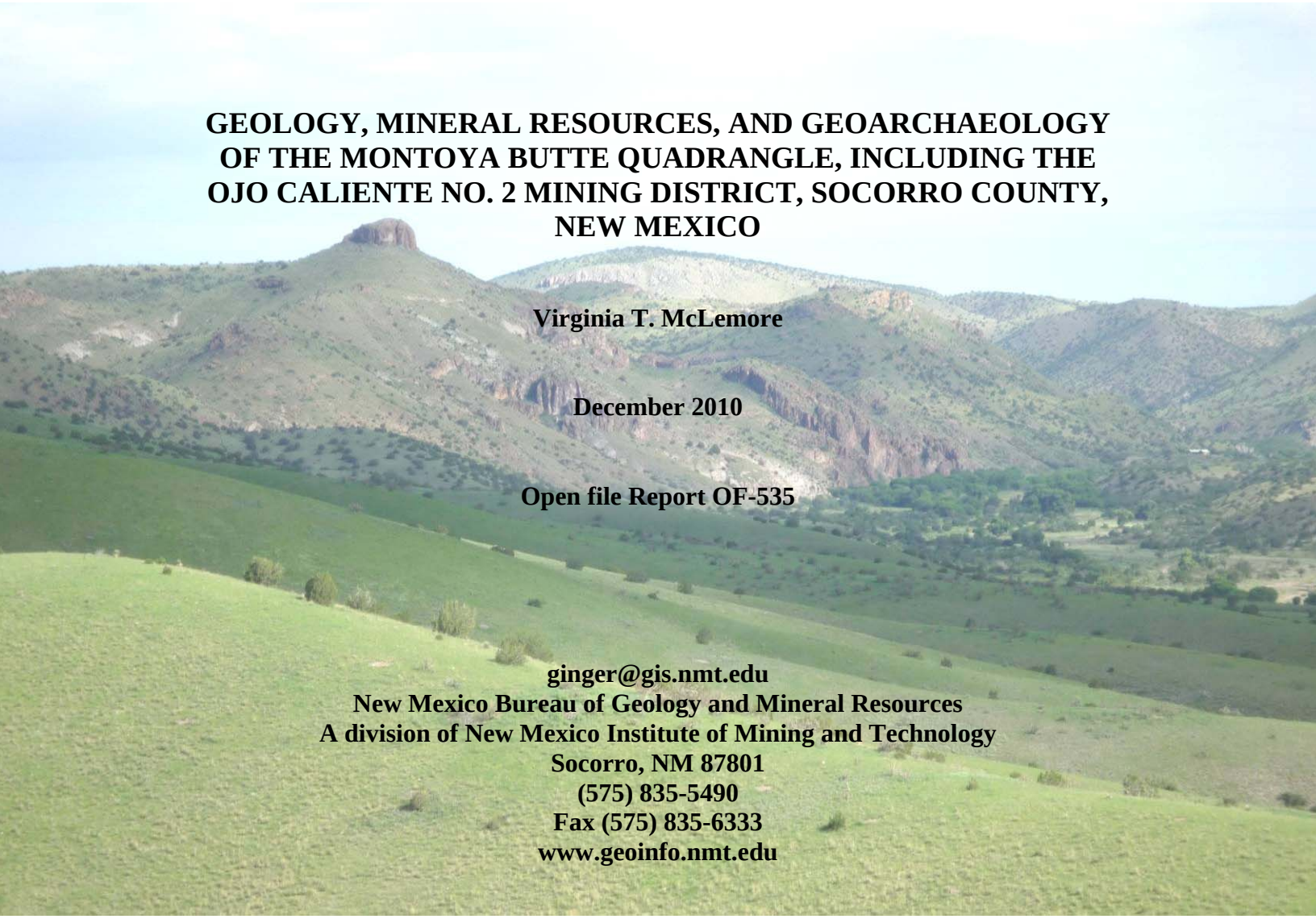

GEOLOGY, MINERAL RESOURCES, AND GEOARCHAEOLOGY OF THE MONTOYA BUTTE QUADRANGLE, INCLUDING THE OJO CALIENTE NO. 2 MINING DISTRICT, SOCORRO COUNTY, NEW MEXICO

Virginia T. McLemore

December 2010

Open file Report OF-535

ginger@gis.nmt.edu
New Mexico Bureau of Geology and Mineral Resources
A division of New Mexico Institute of Mining and Technology
Socorro, NM 87801
(575) 835-5490
Fax (575) 835-6333
www.geoinfo.nmt.edu

Montoya Butte looking north. Black Mountain is on the skyline.

This report is preliminary and could undergo revision. It is being distributed in this draft form to make the information available as quickly as possible, with the understanding that this work has not necessarily met the stringent peer review and editorial standards of more formal publications. The views and conclusions are those of the author, and should not be interpreted as necessarily representing the official policies, either expressed or implied, of the State of New Mexico. Any resource or reserve data presented here are historical data and are provided for information purposes only and do not conform to Canadian National Instrument NI 43-101 requirements.

ABSTRACT

The Montoya Butte quadrangle lies in the northeastern part of the Mogollon-Datil volcanic field in the northern Sierra Cuchillo range and western San Mateo Mountains in Socorro County, central New Mexico. Cañada Alamosa (also known as Alamosa Creek, Alamosa River, and Rio Alamosa) is the main drainage through the quadrangle. Monticello Box is a prominent rock-walled canyon along Cañada Alamosa in the northern portion of the quadrangle. Permian sedimentary rocks are exposed in the southwestern portion of the quadrangle and likely underlie much of the area at depth. Volcanic rocks include an older sequence of andesite, lahar, and latite (around >38-36 Ma) followed by a younger sequence of ash flow tuffs and rhyolite lavas (around 22-29 Ma) associated with the formation of the Nogal Canyon (28.4 Ma) and Bear Trap Canyon (24.4 Ma) calderas in the San Mateo Mountains. Local alkaline basalt flows overlie or are interbedded with the older Quaternary-Tertiary sedimentary rocks and are similar in composition to basalt flows in central New Mexico that are 2-6 Ma. Local and regional faulting formed the Monticello graben where Alamosa Creek flows, between the San Mateo Mountains and Sierra Cuchillo. Quaternary sedimentary rocks eroded from the San Mateo Mountains and Sierra Cuchillo filled the Monticello graben and formed a series of alluvial fans, pediments and younger stream terraces. Alamosa Creek has cut through the Quaternary sedimentary rocks and the 2-6 Ma basalt flows.

Since the volcanic flows and rhyolite domes in the Sierra Cuchillo and San Mateo Mountains are grossly similar, but erupted over a long period of time (i.e., 22 to >38 Ma), they likely represent a series of small, but discrete magma pulses: 1) pre-caldera volcanic rocks around >38-36 Ma (possibly related in part to the eruption of the Emery caldera at 34.9 Ma), 2) Nogal Canyon caldera-related rhyolites at 27-29 Ma, 3) rocks related to the Bear Trap caldera (24 Ma), 4) post-caldera rhyolites and andesites (20-24 Ma), and 5) alkali basalts (around 2-6 Ma?). The 27-29 Ma rhyolites in the Sierra Cuchillo and San Mateo Mountains are similar in geochemistry to topaz-bearing rhyolites and appear to be evolved from partial melts of Proterozoic lower crust in an extensional tectonic setting. In contrast, the older Reilly Peak rhyolite, Sierra Cuchillo laccolith, and monzonite plugs in the Montoya Butte quadrangle are more similar to typical calc-alkaline rhyolites, not topaz rhyolites, and could represent a transition between older arc-related Laramide volcanism and younger extensional Rio Grande volcanism. The formation of the rhyolites can be explained by fractional crystallization. Differences in incompatible trace elements, including beryllium, between various bodies of granite and rhyolite are likely related to either difference in the crustal rocks that were assimilated during magmatic differentiation or by minor potential contamination from crustal sources and/or magma mixing.

At least three separate geothermal systems were/are present in the Ojo Caliente No. 2 (or Taylor) mining district in the Montoya Butte quadrangle: 1) the oldest system forming the volcanic-epithermal veins (~28-36 Ma), 2) the system forming the Apache Warm Springs beryllium deposit and associated alteration (~24.4-28 Ma), and 3) the current, modern system related to Ojo Caliente, Willow Springs, and other warm springs feeding Cañada Alamosa. Copper-silver production has been insignificant from the volcanic-epithermal veins and a small quantity of uranium ore reportedly was produced from the beryllium deposit. The resource potential of the volcanic-epithermal veins is low with a moderate to high degree of certainty because the vein deposits exposed at the

surface are low grade and too small for economic development in the current market. The resource potential of the Apache Warm Springs beryllium deposit is low to moderate with a moderate to high degree of certainty, because the known extent of the beryllium deposit at the surface and in the subsurface where drilled is low grade and too small for economic development in the current market. But, additional exploration drilling could locate additional beryllium at depth. Any potential exploration or subsequent mining would have to plan for environmental issues, especially the affects of mining on the Ojo Caliente and adjacent warm and cold springs (including Alum Spring) feeding the Cañada Alamosa. The mineral-resource potential for geothermal resources, clay, fluorite, and uranium is low with a high degree of certainty. The mineral-resource potential for aggregate for local use is high in the active alluvial and floodplain deposits, but testing would have to be completed to determine the quality of the aggregate resources. There is no resource potential for any other commodities in the quadrangle.

Four major Pueblo sites are found in the Montoya Butte area, which are currently under study: Montoya site (Mimbres phase, A.D. 1000-1130, and Socorro phase, A.D. 1100-1200), Victorio site (Tularosa phase, A.D. 1175-1275, with earlier Pueblo components), Pinnacle ruin (Magdalena Phase, A.D. 1250-1400+), and Kelly Canyon site (Socorro Phase, A.D. 1100-1200). Most Pueblo sites are found along the Montoya (Qtm) and Victorio (Qtv) terraces, downstream of the intersection of Kelly Canyon with Cañada Alamosa. Several pit houses are found on the Montoya terraces. The majority of the lithic artifacts (including stone tools, hammer stones, and projectile points) found at the Pueblo sites are made from local rhyolite and tuff (Vicks Peak Tuff, rhyolite of Alamosa Canyon, and rhyolite dikes), andesite, basalt, and siltstone (latite of Montoya Butte). Some of the lithic artifacts, including obsidian, chert, quartzite, and silicified wood, are not found in the immediate area and were imported into the canyon. Local clays were likely used in the production of common pottery, but some of the glazed pottery was made elsewhere and imported into the canyon. The Pueblo people utilized local boulders for construction of walls. At the Pinnacle ruin, the latite of Montoya Butte was used. At the other sites, predominantly rhyolite boulders (Vicks Peak tuff, rhyolite of Alamosa Canyon, rhyolite dikes, latite of Montoya Butte), andesite and rare alkali basalt found in the terrace and alluvial deposits were used. Adobe walls made from the local soil were locally utilized as well.

TABLE OF CONTENTS

FIGURES

TABLES

APPENDICES

INTRODUCTION

Location and scope

The Montoya Butte quadrangle is located in the northern Sierra Cuchillo Range and western San Mateo Mountains in southwestern Socorro County, central New Mexico (Fig. 1, 2, 3). This area lies in the northeastern Mogollon-Datil volcanic field. The area is accessed by gravel roads, including State Highway 52 from the west and a county road through Cañada Alamosa. Cañada Alamosa, translated as *Canyon of the Cottonwoods*, is the main drainage through the quadrangle and also is known as Alamosa Creek, Alamosa River, and Rio Alamosa. Monticello Box is a prominent rock-walled canyon along Cañada Alamosa in the northern portion of the quadrangle (Fig. 4). The Ojo Caliente No. 2 (or Taylor) mining district is in the northern Sierra Cuchillo, south of Monticello Box (Fig. 5). The Ojo Caliente No. 2 mining district consists of volcanic-epithermal vein deposits (Taylor mine) and the Apache Warm Springs beryllium deposit (also known as the Sullivan Ranch site; Griffitts and Alminas, 1968; Hillard, 1967, 1969; Meeves, 1966). The purposes of this report are to

- Map and describe the structures controlling the mineral resources in the area
- Describe geologic processes that formed the landscape and the rocks in the upper Cañada Alamosa
- Determine the resource potential for mineral deposits in the area
- Describe the geoarchaeology of the area, i.e., how the geology relates to the mineral resources and archaeological features in Cañada Alamosa
- Provide regional correlations of the rocks in the San Mateo Mountains and Sierra Cuchillo based upon mapping, stratigraphic sections, regional field reconnaissance, and previous studies
- Provide the geologic data required for subsequent studies of the surface and ground water in the Cañada Alamosa area.

The quadrangle geologic map is a separate open-file geologic map (McLemore, 2011). The hydrology of Alamosa Creek basin will be described in future aquifer mapping studies by the New Mexico Bureau of Geology and Mineral Resources (NMBGMR). Detailed mapping of the Quaternary geology is underway and also will be in a future report.

Comments to Map Users

A geologic map displays information on the distribution, nature, orientation, and age relationships of rock and mineral deposits and the occurrence of structural features. Geologic and fault contacts are irregular surfaces that form boundaries between different types or ages of bedrock or sedimentary units. Data depicted on this geologic quadrangle are based on field geologic mapping, compilation of published and unpublished work, and photogeologic interpretation. Locations of contacts are not surveyed, but are plotted by interpretation of the position of a given contact onto a topographic base map; therefore, the accuracy of contact locations depends on the scale of mapping and the interpretation of the geologist. Site-specific conditions should be verified by detailed surface mapping or subsurface exploration. Topographic and cultural changes associated with recent development are not always shown on the map.

This report and accompanying map have not been reviewed according to NMBGMR publication standards, but has been informally reviewed by several geologists

with different background specialties (see Acknowledgements below). The contents of the report and map should not be considered final and complete until reviewed and published by the NMBGMR. The views and conclusions contained in this document are those of the author and should not be interpreted as necessarily representing the official policies, either expressed or implied, of the State of New Mexico.

Any resource or reserve data presented here are historical data and are provided for information purposes only and do not conform to Canadian National Instrument NI 43-101 requirements.

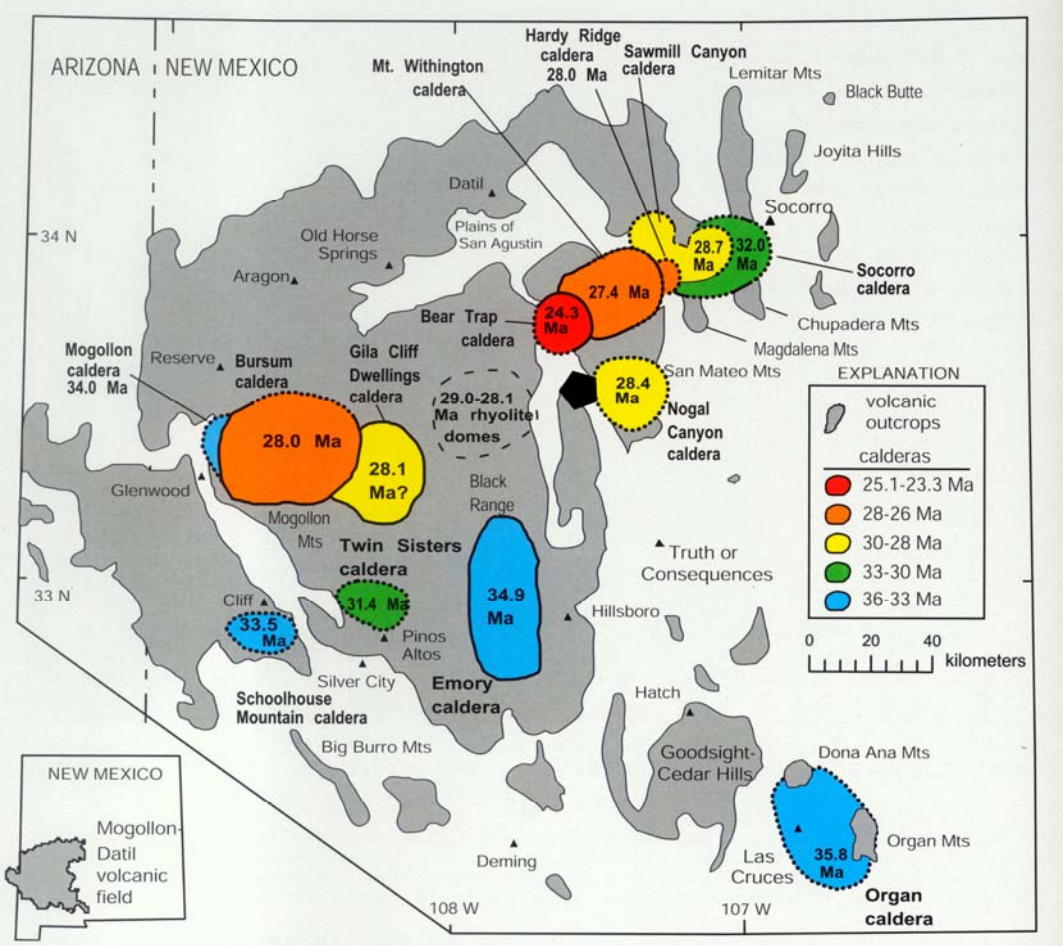

FIGURE 3. Map of the Mogollon-Datil volcanic field showing known calderas color coded by age as in Figure 1. Outcrop area of Taylor Creek Rhyolite shown by dashed line.

FIGURE 1. Map of the Mogollon-Datil volcanic field showing known calderas color coded by age (from Chapin et al., 2004). The Taylor Creek Rhyolite is shown by dashed line. Ages are in millions of years. The black hexagon is the approximate location of the Montoya Butte quadrangle, including the Ojo Caliente No. 2 mining district.

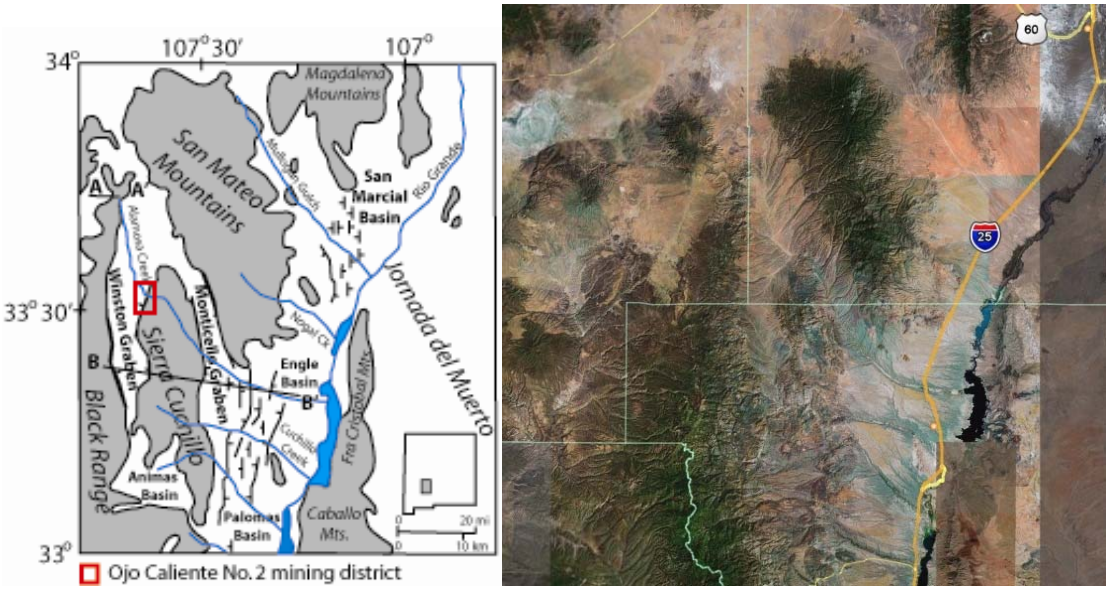

FIGURE 2. Location of the Ojo Caliente No. 2 mining district and geographic features in central New Mexico. Line B-B' is the location of a generalized cross section in Figure 3.

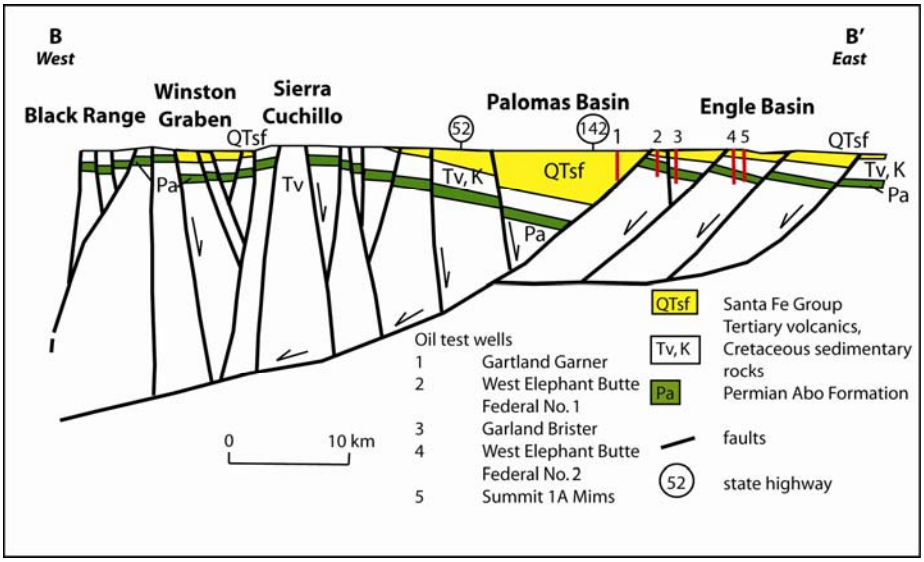

FIGURE 3. Schematic cross section across the Black Range to the Engle Basin. B-B' is slightly modified from Harrison (1992, 1994) and Lozinsky (1987). Detailed information on the oil test wells (1-5) are in Lozinsky (1987). See Figure 2 for approximate location of cross section B-B'. 52 and 142 indicate the locations of State Highways 52 and 142.

FIGURE 4. Monticello Box, looking east, where the spring-fed water flows into the box canyon. Cliffs are formed by andesite of Monticello Box.

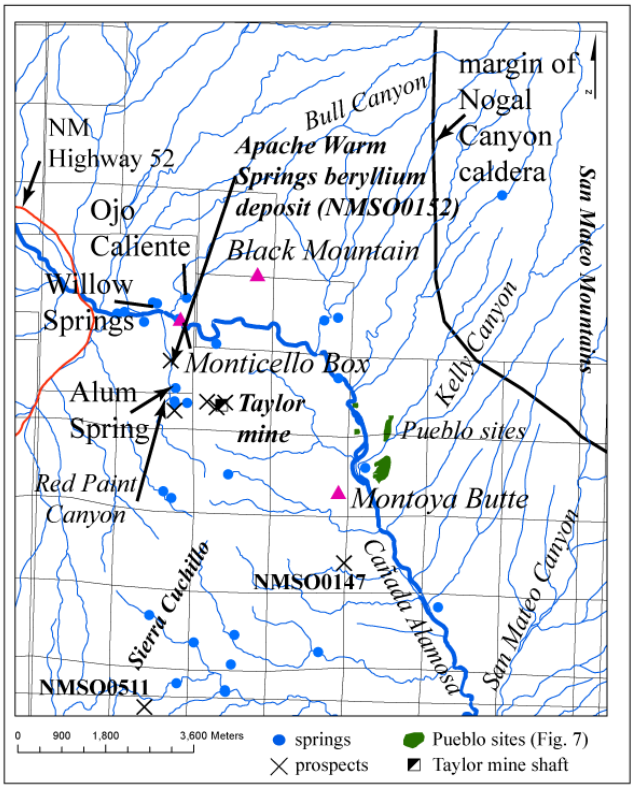

FIGURE 5. Features within the Montoya Butte quadrangle. Red triangles are topographic features and blue-green shading indicates areas with Pueblo sites.

Acknowledgements

This work is part of ongoing research of the economic geology of mineral resources in New Mexico at NMBGMR, Peter Scholle, Director and State Geologist. I appreciate the help and hospitality of the many ranchers who allowed access to their land for mapping, and for those who provided information on their water wells and roads, and their help and hospitality are appreciated. The Monticello Community Ditch Association allowed access to their land for mapping. BE Resources, Inc. (BER) and Kenneth (Tay) Sullivan allowed access to the Apache Warm Springs beryllium deposit, which is on private property. Lewis Gillard, Mark Mansell, Mike Timmons, and Glen Jones provided technical assistance and Kelly Donahue examined and identified clay minerals from soils and altered rocks in the area; their help is greatly appreciated. I also would like to thank Scott Lynch, Pat Hillard, Robert Meyers, Dave Love, Karl Laumbach, Chris Monger, Charles Ferguson, John Hawley, Dennis O'Toole, Ariel Dickinson, Shari Kelly, and Bill McIntosh for the numerous discussions on the geology, history, and archaeology of the area. Portions of this report were reviewed by Daniel Koning, Miles Silberman, Dave Love, Marshall Reiter, Peggy Johnson, John Clema, Shari Kelly, Karl Laumbach, and Dennis O'Toole. This project was funded by the NMBGMR. Chemical analyses were by Diane Johnson, manager of the Washington State University laboratory, and Bonnie Frey, manager of the NMBGMR Chemical Laboratory. $^{40}Ar/^{39}Ar$ ages of three rock samples from the Montoya Butte quadrangle were determined by Lisa Peters and Matt Heizler of the New Mexico Geochronology Research Laboratory. Sample preparation was by Kelly Donahue, Ariel Dickinson, Sam Nunoo, Kwaku Boakye, and Kojo Anim. Thanks to James McLemore, Randy Furr, and Dennis O'Toole for their periodic assistance in the field. Finally, thanks to Donna Furr and Trudi O'Toole for the numerous excellent dinners!

METHODS OF STUDY

The first stage in any geologic investigation is compilation and interpretation of all available published and unpublished geological, geochemical, hydrological, geophysical, and mineral production data. Mineral databases were examined, including the Mineral Resource Data System (MRDS) of the U.S. Geological Survey (USGS; Mason and Arndt, 1996), the Minerals Industry Location System (MILS) of the U.S. Bureau of Mines (U.S. Bureau of Mines, 1995), U.S. Forest Service Abandoned and Inactive Mines database, AMLIS (U.S. Bureau of Land Management), and unpublished files at the NMBGMR. Mineral occurrences, deposits, mines, prospects, and mills were identified using these databases and plotted on base maps, and compiled in a new database (Appendix 1). Locations and other information from water wells and springs were compiled from the literature, New Mexico State Engineers WATERS database, field mapping, and topographic maps (Appendix 2). Ranchers and farmers of the Cañada Alamosa drainage area also were interviewed. Geophysical data (regional magnetic and gravity maps), aerial photographs, and Landsat satellite imagery of the project area were examined.

Using these data, areas of anomalous structural complexity, hydrothermal alteration, mineralization, and anomalous coloration were delineated, examined, mapped and sampled. Field mapping of Montoya Butte quadrangle began in June 2005 and this

report was completed for review in April 2010. The separate quadrangle 1:12,000 scale geologic map will be released in 2011 (McLemore, 2011). Aerial photographs were utilized to aid in geologic mapping. Many of the mines, prospects, and mineral deposits were examined as part of a regional study of mineral resources in Sierra County in 1998-2005 and additional examination of mines, prospects, mineral deposits, springs, wells, and drainages, was conducted in 2005-2009. Geologic mapping of the Montoya Butte quadrangle was at a scale of approximately 1:12,000, using the USGS topographic map as a base by the author as part of the NMBGMR state geologic map and mineral resources programs (McLemore, 2011). Outcrop mapping techniques were employed in mapping where the approximate extent of the actual outcrop of the lithology was mapped in a darker color; the lighter color was used to identify areas of the same lithology that were covered and inferred to be present. Cross sections were constructed (McLemore, 2011). Selected sites were photographed by the author.

Samples were collected and analyzed by a variety of methods. Igneous rock lithologies were identified on the basis of mineralogy and chemistry as defined by LeMaitre (1989). Polished thin sections of samples were examined using standard petrographic techniques and included examination of the texture, mineralogy, and modal analysis. Selected samples collected for this project were analyzed for major and trace elements by X-ray fluorescence (XRF) at the Washington State University; selected samples were analyzed for Be, Li, and U by induced coupled plasma spectroscopy (ICP) at the NMBGMR chemistry laboratory (Appendices 3, 8). Laboratory methods and analytical precision are described in McLemore and Frey (2009) and Johnson et al. (1999).

Structural analysis of geologic data is important to determine the orientation of applied stress fields during deformation of the country rocks and to evaluate the possible relationship between structural style and timing of mineralization. Orientations of faults and foliation and bedding planes of various lithologic units were measured during the course of the field work (Appendix 4). Locally, orientations of fault slickenslides, joints, and fractures also were measured. Stereonet plots were constructed using the computer program RockWorks$^{@}$.

Samples of clay materials also were analyzed by instrumental neutron activation analysis (INNA). Clay mineralogy was determined by X-ray Diffraction methods (XRD) using the procedure by Hall (2004; McLemore and Frey, 2009; Appendix 5). Age determinations of three rock samples from the Montoya Butte quadrangle were determined by $^{40}Ar/^{39}Ar$ (Appendix 6); laboratory methods are described by McLemore et al. (1995) and http://geoinfo.nmt.edu/labs/argon/home.html. Information on exploratory drilling of the Apache Warm Springs beryllium deposit is in Appendix 7 and beryllium analyses are in Appendix 8. The NURE (National Uranium Resource Evaluation) data were obtained from the USGS and examined for the Alamosa Creek drainage basin; methodology and results are described in Appendix 9. Stratigraphic sections are summarized in Appendix 10.

This report assesses the potential of mineral and energy resources (excluding petroleum resources) on the surface and within the subsurface in the Montoya Butte quadrangle. Mineral-resource potential is the likelihood for the occurrence of undiscovered concentrations of metals, nonmetals, industrial materials, and energy resources. The evaluation of mineral-resource potential involves a complex process based

on obtaining geologic data of the study area comparing these to favorable geologic settings that contain known economic deposits (geologic models; Cox and Singer, 1986). Such subjective assessments or judgments depend upon available information concerning the area as well as current knowledge and understanding of known deposits. This assessment will provide land managers with appropriate data to make land-use decisions and to mining companies looking for prospective mineral deposits. This project conforms to mineral assessment guidelines and procedures required by the U.S. Bureau of Land Management (Goudarzi, 1984). More detailed information on assessing the mineral-resource potential is in Appendix 11 and described by McLemore (1985), Bartsch-Winkler and Donatich (1995), McLemore et al. (2001), and others. McLemore (2010b, c) includes a summary of the economics of beryllium.

PREVIOUS INVESTIGATIONS

The Montoya Butte quadrangle is an important area for understanding the geology, mineral resources, and tectonics of south-central New Mexico, because it includes portions of both the San Mateo Mountains and Sierra Cuchillo range and the intervening Monticello graben (Fig. 5). This study is a continuation of numerous previous studies (Fig. 6). Willard (1957) first mapped the region. Previous geologic mapping of the western Montoya Butte quadrangle, including the Ojo Caliente No. 2 mining district, was by Hillard (1967, 1969) and Maldonado (1974, 1980). Lynch (2003) mapped the northeastern portion of the quadrangle. The southern San Mateo Mountains, east of the study area, was mapped by Farkas (1969), Cox (1985), Hermann (1986), and Smith (1992). The Sierra Cuchillo range was mapped by Jahns (1943, 1944a, b, 1955), Jahns et al. (1978, 2006), Davis (1986a, b), and Robertson (1986). Osburn (1984) compiled a geologic map of Socorro County, which included the Montoya Butte quadrangle. McGraw (2003a) mapped the Quaternary geology of Montoya Butte quadrangle. Ferguson et al. (2007) mapped the Welty Hill quadrangle north of the Montoya Butte quadrangle. Jahns et al. (2006) mapped the Chise quadrangle. Heyl et al. (1983) mapped the Priest Tank quadrangle. Maxwell and Oakman (1990) mapped the Cuchillo quadrangle. Harrison (1989, 1992) mapped the Winston quadrangle and Harrison (1992) mapped the Iron Mountain quadrangle. All of these quadrangles, except for Welty Hill, are south of Montoya Butte quadrangle (Fig. 6). Blodgett (1973), Blodgett and Titus (1973), Roybal (1991), Myers et al. (1994), and Basabilvazo (1996) described the water resources of San Augstin and Alamosa Creek basins, northwest (upstream) of Monticello Box. P and E Mining Consultants, Inc. (2009) summarized the minerals resources of the Apache Warm Springs deposit and included results of past drilling (Appendix 7). McLemore (2010b, c) summarized the beryllium resources in New Mexico, Utah, Texas, and Mexico, including the Apache Warm Springs deposit in the Ojo Caliente No. 2 mining district.

An earlier unpublished preliminary progress report by McLemore (2008) described the beryllium resources and preliminary geologic mapping of the Ojo Caliente No. 2 mining district. This open-file report is an update of the earlier report by McLemore (2008) and replaces that report.

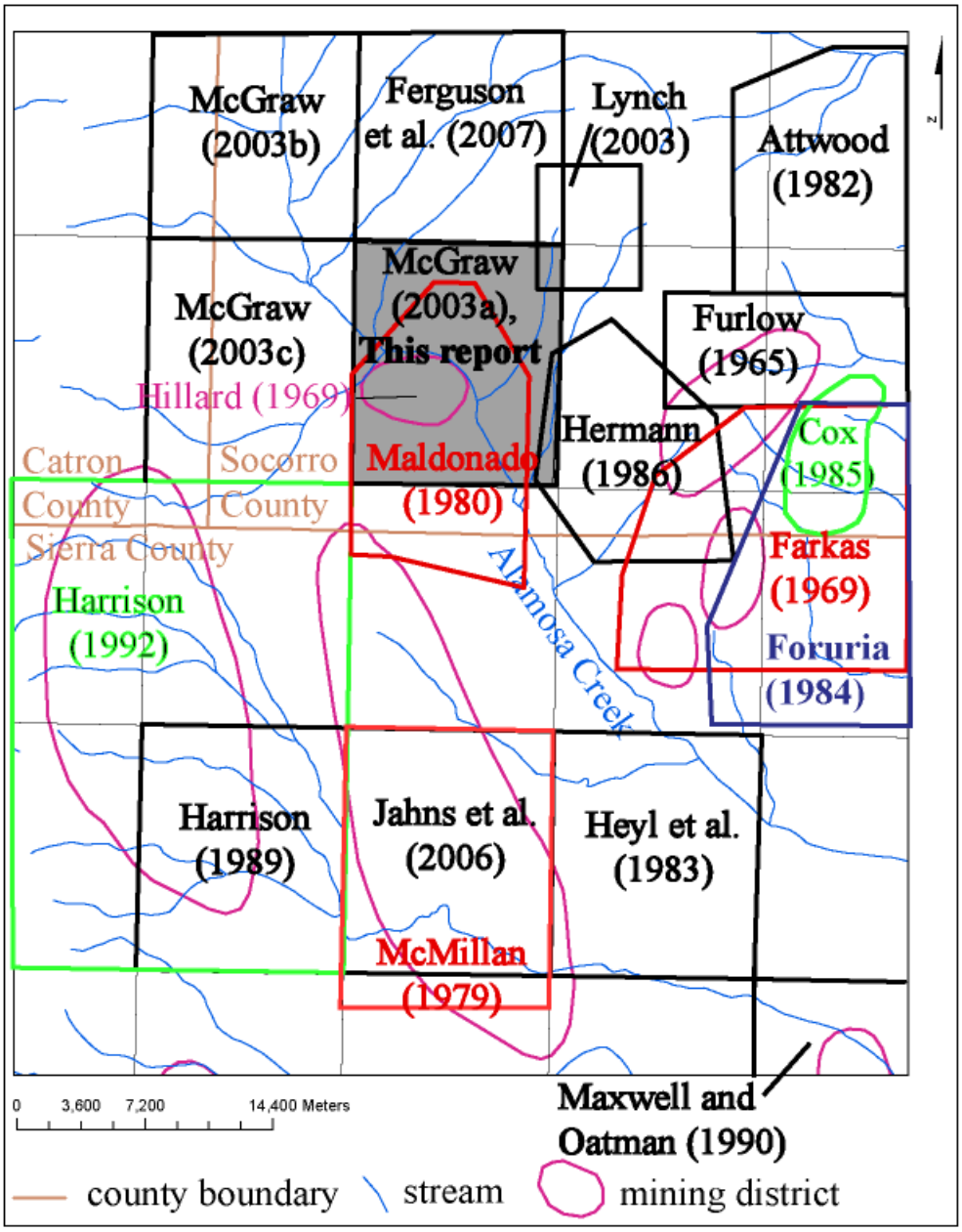

FIGURE 6. Previous geologic mapping studies in the southern San Mateo Mountains and northern Sierra Cuchillo, central New Mexico. See Figure 8 for identification of mining districts, shown as red polygons.

GEOGRAPHY AND HISTORY

Geography

The topography, climate, and land use of the Montoya Butte quadrangle are typical for south-central New Mexico. The terrain of the Cañada Alamosa drainage area in the Montoya Butte quadrangle includes mountains, foothills, plains, and valleys, which results in significant variations in local climate. The elevation of the Montoya Butte quadrangle ranges from 1,758 to 2,320 meters above sea level. The general climate in the

area is semi-arid, and varies from desert to alpine. Winters here can be cold and snowy, while summers are moderate to hot and experience monsoonal precipitation during July through September. Temperatures range from lows below -18°C (0°F) in the mountains to highs in excess of 38°C (100°F) in the valley (data from National Climatic Data Center). Precipitation also varies across the area and is influenced by location and elevation. Average precipitation, including both snowmelt and rainfall, ranges from approximately 203 to 508 mm (8 to 20 inches) per year (data from National Climatic Data Center). Alamosa Creek flows all year long east of Monticello Box to Placitas, mostly through the Community Ditch. Other drainages and the southern Cañada Alamosa, south of the intersection of the county road with Cañada Alamosa below Placitas, generally flow only after intense rain storms or during the wetter seasons. Summer rains typically cause flash floods in the drainages. Ranching is the predominant land use of the area, although small farms are found along Cañada Alamosa, south of the Montoya Butte quadrangle.

The major biotic zones within Montoya Butte quadrangle are Chihuahuan Desert zone, the forested Upland zone, and a transition zone in between. The Chihuahuan Desert is along Cañada Alamosa. Large cottonwood trees along with oak, walnut, and willow trees grow along the banks of the Cañada Alamosa. The Upland zone is in the surrounding mountains and consists of ponderosa pine, piñon, juniper, oak, aspen, and spruce trees. The transitional zone is primarily piñon-juniper grassland. However, ponderosa pines are found in and near Red Paint Canyon (transition zone) and are associated with the acid-sulfate alteration. All three zones include a variety of grasses, small to large shrubs, and cacti. The perennial flow of the stream results in lush, green vegetation in the canyon bottom during the warmer months.

The warm spring in Spring Canyon is called Ojo Caliente, which is Spanish for *warm spring*. Carlton (1992) proposed a name change to Tchihene Apache Ojo Caliente in order to avoid confusion with Ojo Caliente found in Taos and Cibola Counties. Tchihene means *red-painted people*, which was the name given to the Apache Indians in the area. Ojo Caliente in Spring Canyon also is known as Victorio Spring. Additional warm springs, including Willow Springs, are found west of Ojo Caliente (Fig. 5). The warm springs provide much of the water to Cañada Alamosa. Cold springs are found further upstream and south of in Alamosa Creek and along Red Paint Canyon. Runoff from the adjacent mountains and cold springs throughout the area (Appendix 2) provide additional sources of water to Cañada Alamosa.

General History

Cañada Alamosa was first occupied by Pueblo people from about AD 600 to AD 1400. These people lived in small- to medium-sized pueblos along Cañada Alamosa constructed from rock and adobe (Fig. 7). They farmed the river bottom, drainages, and terraces near the pueblos. Four major Pueblo sites are found in the Montoya Butte quadrangle and were excavated over the last 10 yrs by Karl Laumbach and associates (Laumbach and Laumbach, 2009). The Montoya (Mimbres Phase, A.D. 1000-1130, and Socorro Phase, A.D. 1100-1200), Victorio (Tularosa Phase, A.D. 1175-1275, with earlier pit house and Pueblo components), Kelly Canyon (Socorro Phase, A.D. 1100-1200), and Pinnacle Ruin Sites (Magdalena Phase, A.D. 1250-1400+) represent distinct temporal

periods of occupation. By the time the Spanish explorers traveled through this area in 1581, Cañada Alamosa was unoccupied.

The Apache Indians settled in southwestern New Mexico in the 16th or 17th century. The tribe known as the Warm Spring Apache Indians (also known as Tcihene Apache or Red-Painted People and Ojo Caliente Apaches; Carlton, 1992) settled in the Ojo Caliente area by the 1860s, certainly by 1873 (Sullivan, 1994). This group of people had several leaders including Mangas Coloradas, Nana, Loco, and Victorio. The altered area in Red Paint Canyon (defined by the author in this report) south of Monticello Box was exploited by the Warm Springs Apache Indians, who used the red hematitic clay for body paints. It is likely that Pueblo people before the Apaches also used the clay material from Red Paint Canyon for paint and pottery.

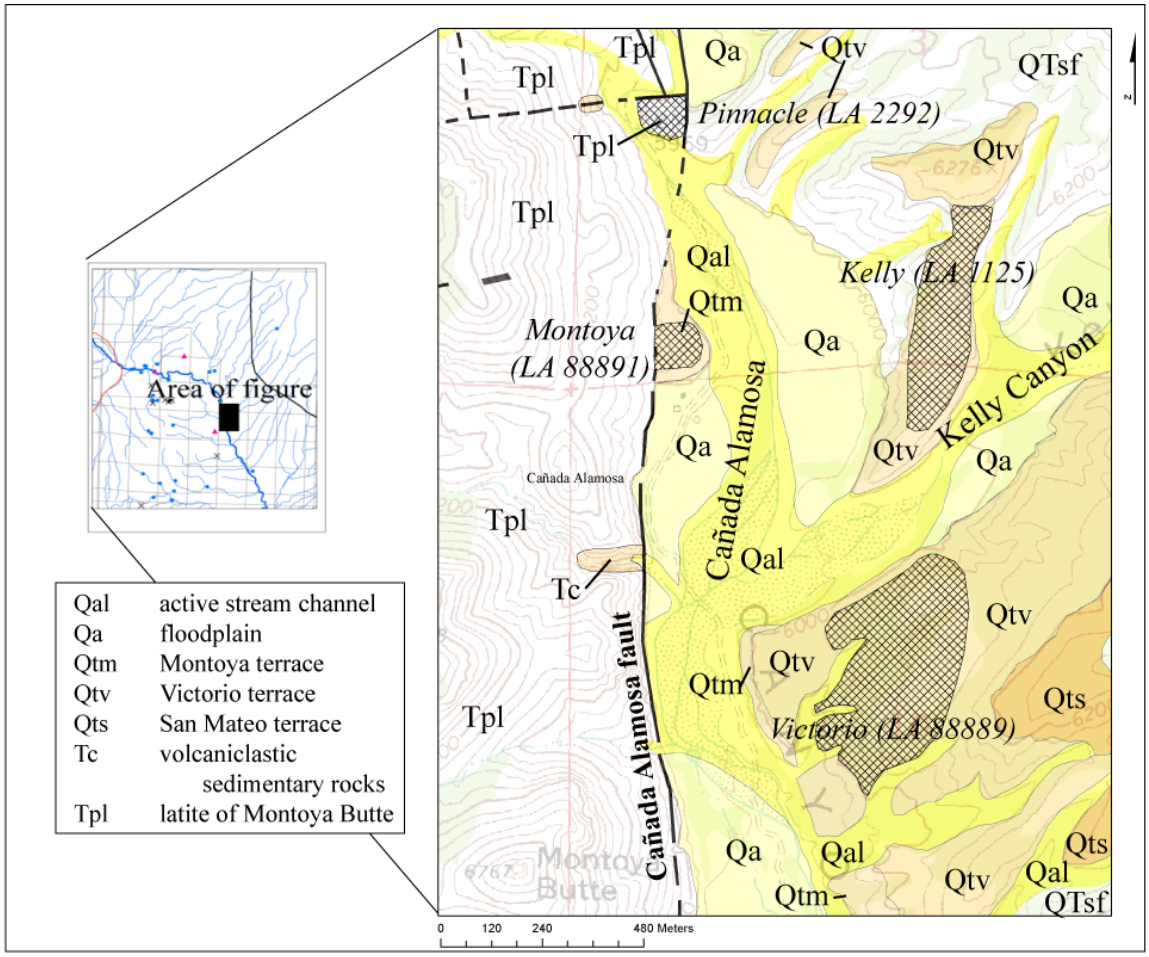

FIGURE 7. Location of Pueblo occupation sites in Cañada Alamosa area. Kelly and Victorio sites that show evidence of local farming are (Qtm, Qtv) terrace. Montoya site is on the Montoya (Qtm) terrace. Units are described below. From McLemore (2011).

In 1874, the U.S. Government established a reservation for the Warm Springs Apache tribe at Ojo Caliente, west of Monticello Box, but in 1875-1876, the U.S. Government moved the tribe to the San Carlos reservation in Arizona and eventually placed the reservation in the public domain. Eventually, the Warm Springs Apache

Indians were relocated to Florida and later to Fort Sill, Oklahoma and the Mescalero Apache Reservation in central New Mexico. The former reservation is now under private ownership.

The first village of Cañada Alamosa (Fig. 8), also known as San Tgnacio de la Alamosa, was established at the mouth of Cañada Alamosa near the Rio Grande about 1859 and was included in the 1860 census. But this village ceased to exist by the 1870 census (Wilson, 1985). Abandonment probably occurred in 1866 or 1867. Monticello originally named Cañada Alamosa was established by 1863 upstream of the first village of Cañada Alamosa at the Rio Grande (Fig. 8; Wilson, 1985). Julyan (1998) reported that the village was settled in 1856. Monticello became the official name of the upstream village in 1881 and the spelling was changed in 1892 (Julyan, 1998; Bailey, 2006). Placitas (*Little Plaza*) was established south of Monticello (Fig. 8). The Monticello Community Ditch Association was established in the 1880s to provide water from the springs in the Alamosa Creek to the farms in the southern portion of the canyon, near the villages of Monticello and Placitas. An irrigation canal in Cañada Alamosa was noted by U.S. Army troops in 1863 (Bailey, 2006). A saw mill was established west of Monticello Box about 1870 (Carlton, 1992).

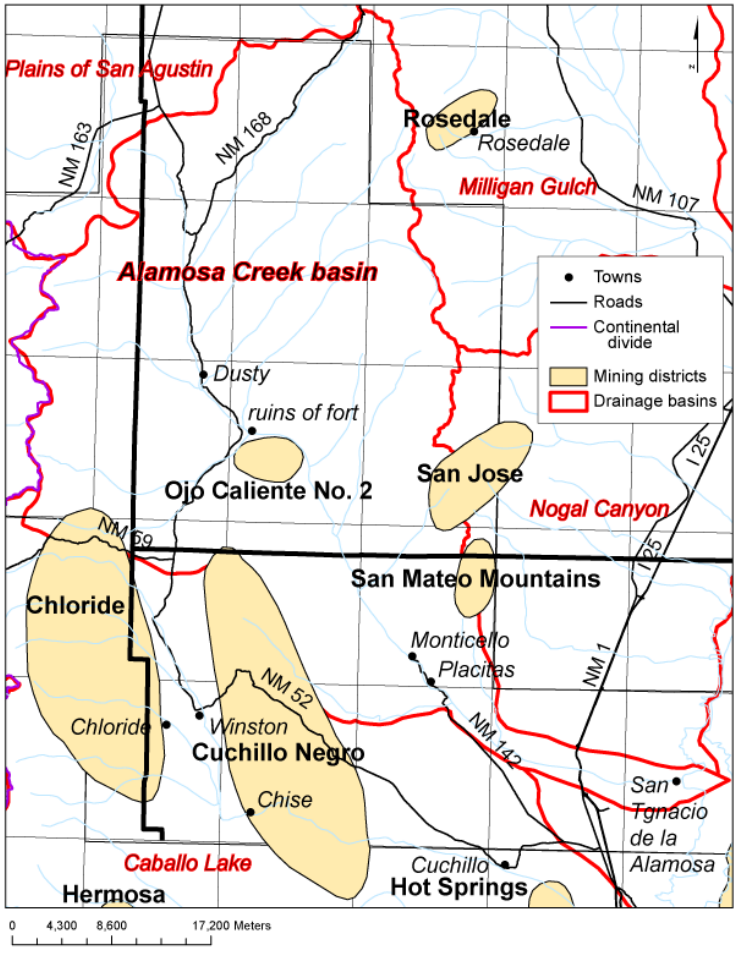

FIGURE 8. Geographic and cultural features of the Cañada Alamosa drainage basin in the Monticello area.

Mining History

Numerous mining districts are found in southern Socorro and northern Sierra Counties (Fig. 8,10, Table 1), but only the Chloride district near Winston and the copper porphyry and Laramide veins in the Hillsboro mining district had significant production. The Ojo Caliente No. 2 mining district (Lasky, 1932; district identification number DIS230, New Mexico Mines Database, McLemore et al., 2005a, b) is the only mining district in the Montoya Butte quadrangle and is south of Monticello Box (Fig. 5, 9). Mineral deposits in the Ojo Caliente No. 2 district include volcanic epithermal vein deposits (McLemore, 1996) and volcanogenic Be (volcanic-hosted replacement, volcanic-epithermal, Spor Mountain Be-F-U deposits; Lindsey and Shawe, 1986; Foley et al., 2010). Only one mine has yielded metals production from this district, the Taylor mine (mine identification number NMSO0073, New Mexico Mines Database), which yielded one car load of copper, silver, and lead ore about 1950. Several veins of calcite, quartz and locally fluorite, possibly with trace base metals, are found throughout the district (McLemore, 2011). During the uranium boom a small amount of uranium was produced from Red Paint Canyon, according to Hillard (1967, 1969).

TABLE 1. Mining districts found in the vicinity of Montoya Butte quadrangle in Sierra and Socorro Counties, New Mexico (Fig. 9). Names of districts are after File and Northrop (1966), North and McLemore (1986), McLemore and Chenoweth (1989), and McLemore (2001) wherever practical, but many districts have been combined and added. Estimated value of production is in original cumulative dollars and includes all commodities in the district, except aggregate (sand and gravel) and dimension stone. Type of deposit is after North and McLemore (1986) and McLemore (2001). Production data modified from Lindgren et al. (1910), Anderson (1957), U.S. Geological Survey (1902–1927), and U.S. Bureau of Mines (1927–1994).

District identification number	District (Aliases)	Year of Discovery	Years of Production	Commodities Produced (Present)	Estimated Cumulative Value of Production (In Original Dollars)	Type of Deposit
DIS049	Carpenter (Swartz, Schwartz)	1891	1891-1969	Cu, Pb, Zn, Au, Ag (F, W, Be, Ba, Nb, Ta)	$1,360,000	Carbonate-hosted Pb-Zn replacement, skarns
DIS191	Chloride (Black Range, Apache, Bear Creek, Fairview-Chloride, Fluoride, Gratton, Phillipsburg, Readjustor, Winston)	1879	1879–1988	Au, Ag, Cu, Pb, Zn, Sn, zeolite (F, Mo, Ba)	$20,000,000	volcanic-epithermal, placer gold, Laramide skarn, zeolite
DIS192	Cuchillo	1879		Ag, Cu, Pb,	$205,000	carbonate-hosted

District identification number	District (Aliases)	Year of Discovery	Years of Production	Commodities Produced (Present)	Estimated Cumulative Value of Production (In Original Dollars)	Type of Deposit
	Negro (Cuchillo, Chise, Negro, Iron Mountain, Limestone, Cross Mountain)			Zn, W, Fe, U, F (Au, Be, Sn, Mo)		Pb-Zn replacement, sedimentary-copper, replacement iron, placer tin, tin veins
DIS194	San Mateo Mountains (Goldsboro, Goldsborough, Argon Hill, Monticello)	1900s		Au, Ag, U (Sn, V, Sb, Mo, Cu)	<$10,000	volcanic-epithermal vein
DIS196	Hermosa (Palomas)	1879	1879–1956	Ag, Au, Pb, Cu, Zn (Sb, Mo)	<$2,000,000	carbonate-hosted Pb-Zn replacement, carbonate-hosted Ag-Mn replacement
DIS197	Hillsboro (Las Animas)	1877	1877–1982	Au, Ag, Pb, Zn, Cu, V, Mn (As, Mo, Te, W)	$8,500,000	porphyry Cu, Laramide vein, Laramide skarn, carbonate-hosted Pb-Zn-Ag-replacement, carbonate-hosted Mn-Ag-replacement, placer gold
DIS198	Hot Springs (Mud Springs, Iron Reef, Black Chief, Ellis, Lucky Strike)	1930	1934–1954	Ag, Cu, Pb, Mn	$70,000	carbonate-hosted Ag-Mn replacement
DIS199	Kingston (Black Range No. 2)	1880	1880–1957	Au, Ag, Cu, Pb, Zn, Mn (W, Sb)	$6,600,000	carbonate-hosted Ag-Mn replacement, carbonate-hosted Pb-Zn replacement
DIS200	Lake Valley	1878	1878–1957	Au, Ag, Mn, Pb, Cu (Mo, V, As, Sb)	$5,400,000	carbonate-hosted Ag-Mn
DIS201	Macho	1879	1879–1977	Au, Ag, Pb, Zn, Cu (V, Mn, Ba, Mo)	$679,000	volcanic-epithermal vein, carbonate-hosted Ag-Mn

District identification number	District (Aliases)	Year of Discovery	Years of Production	Commodities Produced (Present)	Estimated Cumulative Value of Production (In Original Dollars)	Type of Deposit
						replacement
DIS204	Taylor Creek (Black Range) (Catron County)	1918	1919–1943	Sn, Mn (kaolin)	$7,000–8,000	tin veins and placers, rhyolite-hosted tin
DIS205	Tierra Blanca (Percha, Bromide No. 1, Silver Tail)	1885	1885–1955, 1971–1972	Au, Ag, Cu, Pb, Zn, W (Te)	$270,000	Carbonate-hosted Ag-Mn replacement, volcanic-epithermal vein
DIS225	Rosedale (San Mateo Mtns)	1882	1882-1981	Au, Ag (F, U, Cu, Mn)	$500,000	volcanic-epithermal, placer gold
DIS226	San Jose (Nogal, San Mateo, Rhyolite)	prior to 1900	prior to 1946	Au, Ag, Cu, Pb, Zn (Mo)	$40,000	volcanic-epithermal
DIS230	Ojo Caliente No. 2 (Talyor)	1900s		Ag, Cu, Pb (Au, Mn)	<$1,000	volcanic-epithermal, volcanogenic Be

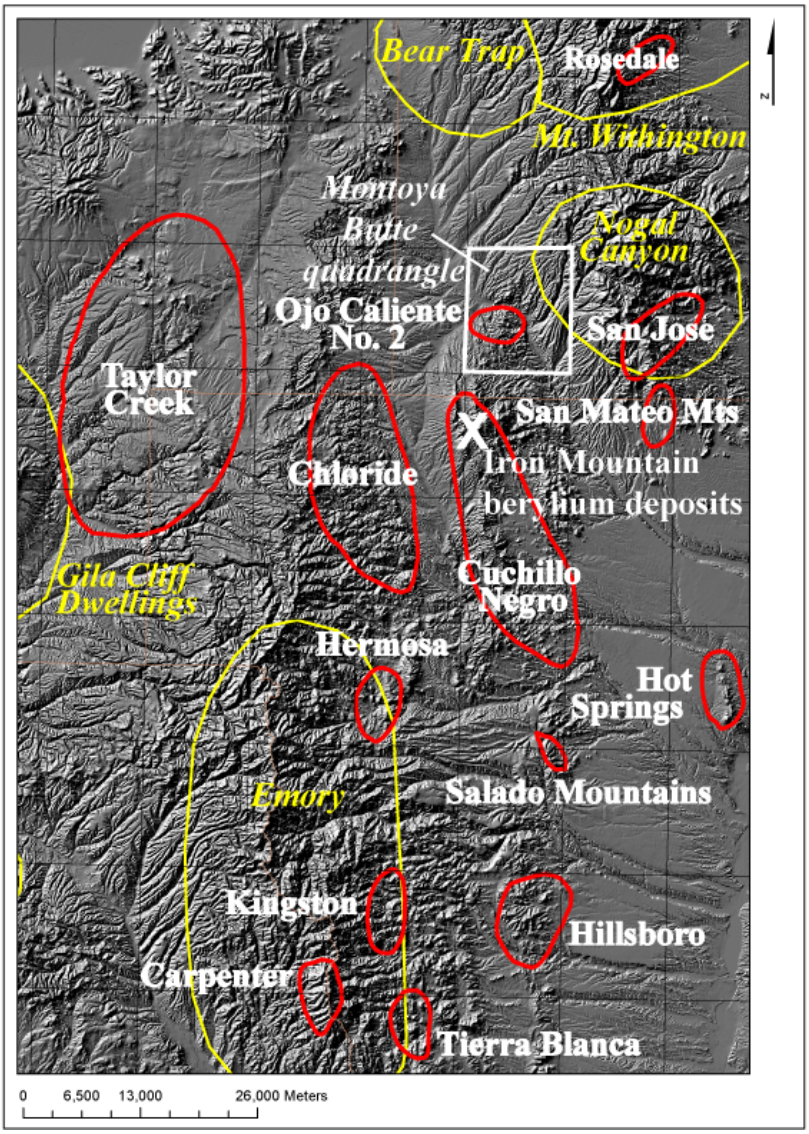

FIGURE 9. Mining districts (red) and calderas (yellow) found in the vicinity of Montoya Butte quadrangle, southern Socorro and northern Sierra Counties, New Mexico. Iron Mountain beryllium deposit in the Cuchillo Negro district is denoted by a white X.

Beryllium, found as mostly as bertrandite ($H_2Be_4Si_4O_9$), was first noted in Red Paint Canyon about 1961 by M. Howard Milligan (NMBGMR files). Shawe (1966) included the Apache Warm Springs beryllium deposit as part of the New Mexico-Arizona beryllium belt, which also includes Iron Mountain to the south. Meeves (1966) described the results of field reconnaissance mapping, trenching, and drilling for beryllium by a commercial company under contract to the U.S. Bureau of Mines. Eighteen holes were drilled as part of these early exploration efforts (Appendix 7).

The Beryllium Group, LLC controlled the Apache Warm Springs beryllium deposit in 2001-2002, drilled 14 holes, and reported a resource of 39,063 metric tones (43,060 short tons, not NI 43-101 compliant; Mining Engineering, 2002). Great Western

Exploration, LLC controlled the property from 2004-2007 (P and E Mining Consultants Inc., 2009). In October 2007, BE Resources Inc. acquired the property and has applied for and been awarded exploration permits for additional drilling. Drilling began in September 2010. There has been no beryllium production from the property.

Beryllium, tungsten, and iron have been produced from the Iron Mountain deposit (Cuchillo Negro mining district), which is south of the Apache Warm Springs deposit in the Sierra Cuchillo (Fig. 9; Lovering and Heyl, 1989). Griffitts and Alminas (1968) conducted a stream-sediment reconnaissance of the Monticello Box area for base metals and found the area to have numerous minor geochemical anomalies; beryllium was not analyzed for.

REGIONAL GEOLOGIC AND TECTONIC SETTING

Introduction

The Montoya Butte quadrangle, including the Ojo Caliente No. 2 mining district, lies in a tectonically active and structurally complex area of the southwestern U.S. that is known for numerous types of mineral deposits. The Mogollon-Datil volcanic field is part of a late Eocene-Oligocene volcanic province that extends from west-central New Mexico southward into Chihuahua, Mexico (Fig. 1; McDowell and Claubaugh, 1979; McIntosh et al., 1991, 1992a, b; Chapin et al., 2004). In southwestern North America, Tertiary volcanic activity began about 40-36 Ma with the eruption of andesitic volcanism, followed by episodic bimodal silicic and basaltic andesite volcanism during ~36 to 24 Ma (Cather et al., 1987; Marvin et al., 1988; McIntosh et al., 1992a, b). Approximately 25 high- and low-silica rhyolite ignimbrites (ash-flow tuffs) were erupted and emplaced throughout the Mogollon-Datil volcanic field during the second event; source calderas have been identified for many of the ignimbrites (McIntosh et al., 1992a, b; Chapin et al., 2004). The western edge of the Nogal Canyon caldera lies in the eastern portion of the Montoya Butte quadrangle (Fig. 1, 5). Subsequent faulting, hydrothermal alteration, and volcanism have offset, altered, and covered portions of the ignimbrites, which creates difficulties for regional correlations.

The Monticello graben lies between the Black Range and Sierra Cuchillo range to the west and the San Mateo Mountains to the east (Fig. 2, 5). The Winston graben is west of the Monticello graben and the Sierra Cuchillo range (Fig. 2). Both grabens are terminated on the north by the Morenci lineament of Chapin et al. (1978), now called the Socorro accommodation zone of Chapin (1989). The deflection in the southern Monticello graben (i.e., Cañada Alamosa) corresponds with the Chise lineament of Harrison (1992).

The Ojo Caliente No. 2 mining district is one of numerous epithermal-vein deposits found in southwestern New Mexico (Table 1; McLemore, 1996, 2001) and southeastern Arizona (Keith et al., 1983) and is one of few volcanic-epithermal districts not associated with any caldera. The district also is one of a few districts in New Mexico to contain significant beryllium deposits not hosted by pegmatites (McLemore, 2010b, c).

Age of regional lithologic units

Numerous studies have examined the age of volcanic and intrusive rocks similar to those found in the Montoya Butte quadrangle and are summarized in Table 2. Three

samples from the quadrangle were submitted for $^{40}Ar/^{39}Ar$ age dating. The results of these studies are in Table 2 and Appendix 6.

TABLE 2. Ages of various lithologic units in the San Mateo Mountains, Sierra Cuchillo, and Taylor Creek areas (Black Range), Sierra, Socorro, and Catron Counties, New Mexico.

Lithologic unit	Age (Ma)	Method of dating	Comments	Reference
Quaternary-Tertiary basalt flows				
Mud Springs Mountains	2.1-2.9			Bachman and Mehnert (1978), Maxwell and Oatman (1990)
Hillsboro	4.2±0.1	K-Ar	Overlies gravels	Seager et al. (1984), Harrison (1994)
Hillsboro	4.5±0.1	K-Ar	Underlies Palomas surface	Seager et al. (1984)
Table Top Mountain	4.8±0.1	K-Ar	Flow overlies Santa Fe beds and fault	Seager et al. (1984)
Mimbres basalt	6.9			Elston et al. (1968)
San Mateo Mountains				
Turkey Springs Tuff (Tts)	24.38±0.03, 24.50±0.04	$^{40}Ar/^{39}Ar$	Weighted mean	Lynch (2003), this report, Appendix 6
Volcaniclastic sediment (Tvc1)	27.89±0.10	$^{40}Ar/^{39}Ar$		Lynch (2003)
Rhyolite lava (Tac, MONT-104)	28.38±0.03	$^{40}Ar/^{39}Ar$		This report, appendix 6
Rhyolite intrusion (Ti2)	28.31±0.15	$^{40}Ar/^{39}Ar$	Weighted mean	Lynch (2003)
Rhyolitic ignimbrite (Trlt)	28.28±0.06	$^{40}Ar/^{39}Ar$	Weighted mean	Lynch (2003)
Rhyolite lava (Trl)	28.36±0.11	$^{40}Ar/^{39}Ar$	Weighted mean	Lynch (2003)
Granite porphyry (Ti1)	28.34±0.06	$^{40}Ar/^{39}Ar$	Weighted mean	Lynch (2003)
Vicks Peak Tuff (Tvp)	28.39±0.19	$^{40}Ar/^{39}Ar$	Weighted mean	Lynch (2003)
Taylor Creek, Black Range				
Taylor Creek Rhyolite	27.92±0.04	$^{40}Ar/^{39}Ar$	Weighted mean	Dalrymple and Duffield (1988), Duffield et al. (1990), Duffield and Dalrymple (1990)
Sierra Cuchillo				
Upper andesite sequence	18.3			Seager et al. (1984)
Porphyritic rhyolites	22.6±0.8	K-Ar	Sample 84-064, perthitic microcline	Davis (1986a, b)
Scheelite skarn	27.3±0.6	K-Ar	Adularia from skarn	Davis (1986a, b)
Rhyolite of Willow Springs	27.8±1.0	Fission track	zircon	Heyl et al. (1983)
Rhyolite of Willow Springs	28.2±0.5	U-Pb		Michelfelder (2009)
Rhyolite aplite, Sierra Cuchillo	29.2±1.1	K-Ar	Accessory minerals include biotite, apatite, fluorite and topaz	Chapin et al. (1978), Robertson (1986)

Lithologic unit	Age (Ma)	Method of dating	Comments	Reference
Latite of Montoya Butte (Tpl, MONT-108)	35.70±0.05	$^{40}Ar/^{39}Ar$	biotite	This report, appendix 6
Latite-andesite	36.2±0.6	U-Pb	zircon	Michelfelder (2009), Michelfelder and McMillan (2009)
Dacite-rhyolite	36.5±0.7	U-Pb	zircon	Michelfelder (2009), Michelfelder and McMillan (2009)
Iron Mountain monzonite	29.2±1.1	K-Ar		Chapin et al. (1978)
Reilly Peak rhyolite	36.0 ±1.4	K-Ar	Sample 84-031, whole rock	Davis (1986a, b)
Vindicator sill (rhyolite)	37.7±0.7	U-Pb	zircon	Michelfelder (2009), Michelfelder and McMillan (2009)
Sierra Cuchillo laccolith (monzonite)	38.2±0.9	U-Pb	zircon	Michelfelder (2009), Michelfelder and McMillan (2009)
Andesite dike	41.0±7.4	K-Ar	Sample 84-039, whole rock	Davis (1986a, b)

LITHOLOGIC DESCRIPTIONS

General statement

Figure 10 is a simplified geologic map of the Montoya Butte quadrangle, modified from the detailed geologic quadrangle McLemore (2011). McLemore (2011) also includes cross sections of the area. The rock units are described in Table 3 and below (updated from McLemore, 2008). The Montoya Butte quadrangle consists of Mid-Tertiary volcanic rocks, typical of the Mogollon-Datil volcanic province and sediments correlative to the Quaternary-Tertiary Santa Fe Group (Table 3). A major fault zone, Red Paint Canyon fault zone (new name defined by the author), separates the volcanic rocks in the Ojo Caliente No. 2 mining district from Quaternary sedimentary rocks of the upper Alamosa Creek basin. The Red Paint Canyon fault zone consists of several parallel and subparallel faults and fractures west of Monticello Box (Fig. 10; McLemore 2011). The beryllium deposits are along the southern portion of this fault zone and the volcanic-epithermal copper-silver vein deposits are east and south of the Red Paint Canyon fault zone. Ojo Caliente, Willow Springs, and other the warm and cold springs feeding the Cañada Alamosa, Alum Spring, and two water wells also are within the Red Paint Canyon fault zone. This fault zone truncates and offsets older faults.

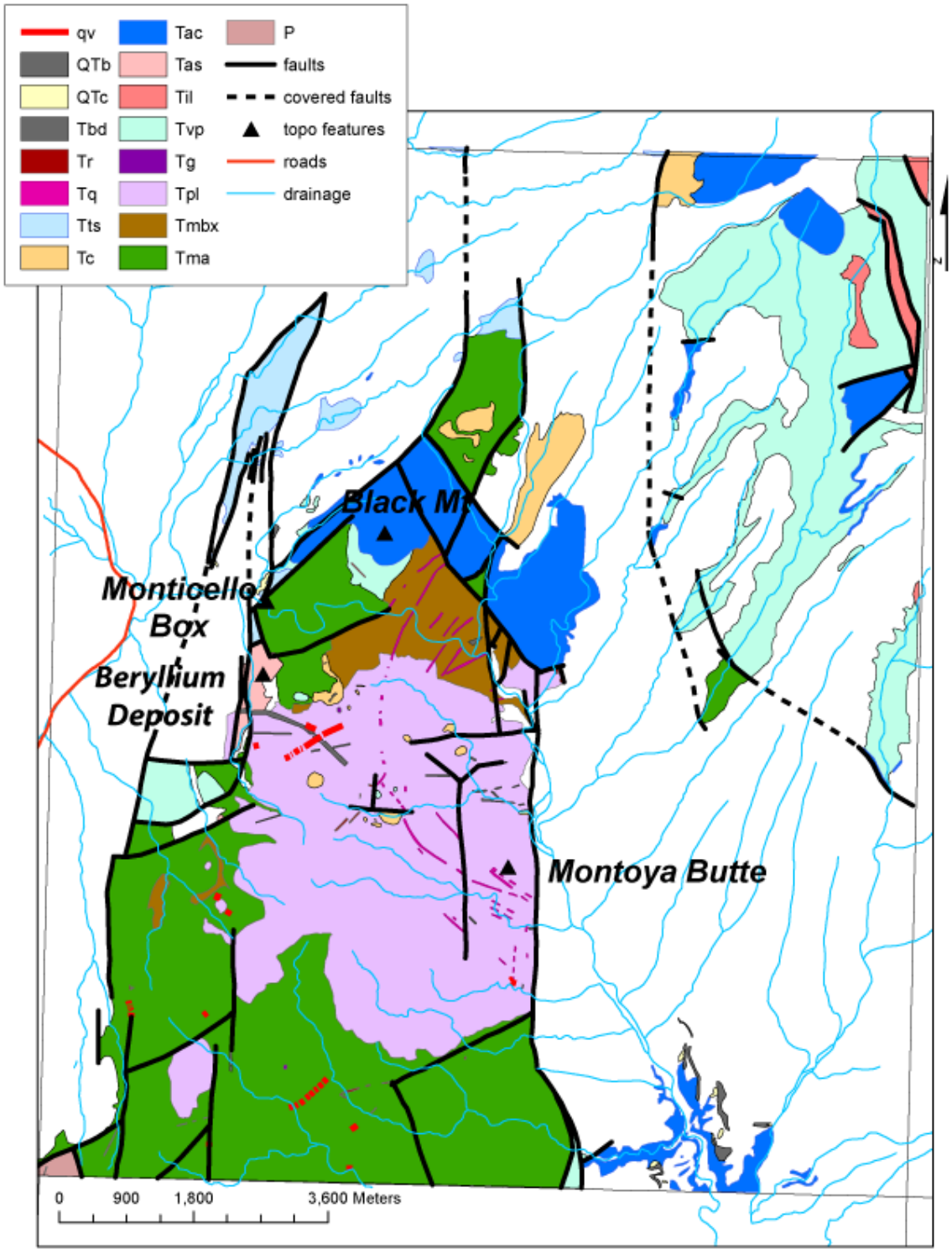

FIGURE 10. Simplified geologic map (simplified from McLemore, 2011). See Table 3 for definition of legend symbols.

TABLE 3. Descriptions of geologic units in the Montoya Butte quadrangle, Socorro County, youngest to oldest (age dates, thickness, and descriptions are modified from Jahns et al., 1978; Hillard, 1967, 1969; Maldonado, 1974, 1980; McGraw, 2003a; Lynch, 2003; and McLemore, 2011).

Symbol	Unit (age)	Description	Thickness (m)
af	Artificial fill	areas of disturbed, excavated, or filled ground due to human activity, commonly earthen dams or stock tanks	
Qal	Modern alluvium	valley bottom clays, sands, and volcanic gravel deposits found in modern and active stream channels and adjacent floodplain deposits	0-2
Qa	Valley-floor alluvium	alluvium occupying the floors of modern valleys that is composed of fine-grained sediment with minor coarse channel-fills. Historical erosion has formed low terraces whose upper surface (i.e., tread) lies less than 2-3 m above adjacent major streams	2-6
Qc	colluvium and talus, undivided	colluvium and talus deposits on hill slopes that are composed of sand and volcanic gravels; these deposits conceal bedrock.	0-6
QTsf	Santa Fe Group	undivided, poorly to moderately consolidated clay-silt, sand, and gravels comprising the main piedmont alluvial fans and bajadas adjacent to uplands, locally includes some terrace deposits (Qt); thickness 0-300+ m (in part after McGraw, 2003)	0-390+ (includes QTc, Qt, Qp, Qa, Qal)
Qt	Terrace surfaces, undivided	clays, silts, sands and volcanic gravels forming upper terrace deposits (above active stream channels and floodplains), subdivided by age/inset relationships where possible (Qtm, Qtv, Qts) (in part after McGraw, 2003)	3-8
Qtm	Montoya terrace (youngest)	tread lies 3-15 m above modern grade of Cañada Alamosa; unit consists of silt, sand, gravel, and boulders (mostly rhyolite), generally well-developed, cemented soils; locally unconformable on Tertiary volcanic rocks; 3-8 m thick	3-8
Qtv	Victorio terrace (second youngest terrace)	tread lies 10-30 m above modern grade of Cañada Alamosa; unit consists of silt, sand, gravel, and boulders (mostly rhyolite), generally well-developed, cemented soils; 3-8 m thick	3-8
Qts	San Mateo terrace (third youngest terrace)	tread lies 15-45 m above modern grade of Cañada Alamosa; unit consists of silt, sand, gravel, and boulders (mostly rhyolite), generally thin soil and some caliche development; 3-8 m thick	3-8
Qp	Burma Pediment deposits	Poorly to moderately consolidated sand and gravel similar to that found on terraces; larger surfaces are included in QTsf	0-8
QTb	Basalt (~2-4 Ma?)	fine grained, black to dark gray basalt flows and sills, <1% phenocrysts of feldspar, olivine, and late-stage calcite, vesicular to massive with local pillow-like texture	0-10
QTc	Santa Fe Group—basal conglomerate	well-cemented, orange to brown to buff, poorly sorted conglomerates and sandstones composed of volcanic material, up to 9 m thick	0-5
Tc	Volcaniclastic sedimentary rocks	well-cemented, massive to thin-bedded, volcaniclastic conglomerate, sandstone, and siltstone; includes a	0-7

Symbol	Unit (age)	Description	Thickness (m)
		white ash-fall or ash-flow tuff north of Black Mountain	
Tan	Andesite flows	andesite flows interbedded with volcaniclastic sedimentary rocks (Tc)	0-7
Tt	Turkey Springs Tuff (24.4 Ma; Lynch, 2003; 24.5 Ma, this report, Appendix 6)	gray, welded to nonwelded tuff containing 5-30% phenocrysts (quartz, sanidine, biotite) (Ferguson and Osburn, 2007)	0-60
Tas	rhyolite of Alum Spring	interbedded rhyolite ash-flow tuff, lava and volcaniclastic beds with strong argillic (acid-sulfate) alteration, thickness 0-350 m in drill holes	0-350?
Til	granite of Kelly Canyon (28.3 Ma; Lynch, 2003)	pinkish gray to gray holocrystalline to porphyritic granitic stocks, typically with large K-feldspar phenocrysts	intrusion
Tac	rhyolite of Alamosa Canyon (28.4 Ma; Lynch, 2003; this report, Appendix 6)	pinkish gray to gray rhyolite lava, phenocryst poor (1-3% sanidine, 1-3% quartz, locally amethyst or smokey, 1-5% biotite, pseudobrookite), with contorted flow bands, brecciated and vuggy (especially near the top), local sphereulitic texture, interbedded with local ash-flow tuffs and vitrophyre, thickness 0-300+ m	0-220+
Tvp	Vicks Peak Tuff (28.4 Ma; Lynch, 2003)	pinkish-gray, welded rhyolite ash flow tuff, phenocryst poor (1-10% sanidine, biotite), 4-15% pumice, locally columnar jointed	0-690+
Tr	rhyolite dikes	pink gray rhyolite dikes	intrusion
Tbd	andesite to basalt dikes	dark gray to black to olive green andesite to basalt dikes, locally with porphyritic texture	intrusion
Tgr	granite to quartz monzonite	pink to gray, coarse- to fine-grained granite to quartz monzonite, consisting of K-feldspar, plagioclase, quartz, and biotite (Hillard, 1963)	intrusion
Tql	Latite to quartz latite dikes	greenish gray to brown gray, porphyritic quartz latite dikes, 5-10% phenocrysts of albite, some Carlsbad twins, xenoliths common (Hillard, 1963)	intrusion
Tpl	latite of Montoya Butte (35.7 Ma, this report, Appendix 6)	platy, gray to brown gray latite, up to 60% phenocrysts of sanidine, plagioclase, and biotite, locally interbedded with green to gray siltstone and sandstone	0-185
Tmbx	lahar (mudflow)	mudflow, matrix supported, contains andesite and rhyolite boulders and cobbles	0-220
Tmb	andesite of Monticello Box	black to gray, porphyritic to aphanitic andesite	0-120
Py	Yeso Formation and San Andres Limestone, undivided (Permian)	brown thin- to medium-bedded sandstone and siltstone, and dark gray, fine-grained limestone	<643 in Sierra Cuchillo

Sedimentary and volcaniclastic deposits

Permian Yeso/San Andres Formations (Py)

The oldest rocks exposed in the Montoya Butte quadrangle are marine sedimentary rocks belonging to the Permian Yeso and San Andres Formations. Fault blocks in the southwestern corner of the quadrangle consist of orange- to reddish-brown, well- to moderately-sorted sandstones and siltstones that are interbedded and overlain by dark gray, fine-grained, massive limestones. These units are as thick as 640 m elsewhere

in the Sierra Cuchillo (Jahns et al., 1978). It is likely that these Permian rocks underlie much of the Montoya Butte quadrangle at depth (Maldando, 1974; Jahns et al., 1978).

Andesite of Monticello Box (Tmb)

The andesite of Monticello Box in this report is the name given to the andesite forming the Monticello Box and is the oldest volcanic rocks exposed in the Montoya Butte quadrangle. Maldonado (1974, 1980) combined the andesite with the overlying lahar (mudflows) and latite (latite of Montoya Butte) and called the combined unit andesite-latite of Montoya Butte. The andesite is fine grained to aphanitic to locally porphyritic, dense to locally amygdaloidal, dark gray to reddish gray to reddish brown (Fig. 11) and consists of plagioclase, pyroxene, biotite, and hornblende in a fine-grained groundmass. Amygdaloids (vesicles) are locally filled with calcite and/or quartz. In the Monticello Box area, the andesite is up to 120 m thick and forms steep cliffs, whereas in the southern Sierra Cuchillo the lower andesite sequence is 250 to 550 m thick (Jahns et al., 2006). The base is not exposed. The andesite of Monticello Box could correlate with the Red Rock Ranch Formation in the southern San Mateo Mountains as mapped by Hermann (1986) and Farkas (1969) and with the lower andesite sequence in the Sierra Cuchillo as mapped by Jahns et al. (1978, 2006).

FIGURE 11. Andesite of Monticello Box, near the entrance.

Lahar (mudflow)(Tmbx)

The lahar consists of 220 m of massive, poorly sorted, matrix-supported, greenish- to purplish-gray to dark gray, mudflows, breccias, and lahars, with numerous rounded to subangular boulders, cobbles, gravel, and sand in a fine-grained matrix of

plagioclase, K-feldspar, biotite, magnetite, and clay minerals. The lithic clasts are as large as 2 m and consist of andesite and latite. In places, the unit could have been deposited in water as evidenced by local moderate sorting and fining upwards sandstone beds. The beds are near horizontal or dip to the southeast and form the cliffs on the south side of the upper Cañada Alamosa (Fig. 12). It overlies the andesite of Monticello Box and is overlain by the latite of Montoya Butte. Maldonado (1974, 1980) mapped these as tuff-breccias and combined them with the andesite as part of the andesite-latite of Montoya Butte. At Iron Mountain, Jahns (1943, 1944a) described similar lahars at the base of the andesite-latite sequence.

FIGURE 12. Lahar flows forming the cliffs along the upper Cañada Alamosa, looking south.

Latite of Montoya Butte (Tpl)

The latite of Montoya Butte is as much as 185 m thick south of Cañada Alamosa and consists of multiple, thinly foliated (platy), gray beds of latite to quartz latite lava flows and ash-flow tuffs. The latite is porphyritic and contains plagioclase, sanidine, and pyroxene in a fine-grained matrix (Fig. 13). Locally, andesite flows similar to the andesite of Monticello Box are interbedded in the latite, especially near the base. Siltstone beds are interbedded within the latite flows locally, and typically are less than 1-2 m thick. In sections 5 and 6, some of the siltstone beds have been altered by hydrothermal fluids related to the volcanic-epithermal veins and/or the Apache Warm Springs beryllium deposit. A sample was dated as 37.5±0.5 Ma ($^{40}Ar/^{39}Ar$, Table 2, Appendix 6).

FIGURE 13. Platy foliation typical of the latite of Montoya Butte looking east at the Pinnacle site (see Fig. 7).

Vicks Peak Tuff (Tvp)

The Vicks Peak Tuff erupted from the Nogal Canyon caldera and is a pinkish gray to brown gray, moderately to densely welded, phenocryst-poor rhyolite ignimbrite (ash flow tuff) that exhibits local columnar jointing or multiple fractures. Phenocrysts include tabular to euhedral sanidine (1-3 mm, 1-10%), biotite (trace-1%), and trace quartz and are in a devitrified welded ash and pumice matrix with local rock fragments of andesite and rhyolite. Abundant flatten pumice and gas cavities can be found locally at the top of individual flows, and feldspar and quartz crystals are commonly found in the gas cavities (Fig. 14). In the western portion of the quadrangle, the ash flow tuff contains abundant spherulites. The Vicks Peak Tuff is more than 690 m thick inside the caldera boundary in the northeastern portion of Montoya Butte quadrangle (Lynch, 2003; this report) and ranges in thickness from 5-200 m thick west of the caldera boundary (Maldonado, 1974, 1980; this report). The tuff unconformably lies on top of the lahar and andesite of Monticello Box north of Cañada Alamosa at Black Mountain and rests on top of latite of Montoya Butte south of the Cañada Alamosa (Fig. 10; McLemore, 2011). A 1-3 m thick, basal vitrophyre is locally present. Lynch (2003) determined that the age of the Vicks Peak Tuff is 28.4 Ma ($^{40}Ar/^{39}Ar$).


FIGURE 14. Close-up of Vicks Peak Tuff showing pumice fragments.

Rhyolite of Alamosa Canyon (Tac)

The rhyolite of Alamosa Canyon (Tac) was named by Maldonado (1974, 1980) and was called rhyolite lavas by Lynch (2003) and Ferguson et al. (2007). These lava flows overlie the Vicks Peak Tuff and locally form rhyolite dome complexes that conceal local fault zones. Locally, the unit forms cliffs and mesa tops. A basal vitrophyre (1-3 m thick) locally forms the contact between the Vicks Peak Tuff and the lava flows. Thin (1-3 m thick) moderately- to poorly-welded, phenocryst-poor (1-10%) ignimbrites are interbedded with the lava flows, especially in areas of rhyolite domes. These ignimbrites contain phenocrysts of tabular sanidine, plagioclase, and trace biotite and quartz. The rhyolite flows can be difficult to distinguish from the Vicks Peak Tuff because of their similar composition. The rhyolite lava flows commonly have undulatory flow banding, rounded quartz phenocrysts (<5%, except in gas cavities), and locally contorted and overturned folds. The top of the rhyolite flows commonly contain abundant gas cavities that can be filled with clear, smokey, and amethystine quartz, anorthoclase, magnetite, titanite, and pseudobrookite (Fig. 15; Maldonado, 1974). The rhyolite of Alamosa Canyon is as much as 60 m thick inside the caldera (Lynch, 2003) and 50-220 m thick west of the caldera boundary (this report). Lynch (2003) determined that the age of the rhyolite of Alamosa Canyon is 28.4 Ma ($^{40}Ar/^{39}Ar$ dating) and is indistinguishable from the age of the Vicks Peak Tuff. A sample collected in the southern portion of the quadrangle (MONT-104) was dated as 28.4±0.04 Ma by $^{40}Ar/^{39}Ar$ (Table 2; Appendix 6).

FIGURE 15. Rhyolite of Alamosa Canyon, showing amethystine quartz.

Rhyolite of Alum Spring (Tas)

The rhyolite of Alum Spring is exposed along Red Paint Canyon, south of Cañada Alamosa and is at least 100 m thick; the base is not exposed. The unit consists of thin rhyolite lava flows, ash-flow tuffs, and volcaniclastic sedimentary rocks (Fig. 16). The volcaniclastic sedimentary rocks consist of interbedded fine-grained sandstone, siltstone, and tuff, some of which are water laid sediments. Most of the unit is altered and varies in color from white to gray to variegated purple to red to green to buff colors, mostly as a result of acid-sulfate alteration (i.e., advanced argillic alteration). This unit can be as much as 61 m thick as determined from mapping and examination of the drill logs (Appendix 7; called clay/tuff by P and E Mining Consultants, Inc., 2009). Although, stratigraphic relationships between the rhyolite of Alum Spring and other volcanic rocks are not well exposed in the area, some interpretations can be made based upon outcrop exposure and examination of the drill logs (Appendix 7). The rhyolite of Alum Spring overlies the andesite of Monticello Box in the southern Red Paint Canyon and is overlain by the Turkey Springs Tuff. It could be correlative to the rhyolite of Alamosa Canyon on the basis of similar chemical composition (Appendix 3, see below). The rhyolite of Alum Spring could be correlative to the volcaniclastic sedimentary rocks (Tc) found north of Black Mountain and east of Red Paint Canyon. The rhyolite of Alum Spring is likely part of a rhyolite dome or intrusive complex along Red Paint Canyon fault zone. A high magnetic geophysical anomaly supports this interpretation (see Aeromagnetic map below).

FIGURE 16. Volcaniclastic rocks in the rhyolite of Alum Spring, east of Red Paint Canyon.

Turkey Springs Tuff (Tt)

The Turkey Springs Tuff erupted from the Bear Trap Canyon caldera in the northern San Mateo Mountains and is exposed in drainages in the northern and northwestern portion of the Montoya Butte quadrangle (north of Cañada Alamosa). These drainage outcrops likely represent topographic valleys or channels that were filled by the tuff. Many outcrops were mapped as the rhyolite tuff of Spring Canyon by Maldando (1974, 1980), but an age determination of a sample near the Monticello Box has the same age as the Turkey Springs Tuff. Therefore, the rhyolite tuff of Spring Canyon is correlated with the Turkey Springs Tuff and the term rhyolite tuff of Spring Canyon is no longer used. The Turkey Springs Tuff typically is gray to pinkish gray, phenocryst-poor (3-8%), poorly- to moderately-welded ignimbrite (Fig. 17). Locally a more phenocryst-rich phase (up to 20%) is present. Phenocrysts include tabular sanidine (1-3 mm, 5-10%), euhedral to subhedral quartz (1-3 mm, 0-10%), and trace plagioclase, biotite, magnetite/hematite, and titanite in a devitrified groundmass of ash and pumice. Rock fragments of rhyolite and andesite are common locally. Linear pumice fragments (1-3 cm) are locally common. The Turkey Springs Tuff is as much as 60 m thick in the Montoya Butte quadrangle and 70-105 m thick elsewhere in the San Mateo Mountains (Lynch, 2003). Lynch (2003) determined that the Turkey Springs tuff is 24.4 Ma ($^{40}Ar/^{39}Ar$ dating) and a sample collected for this report near Monticello Box was 24.5±0.04 Ma (Appendix 6).

FIGURE 17. Turkey Springs Tuff, north of Cañada Alamosa.

Andesite flows (Tan)

Younger andesite flows (Tan) are found north of Black Mountain and are interbedded with volcaniclastic sedimentary rocks (Tc). The andesite flows are fine grained to aphanitic, dense to vesicular, gray to brown-gray flows that consist of pyroxene, hornblende, biotite, and iron-oxide minerals. They are less than 2 m thick.

Volcaniclastic sedimentary rocks (Tc)

Volcaniclastic sedimentary rocks are exposed north of Black Mountain and elsewhere, and consist of well-cemented, massive to thin-bedded, volcaniclastic conglomerate, sandstone and siltstone. This unit includes a white ash-fall or ash-flow tuff north of Black Mountain. This unit could be correlated to the rhyolite of Alum Spring (Tas) in Red Paint Canyon. The sandstone and conglomerate contains rock fragments of rhyolite tuff and andesite. These rocks overlie the Vicks Peak Tuff north of Black Mountain and overlie latite of Montoya Butte south and west of Cañada Alamosa.

Quaternary-Tertiary Santa Fe Group (QTsf, Pleistocene to Miocene)

Since formation of the Nogal Canyon caldera and eruption of rhyolite lavas during the Miocene, large amounts of detritus were shed into the Alamosa Creek basin from the San Mateo Mountains and, to a lesser extent, from the Sierra Cuchillo Range. This detritus was derived largely from erosion of rhyolite ash-flow tuffs and rhyolite and andesite flows. Over time, this erosion resulted in deposits that may be as much as 390 m thick in places. These piedmont deposits consist of reddish-brown, pale-brown, tan, and

orange, poorly-sorted, poorly consolidated, intertonguing beds of massive conglomerates and thin, massive to cross-bedded, fine-grained sandstones, siltstones, and clay beds. Organic material is rare and, if present, consists predominantly of plant roots. Graded bedding and cross-bedding are common in thin lenses (several meters thick). The deposits eroded from the San Mateo Mountains are thicker and more extensive than deposits eroded from the Sierra Cuchillo. These sedimentary units have been correlated to the Gila Conglomerate (Myers et al., 1994) or the Winston Formation (Hillard, 1967, 1969), but are better correlated with the Palomas Formation of the Santa Fe Group (Harley, 1934; Heyl et al. 1983; Lozinsky, 1986; Maxwell and Oatman, 1990; McGraw, 2003a, b, c). The piedmont deposits typically are incised, so that younger deposits are inset into them.

The thickness of the Santa Fe Group varies throughout the quadrangle (Table 4). In the Red Paint Canyon area, Quaternary(?) sediment is 6-12 m as determined by drilling of water wells (Appendix 2) and the exploration drilling by BE Resources, Inc. (Appendix 7; P and E Mining Consultants Inc., 2009). East of Cañada Alamosa, the Santa Fe Group is as much as 390 m thick, as determined from mapping and drilling of water wells (Appendix 2).

TABLE 4. Estimated thickness of Quaternary-Tertiary sedimentary units in Montoya Butte quadrangle (water well data in Appendix 2).

Location	Estimated thickness (m)	Source of sediment	Comments
Sim Yaten Canyon	198	San Mateo Mountains	Includes 82 m found in Sim Yaten water well
Post Canyon	213	San Mateo Mountains	Includes 27 m found in water well
Pine Canyon	198	San Mateo Mountains	
Arroyo west of Spring Canyon	73	San Mateo Mountains, volcanic rocks at Monticello Box and Red Paint Canyon	Turkey Springs Tuff exposed in the bottom of the arroyo
Spring Canyon (north of Ojo Caliente)	152	San Mateo Mountains, volcanic rocks at Monticello Box	Includes 27 m found in Spring Canyon water well
Hills west of Red Paint Canyon	6-12	Sierra Cuchillo	Includes 6 m found in Be exploration drill holes (Appendix 7)
Kelly Canyon	244	San Mateo Mountains	
San Mateo Canyon	219-262	San Mateo Mountains	Includes 18 m found in Eds water well
Cañada Alamosa (east of 74 ranch)	390	San Mateo Mountains, Sierra Cuchillo	Includes 91 m found at 74 water well
Cañada Alamosa (north of Sam Hill Canyon)	183	San Mateo Mountains, Sierra Cuchillo	From mapping, this report

The base of the Santa Fe Group in the Montoya Butte quadrangle is locally characterized by as much as 9 m of interbedded orange to brown to buff, well- to moderately-cemented, poorly-sorted, angular to subrounded conglomerates, sandstones, and siltstones composed of volcanic material (QTc). This basal unit is found in local

areas of the quadrangle (i.e., Spring Canyon, adjacent arroyos west of Ojo Caliente, and on top of the rhyolite flows exposed in the southern part of Cañada Alamosa and in San Mateo Canyons). In the southern Cañada Alamosa, San Mateo Canyon, and Spring Canyon (upstream of Ojo Caliente), these beds are overlain or interbedded with alkali, olivine basalt flows. Elsewhere, these beds are typically overlain by poorly-consolidated, poorly-sorted gravels, sandstones, siltstones, and thin clay beds of the Santa Fe Group. These beds could be correlative to the Jornada deposits or the lower Palomas Formation of Lozinsky (1986), because of their reddish color and their being older than the basalt flows.

Basalt flows (QTb)

Basalt and scoria flows are found interbedded with the Quaternary-Tertiary sediments of the Santa Fe Group along the southern Cañada Alamosa (lower box), San Mateo Canyon, and in Spring Canyon near the Spring Canyon well, north of Ojo Caliente. These basalt flows are up to 10 m thick, black to dark gray, fine grained, locally porphyritic, dense to vesicular, and exhibit local pillow-like structures (Fig. 18). Locally, the basalt flows overlie either a well-cemented, poorly sorted, orange-gray to brown conglomeratic sandstone (QTc) or the rhyolite of Alamosa Canyon (Tac), and the basalt flows are overlain by unconsolidated sediments of the Santa Fe Group (QTsf). The basalt consists of phenocrysts of plagioclase, pyroxene, and trace olivine (altered to iddingsite), magnetite, calcite, and iron oxides in a fine-grained groundmass.

Chemically, the basalt flows are alkaline, similar to the chemical composition of the basalts in the Elephant Butte, Hillsboro, and Winston areas (Fodor, 1975, 1978; Haag, 1991; Anthony et al., 1992; McMillan et al., 2000), and exhibit typical trace element signature of with-in plate basalts (Fig. 19). The basalt flows are similar in texture and composition to the basalt flow capping Tabletop Mountain, east of Winston, which is 4.8±0.1 Ma (Seager et al., 1984; Harrison, 1994). The basalt flows in the Chise area are as much as 100 m thick (Jahns et al., 2006). The ages of regional basalt flows are in Table 2. The similarity in lithology, texture, and chemical composition between the basalts in the Montoya Butte, Winston and Hillsboro areas, suggests a similar age of 2-6 Ma. These Quaternary basalts are a result of crustal thinning and upwelling asthenosphere in the Rio Grande rift (McMillan et al., 2000).

a)

b)

FIGURE 18. a) Pillow-like structures in the basalt flow near the Burma Road. b) Vesicular basalt in the southern Cañada Alamosa, overlying Quaternary sedimentary rocks and rhyolite of Alamosa Canyon.

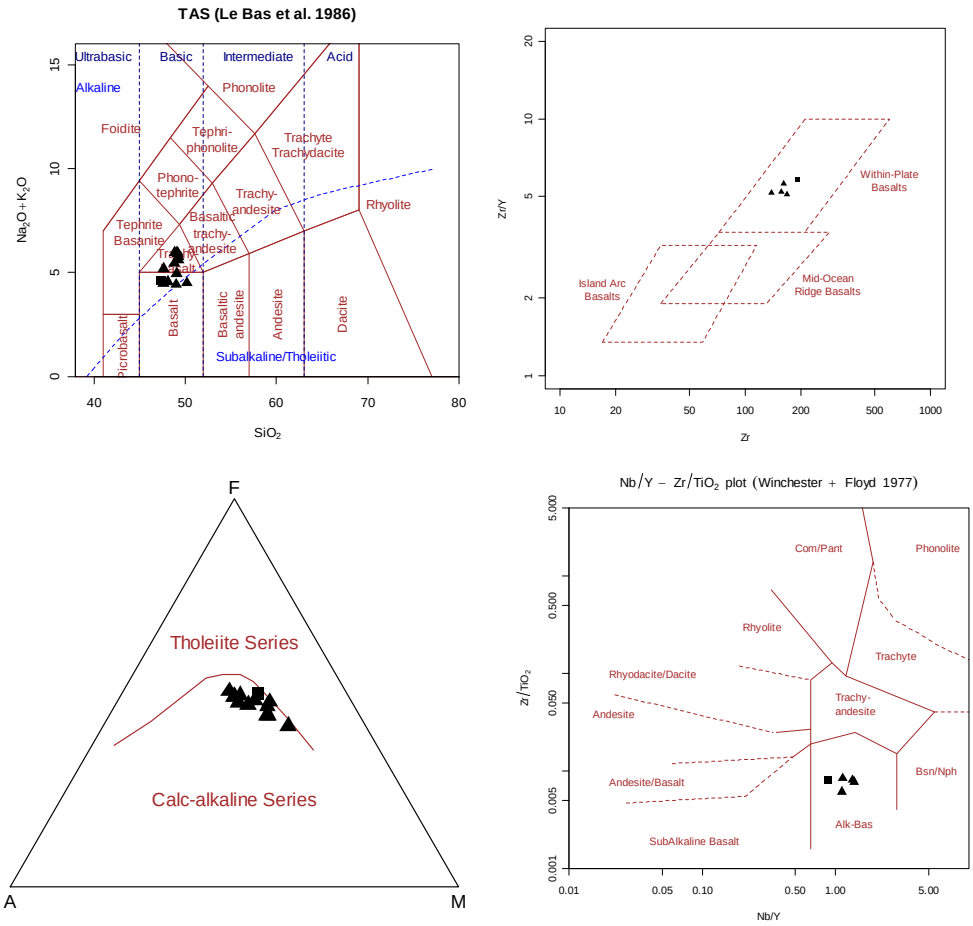

FIGURE 19. Various plots of whole-rock chemical analyses of 2-6 Ma alkaline basalts from Montoya Butte (this report, black squares) and other localities (black triangles), including Hillsboro (Fodor, 1978; McMillan et al., 2000), Mimbres (Fodor, 1978), and Winston (McMillan et al., 2000), showing the similar chemical composition of the basalts. Chemical analyses are in Appendix 3 (Table 3-2 and 3-3).

Quaternary terrace and pediment deposits (Qp, Qt, Qts, Qtv, Qtm)

Pediment deposits occur as alluvial fan deposits flanking the San Mateo Mountains and, to a lesser extent, Sierra Cuchillo range and typically are mapped as Santa Fe Group sediments (QTsf), as previously described. This old surface is called the Burma pediment, named after the Burma Road, which is constructed on the surface. Lozinsky (1986) was able to map three levels of pediment deposits in the Mud Springs Mountains. However, only one level of pediment deposits was mapped in the Montoya Butte quadrangle (Fig. 10; McLemore, 2011), which could be older than the pediment surfaces mapped by Lozinsky (1986), because the Burma pediment is higher in elevation and the San Mateo Mountains are older than the Mud Spring Mountains. Lozinsky (1986) found only one pediment level in the Caballo Mountains. The Burma pediment in the Montoya Butte quadrangle grades into the oldest terrace deposits (Qt, Qts), and is mapped as QTsf. Locally in the Montoya Butte quadrangle, thin veneers of poorly

consolidated, poorly-sorted, gravel and sand form younger pediments and are mapped separately as Qp.

At least four levels of stream terraces deposits flank Cañada Alamosa south of Kelly Canyon (Qtm, Qtv, Qts, Qt). The terraces were named for local geographic sites. The youngest terrace above the Cañada Alamosa was named for the Montoya site, Montoya terrace (Qtm), which could be correlative to the fifth terrace level, Qt5, as mapped by Heyl et al. (1983), Lozinsky (1986), and Maxwell and Oatman (1990). The next terrace above the Montoya terrace is the Victorio terrace, Qtv, named after the Victorio site. The third terrace above Cañada Alamosa is the San Mateo terrace, Qts, named after San Mateo Canyon. The older terraces are difficult to correlate and are not differentiated and designated Qt. The terraces are well developed along Cañada Alamosa, San Mateo Canyon, and Kelly Canyon; terraces also are found along Cañada Alamosa west of the Monticello Box, but are difficult to correlate to the other terraces and are designated Qt. Near the junction of San Mateo Canyon with Cañada Alamosa, the Montoya terrace is developed on top of the rhyolite of Alamosa Canyon (Fig. 10; McLemore, 2011).

The ancestral Alamosa Creek cut into the Santa Fe Group sediments (QTsf) and the terraces are depositional. A diagrammatic cross section showing the stratigraphic relationships of the Quaternary units is in Figure 20 and a photograph in Figure 21. Terrace deposits consist of thin (3-8 m thick), consolidated to unconsolidated, poorly- to moderately-sorted, veneers of gravel and sand with silt lenses derived from the San Mateo Mountains and Sierra Cuchillo. Gravel consists of rounded to subangular boulders, cobbles, and smaller rock fragments of rhyolite and andesite. Similar terraces were developed in the Cuchillo Negro Creek (Heyl et al., 1983; Lozinsky, 1986; Maxwell and Oatman, 1990).

Absolute ages of the terraces is unknown because no organic material has been dated, but the ages of the terraces can be estimated based upon regional correlations with height above the active stream levels and soil development (Hawley and Kottlowski, 1969; Lozinsky, 1986; Pazzaglia and Hawley, 2004). The highest or oldest terraces are developed within the Santa Fe Group sediments, designated as QTsf and Qt, and could be Pleistocene in age (Heyl et al., 1983; Lozinsky, 1986; Maxwell and Oatman, 1990; Pazzaglia and Hawley, 2004).

Incision of the next level of terraces, San Mateo and Victorio terraces (Qtv, Qts) occurred during periods of increased stream flow, possibly during the Pleistocene (Hunt, 1978; Maxwell and Oatman, 1990). The youngest Montoya terrace (Qtm) was developed above the level of the active stream during periods of increased stream flow, probably during the Holocene or earliest Pleistocene (Heyl et al., 1983; Lozinsky, 1986; Maxwell and Oatman, 1990; Pazzaglia and Hawley, 2004).

Formation of these terraces reflects changes in basin hydrology, sediment yield, and/or basin wide tectonics when the streams slowed or ceased its incision, widen its valley bottom, and deposited sediment. Renewed stream flow, possibly related to melting of alpine glaciers, cut into the older deposits and then formed new deposits inset into the older deposits above the newly established floodplain (Pazzaglia and Hawley, 2004). Table 5 shows the terrace levels and compares the terraces in the Montoya Butte quadrangle with those in the Cuchillo Negro and Rio Grande (Lozinsky, 1986).

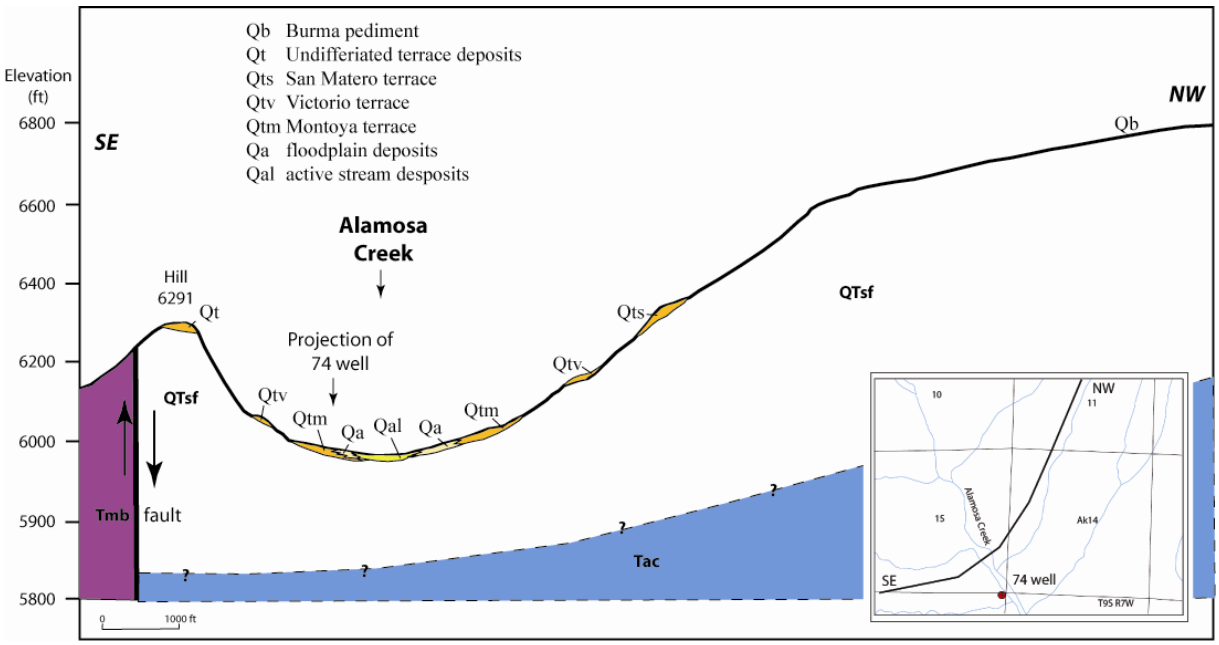

FIGURE 20. Diagrammatic cross section showing the stratigraphic relationships of the Quaternary units along Cañada Alamosa.

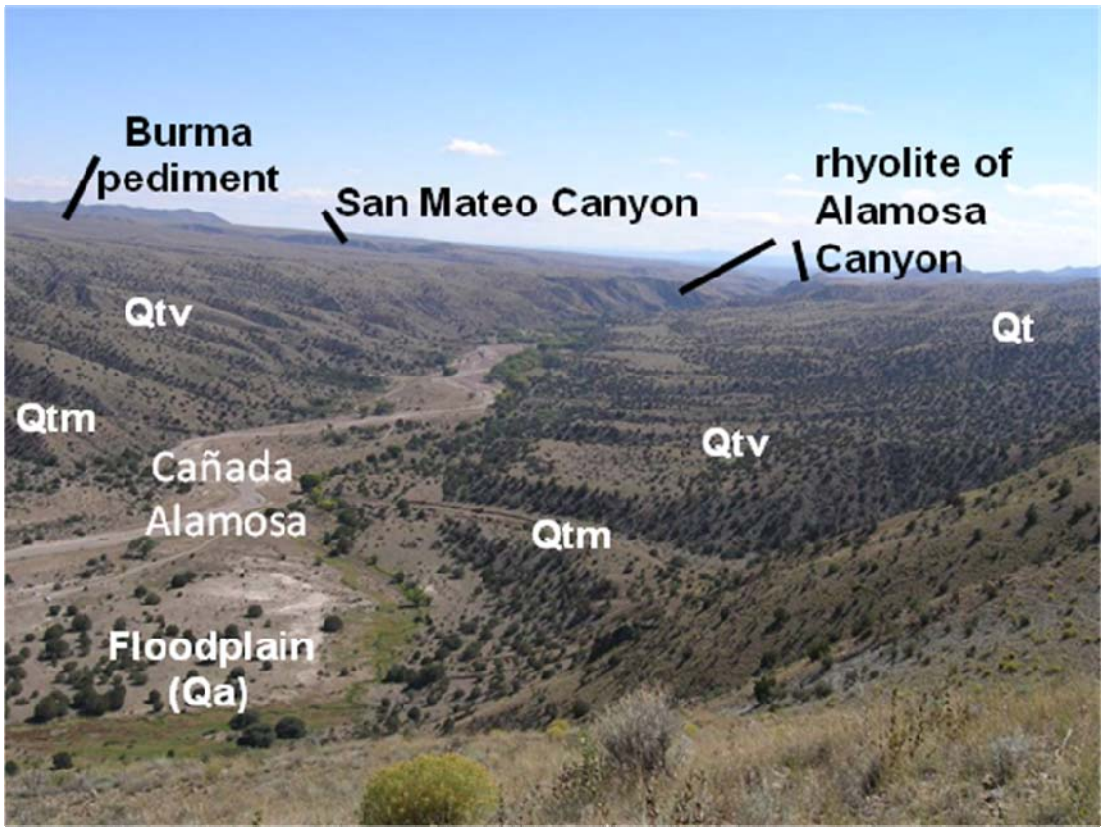

FIGURE 21. Terraces along Cañada Alamosa, looking south from Montoya Butte.

TABLE 5. Terrace-level data for Rio Grande, Cuchillo Negro, Alamosa, Kelley, and San Mateo Creeks. Possible correlation to Hawley and Kottlowski (1969) and Lozinsky (1986), and is based upon regional correlations of height above the active stream levels and soil development, and could change if dateable material is found. Qt is older than the basalt flows, which are believed to be 2-4 Ma.

Terrace in Montoya Butte quad.	Height (m) above floodplain Rio Grande and Cuchillo Negro (Lozinsky, 1986)	Height (m) above floodplain Cañada Alamosa	Height (m) above floodplain San Mateo and Kelly Canyons	Possible correlation to Hawley and Kottlowski (1969)	Type
Montoya Qtm	Qt5—6-12	3-15	3-15	Leasburg	strath
Victorio Qtv	Qt4—18-24	10-30	15-30	Picacho	strath
San Mateo	Qt3—24-30	15-45	20-50	Picacho	strath
Qt2	Qt2—30-36	30-55			strath
Burma pediment		35-60	35-60		pediment

The ancestral Alamosa Creek subsequently cut into these units to form the current active drainage. Basalt flows on top of the basal Santa Fe Group and rhyolite of Alamosa Canyon in the southern portion of Cañada Alamosa in the vicinity of San Mateo Canyon are found on both sides of the canyon and suggests that the river cut into the flows after their deposition, presumably ~2-4 Ma. Thus the river cut through the rhyolite of Alamosa Canyon over the last 2-4 million years. The San Mateo terrace, Qts, is at the same approximate elevation as the basalt flow in the southern part of Cañada Alamosa, suggesting that the lower, younger Montoya and Victorio terraces (Qtm, Qtv) were formed after eruption of the basalt.

Quaternary alluvium (Qal), floodplain (Qa), and colluvium (Qc deposits)

Colluvium deposits (Qc), including minor landslide deposits, are found in local areas of the Montoya Butte quadrangle where thin veneers of unconsolidated gravel, sand, and silt cover the volcanic bedrock. Floodplain deposits (Qa) consist of unconsolidated, moderately sorted, fine- to coarse-grained sand, silt, and clay, are several meters thick, and are cut by the active streams (Qal). The youngest deposits in the area are unconsolidated alluvium deposited by the active streams (Qal), which are found in the active arroyos and stream channels and consist of volcanic rocks, predominantly rhyolite and granite. The larger streams meander and cut as much as 600 m into the older Quaternary-Tertiary sediments (mainly QTsf); Alamosa Creek is the only stream that flows all year. The smaller streams are ephemeral and cut into volcanic bedrock or in broad valleys cut into the older Quaternary-Tertiary sediments (QTsf).

Intrusive rocks

Granite to quartz monzonite (Tgr)

Brown to gray, fine- to medium-grained monzonite to quartz monzonite plugs intruded the latite of Montoya Butte near the Taylor mine in section 8, T9S, R7W and intruded the andesite of Monticello Box in section 20, T9S, R7W. The plugs are circular, 55 m in diameter, and form the cap of two hills south of Monticello Box (McLemore,

2011). The monzonite consists of quartz (20-30%), plagioclase (20-30%), K-feldspar (40-50%), and trace amounts of magnetite, apatite, and biotite (Fig. 22). Although, this monzonite is similar in major-element chemistry to the Vicks Peak Tuff, rhyolite of Alamosa Canyon, and granite of Kelly Canyon, this monzonite is similar in trace element chemistry to the Sierra Cuchillo laccolith and Reilly Peak rhyolite, and chemically distinct in trace element composition from the Vicks Peak Tuff, rhyolite of Alamosa Canyon, and granite of Kelly Canyon (Fig. 23). Thus, the monzonite is probably older than the Vicks Peak Tuff, rhyolite of Alamosa Canyon, and granite of Kelly Canyon and probably related to the Sierra Cuchillo laccolith and Reilly Peak rhyolite.

FIGURE 22. Close-up of monzonite plug near the Taylor mine.

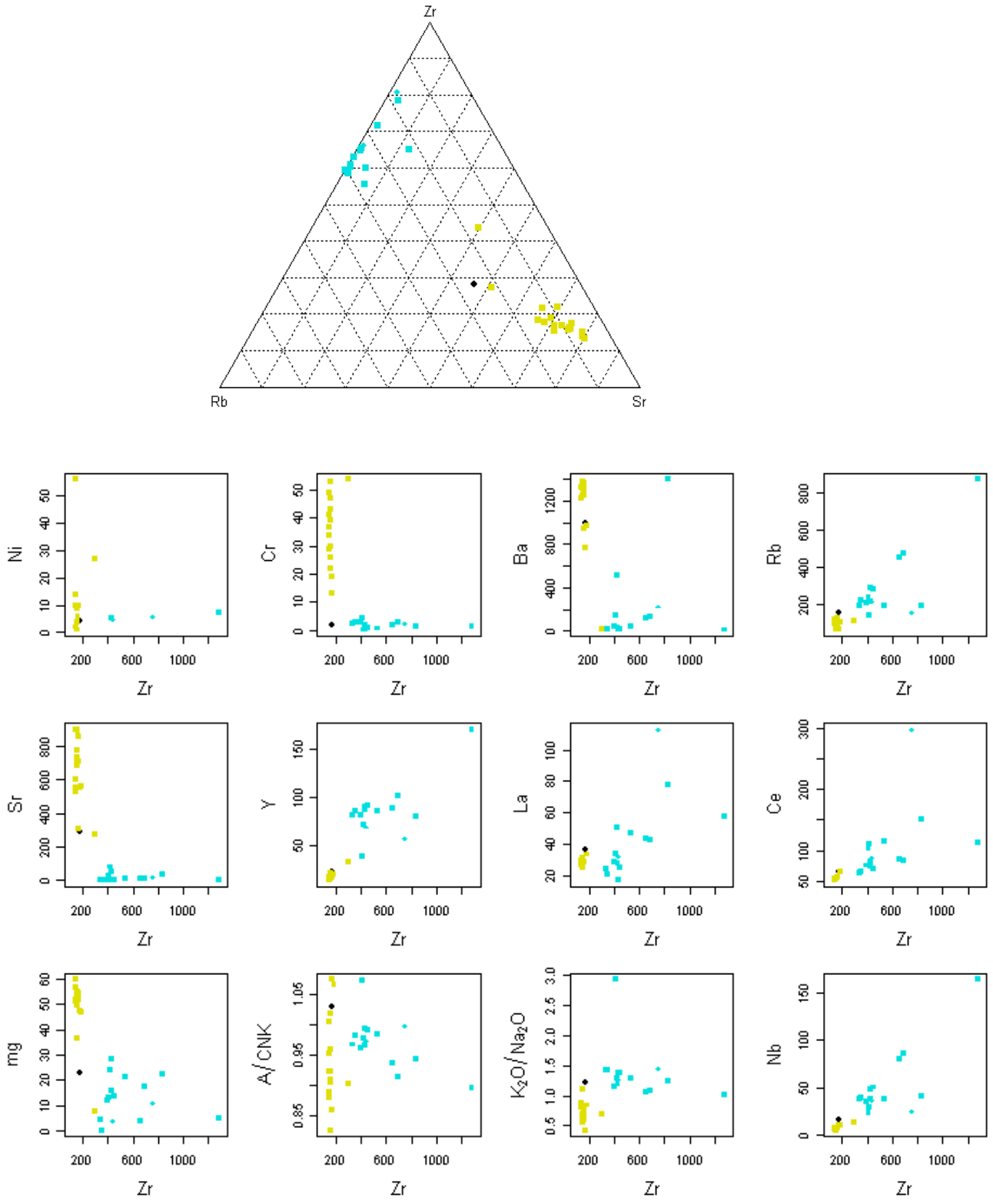

FIGURE 23. Chemical plots of Montoya Butte samples: monzonite (black circle), Vicks Peak Tuff/rhyolite of Alamosa Canyon (blue squares), granite of Kelly Canyon (blue

diamonds), and Sierra Cuchillo monzonite-granite laccolith and Reilly Peak rhyolite (yellow squares). Chemical analyses are in Appendix 3 and are from this report, Robertson (1986), Davis (1986a), and Michelfelder (2009). Trace elements are in ppm and major elements are in percent.

Latite/quartz latite dikes (Tql)

Green gray to brown gray, porphyritic to phaneritic latite to quartz latite dikes intrude the andesite of Monticello Box, lahar, and latite of Montoya Butte, and consist of 5-10% phenocrysts of albite (some Carlsbad twins), biotite, and quartz. Xenoliths of andesite are common. Some of these dikes have similar mineralogy and chemistry as the latite of Montoya Butte and could be feeder dikes for the latite of Montoya Butte flows. Most dikes are only 1-2 m thick and a few meters long. One prominent dike is 20 m wide and nearly 6000 m long, extending from just north of Cañada Alamosa southwards into section 4. This dike has a fine-grained chilled margin, nearly 50 cm wide. The latite/quartz latite dikes are believed to be older than the Vicks Peak Tuff, rhyolite of Alamosa Canyon, and granite of Kelly Canyon, because the dikes do not intrude the Vicks Peak Tuff, rhyolite of Alamosa Canyon, and granite of Kelly Canyon and are chemically distinct from these younger rhyolites (see Petrochemistry section below).

Andesite to basalt dikes (Tbd)

Fine-grained to aphanitic mafic dikes, up to 1-2 m wide, intrude the andesite of Monticello Canyon, lahar, and latite of Montoya Butte. The andesite dikes are fine grained to aphanitic to locally porphyritic, dense to locally amygdaloidal, black to dark to greenish gray to reddish brown and consist of plagioclase, pyroxene, biotite, and hornblende in a fine-grained groundmass. Many are altered, form saddles in between hill tops, and the groundmass consists of calcite, chlorite, and locally epidote. These dikes are believed to be older than the Vicks Peak Tuff, rhyolite of Alamosa Canyon, and granite of Kelly Canyon, because the dikes do not intrude the Vicks Peak Tuff, rhyolite of Alamosa Canyon, and granite of Kelly Canyon and are chemically distinct from these younger rhyolites (see Petrochemistry section below).

Rhyolite dikes (Tr)

Rhyolite dikes, up to 1-2 m wide, intruded the latite of Montoya Butte in the Montoya Butte area and in the southwestern portion of the quadrangle, where they intruded the Permian sedimentary rocks. The rhyolite dikes are pink to reddish-brown, fine-grained to porphyritic, and consist of plagioclase, sanidine, and quartz in a fine-grained matrix. These dikes are likely related to the porphyritic rhyolite and rhyolite aplite intrusions found throughout the Sierra Cuchillo.

Granite of Kelly Canyon (Til)

Several irregular to elongated stocks of pink to gray granite intruded the Vicks Peak Tuff in Kelly and San Mateo Canyons. Lynch (2003) and Ferguson et al. (2007) called these stocks granite porphyry stocks and in this report they are called granite of Kelly Canyon (Til). The granite is holocrystalline to porphyritic and consists of K-feldspar (2-15 mm, 25-35%) in a finer-grained groundmass of sanidine (20-30%), quartz (20-30%), plagioclase (20-30%), and trace biotite and magnetite (Fig. 24). The chemical

composition of the granite of Kelly Canyon is nearly identical to the chemical composition of the Vicks Peak Tuff and rhyolite of Alamosa Canyon (Fig. 23, Appendix 3). Lynch (2003) determined that the age of the granite of Kelly Canyon is 28.3 Ma ($^{40}Ar/^{39}Ar$ dating), which is indistinguishable from the age of the Vicks Peak Tuff.

FIGURE 24. Granite of Kelly Canyon, in Kelly Canyon.

PETROCHEMISTRY

Samples of various volcanic, volcaniclastic, intrusion, altered, and mineralized rocks and soils from throughout the Montoya Butte quadrangle and adjacent areas were analyzed for major and trace elements in order to classify and chemically characterize the igneous rocks, compare the geochemical composition of the igneous rocks from the Montoya Butte quadrangle to other igneous rocks in central New Mexico, aid in determining the mineral resource potential, and aid in determine the source of archeological artifacts. Geochemical and locational data of samples, including selected published data, are in Appendix 3. Additional chemical analyses of rhyolites and granites are in references cited and available upon request.

Geochemistry is utilized in classifying and characterizing volcanic rocks. The TAS (total alkali-silica; Le Bas et al., 1986) diagram is widely used in classifying volcanic rocks by lithology (Fig. 19; Appendix 3). Winchester and Floyd (1977) developed a lithologic classification scheme on the basis of Zr/TiO_2 and Nb/Y, because these elements are typically immobile during alteration. A similar lithologic classification plot is the popular R1-R2 classification scheme by De La Roche (1980). Most samples in the Montoya Butte quadrangle plot in or near their respective lithologic fields (Fig. 25, Appendix 3); i.e., rhyolites plot in the rhyolite or rhyodacite field and andesites plot in the andesite or rhyodacite/dacite field. Vicks Peak Tuff, granite of Kelly Canyon, and

rhyolite of Alamosa Canyon have similar chemical compositions, suggesting a similar source, which is consistent with the similar age (Appendix 3; Lynch, 2003). Geochemical element plots indicate that the andesites are more altered than the rhyolites or ash-flow tuffs, as observed in the field (Appendix 3).

The samples from the Montoya Butte quadrangle are predominantly peraluminous (i.e., $Al_3O_5/(CaO + K_2O + Na_2O) > 1.0$) to metaluminous (i.e., $Al_3O_5/(CaO + K_2O + Na_2O) < 1.0$), high-Si (silica-saturated), high-K basaltic andesite to rhyolite (Fig. 25; Appendix 3). Most of the samples are calc-alkalic and alkali-calcic (i.e., subalkaline) and form trends typical of calc-alkaline igneous rocks, according to the definition of Irvine and Baragar (1971) and Frost et al. (2001). Some andesites plot in the alkaline field, probably due to regional low-grade hydrothermal alteration. Some Vicks Peak Tuff and rhyolite of Alamosa Canyon are slightly peralkaline (Fig. 25). Most of the rocks are classified as A-type granites (Whalen et al., 1987).

The samples from the Montoya Butte quadrangle are grossly similar in chemical composition to similar lithologies elsewhere in the Mogollon-Datil volcanic field (Appendix 3; Bornhorst, 1980, 1986, 1988; Davis and Hawkesworth, 1995; Davis 1986a, b; McMillan et al., 2000; Michelfelder, 2009). The older rocks in Sierra Cuchillo (30-40 Ma, andesite of Monticello Canyon, latite of Montoya Butte, dikes and granite intrusion) have different trace chemical compositions than the younger rhyolites (20-30 Ma, Turkey Spring Tuff, tuff of Alum Mountain, Vicks Peak Tuff, rhyolite of Alamosa Canyon, and granite of Kelly Canyon) (Fig. 25; Appendix 30), which also is consistent with the variation in age of emplacement. The older Sierra Cuchillo rocks have higher Nb and Y and lower Zr and Sr concentrations than the younger rhyolites (Fig. 25; Appendix 3). Similar differences in geochemical composition between the older (30-40 Ma) and younger (20-30 Ma) volcanic rocks in the Sierra Cuchillo were observed by Robertson (1986), Davis (1986a, b), McMillan et al. (2000), Michelfelder (2009), and Michelfelder and McMillan (2009) and in the northern Black Range by Harrison (1992).

Rhyolites from the Montoya Butte quadrangle are grossly similar in major chemistry as rhyolites/granites associated with beryllium deposits in Spor Mountain (Utah), Victorio (Luna County, New Mexico), Aguachile (Mexico), Sierra Blanca (Texas), and Cornudas Mountains (Otero County, New Mexico), but exhibit different trace element chemical compositions (see chemical plots in Appendix 3; McLemore, 2010b, c). All of these rhyolites/granites associated with beryllium deposits are predominantly peraluminous (i.e., $Al_3O_5/(CaO + K_2O + Na_2O) > 1.0$) to metaluminous (i.e., $Al_3O_5/(CaO + K_2O + Na_2O) < 1.0$), high-K, high-Si (silica-saturated) rhyolite. They are A-type granites found within-plate granite fields of Pearce et al. (1986). Most of the samples are calc-alkalic and alkali-calcic (i.e., subalkaline) and form trends typical of calc-alkaline igneous rocks, according to the definition of Irvine and Baragar (1971) and Frost et al. (2001).

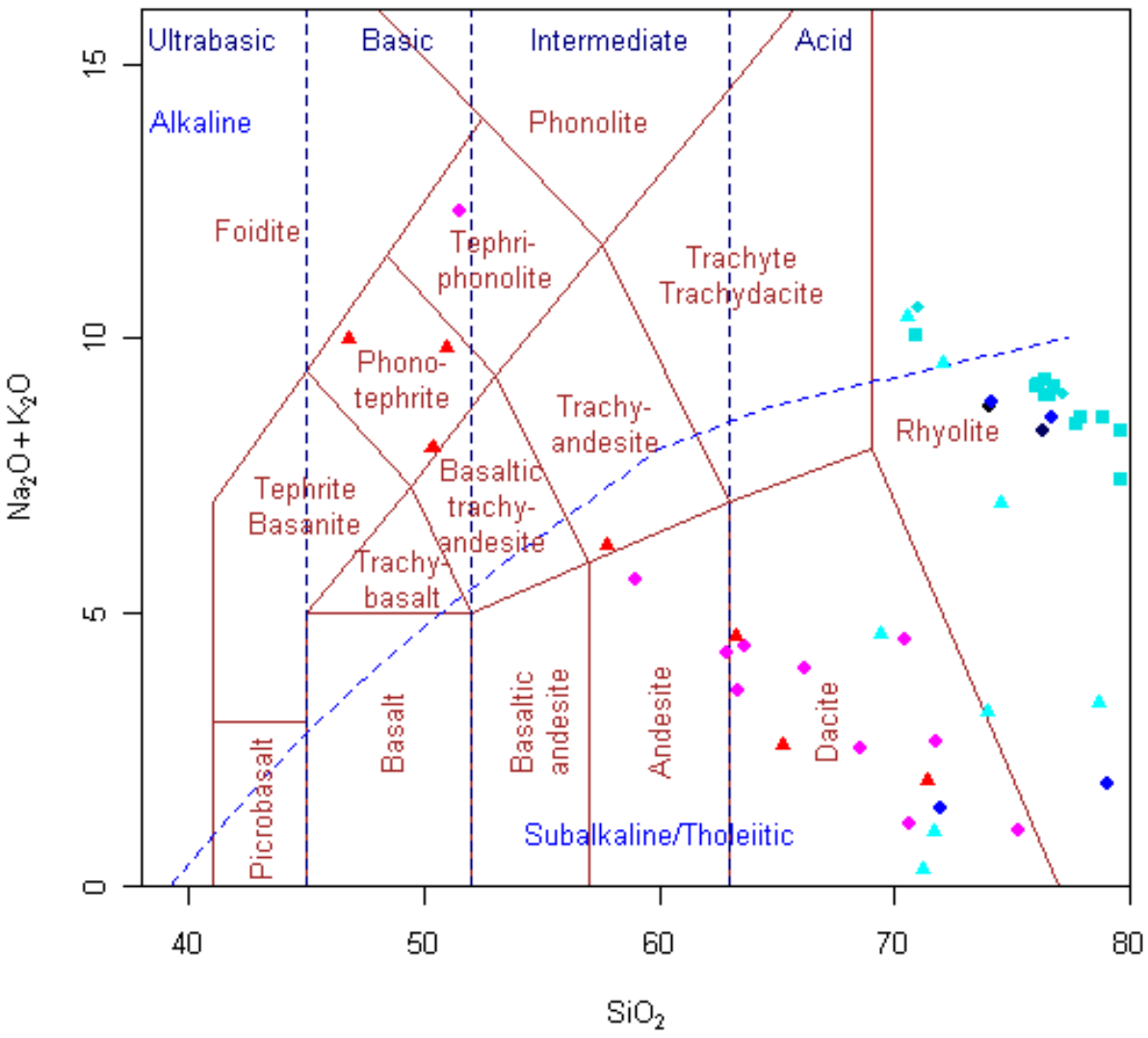

(a) TAS diagram (Le Bas et al., 1986) showing the classification of the samples from Montoya Butte quadrangle as predominantly subalkaline to alkaline rhyolites and subalkaline andesites and dacites. TAS is Total alkali (NaO_2+K_2O) verses SiO_2. Samples in the phonoterphrite field are altered. Symbols are explained in caption below.

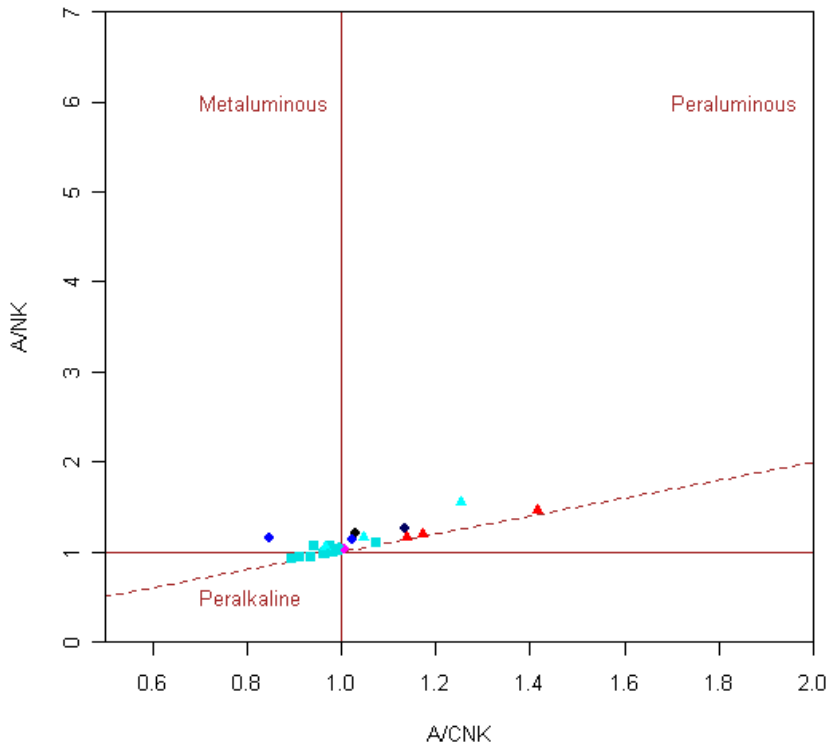

(b) A/CNK-ANK diagram (Shand, 1943) showing the classification of the samples from Montoya Butte quadrangle as predominantly metaluminous to peraluminous with some peralkaline rhyolites. A/CNK (Al_2O_3/(CaO+Na_2O+K_2O) verses ANK (Al_2O_3+Na_2O+K_2O) (Shand, 1943). Symbols are explained in caption below.

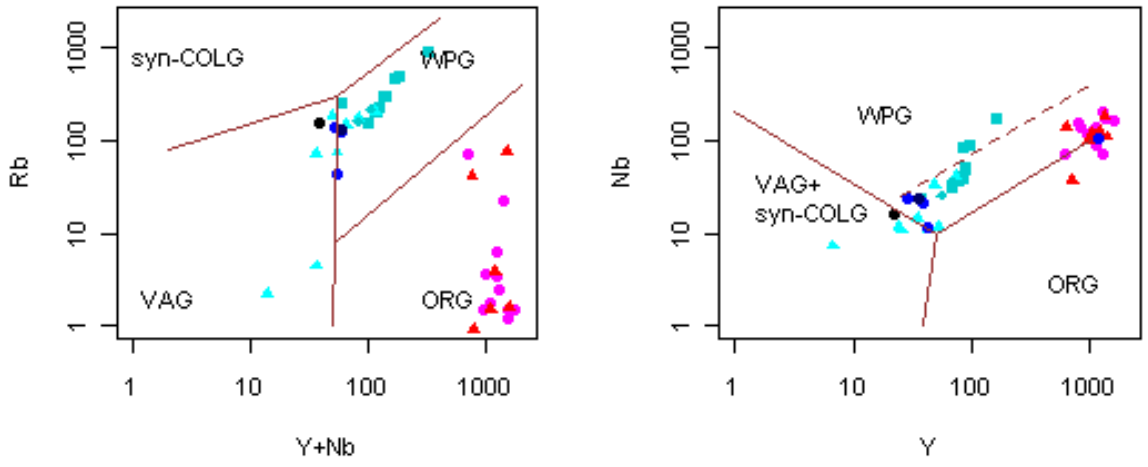

(c) Pearce et al. (1984) tectonic diagrams, showing the samples from the Montoya Butte quadrangle are similar to within plate granitic granites (San Mateo younger rhyolites) and orogenic granites (older Sierra Cuchillo rocks). Syn-COLG—syn-collusion, VAG—volcanic arc, ORG—orogenic, WPG—within plate granitic fields. Symbols are explained in caption below.

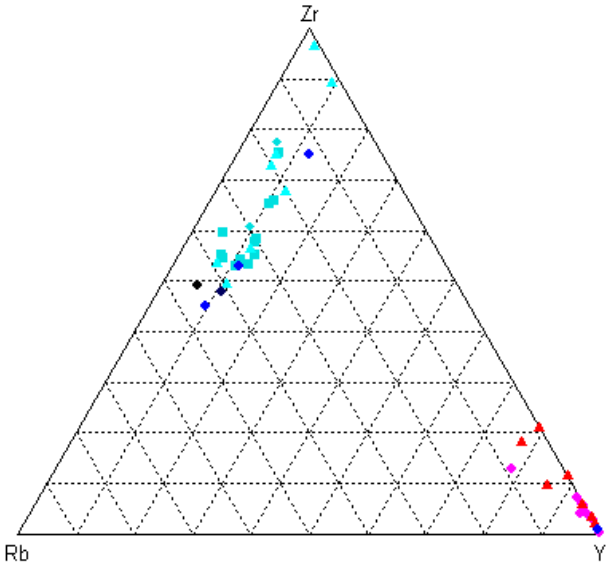

(d) Rb-Zr-Y plot showing the variation in the older Sierra Cuchillo rocks (andesite of Monticello Canyon, latite of Montoya Butte, dikes and granite intrusion) and the younger rhyolites (Turkey Spring Tuff, tuff of Alum Mountain, Vicks Peak Tuff, rhyolite of Alamosa Canyon, and granite of Kelly Canyon) in the Montoya Butte quadrangle. Symbols are explained in caption below.

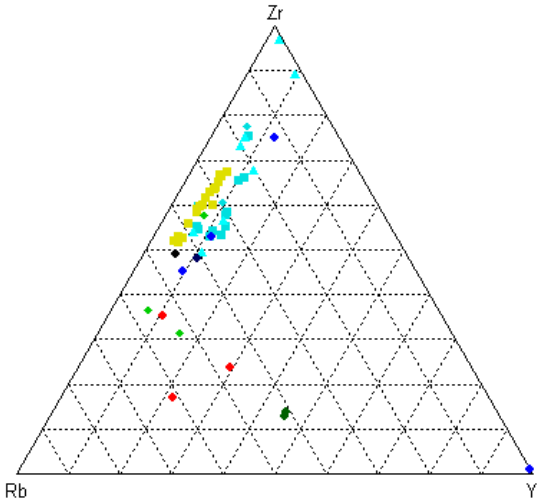

(e) Rb-Zr-Y plot showing the variation in the older Cuchillo laccolith (yellow squares), younger rhyolites in the central and southern Sierra Cuchillo (aplite is red triangles, Iron Mountain rhyolite is dark green diamond, porphyritic rhyolite is light green triangle), and the younger rhyolites in the Montoya Butte quadrangle (Turkey Spring Tuff, tuff of Alum Mountain, Vicks Peak Tuff, rhyolite of Alamosa Canyon, and granite of Kelly Canyon, symbols are explained below). Chemical analyses are by Deal (1973), McMillan (1979), Correa (1980, 1981), Robertson (1986), Davis (1986a, b), Davis and Hawkesworth (1995), Michelfelder (2009), and this report. Symbols are explained in caption below.

FIGURE 25. Selected geochemical plots of igneous rocks from the Montoya Butte quadrangle and adjacent areas. Additional geochemical plots are in Appendix 3. Tuff of Alum Spring (Tas) is blue diamonds. Turkey Springs Tuff (Tt) is dark blue circles. Vicks Peak Tuff (Tvp) and rhyolite of Alamosa Canyon (Tac) are blue squares. Granite of Kelly Canyon (Til) is blue diamond. Andesite dikes and andesite of Monticello Canyon (Tmb) are red triangles. Latite/quartz latite dikes and latite of Montoya Butte (Tql, Tl, Tpl) are pink circles. Granite intrusion (Tg) is black circle. Rhyolite dikes are dark blue diamonds. Chemical analyses are in Appendix 3, except for samples shown in Figure 23-e, which are cited in the caption. Trace elements are in ppm and major elements are in percent.

STRUCTURE

Local structure

The San Mateo Mountains and Sierra Cuchillo form north-trending mountain ranges separated by the Monticello graben (Fig. 26). The predominant structures in these mountains are the Nogal Canyon caldera and Basin and Range faulting (Fig. 26). The volcanic rocks throughout the Montoya Butte quadrangle have been tilted generally westward or, rarely, eastward by Basin and Range faulting. Rose diagrams of strikes of foliations of Monticello Box, latite of Montoya Butte, Vicks Peak Tuff/rhyolite of Alamosa Canyon, and Turkey Springs Tuff are in Figure 27 (measurements are in Appendix 4).

Faults

Numerous normal faults cut the volcanic rocks in the quadrangle; most of them have vertical to steep dips and trend north-northeast (Fig. 28). Faults typically are brecciated, silicified, and exhibit local gouge zones of clay, calcite, and quartz. Fractures and joints locally parallel the fault traces. Many canyons and drainages are offset by or follow faults (Fig. 26). Some, but not all dikes, follow faults; whereas most veins follow faults or dikes (Fig. 28). The dikes and veins have variable directions (Fig. 28). The difference in orientations between the dikes and faults suggest that they represent two separate periods of deformation; the dikes are older than the north-south trending faults.

Red Paint Canyon fault zone

The Red Paint Canyon fault zone south of Monticello Box consists of several subparallel north-south-trending faults and fractures (Fig. 26). North of Ojo Caliente, the fault splays into a complex fault system. Several field observations and other evidence indicate that the Red Paint Canyon fault zone is a major fault system:

- This fault zone consist of three or more subparallel faults that have offset the Turkey Springs Tuff, Quaternary sedimentary rocks, and the rhyolite in the drill holes at the Apache Warm Springs beryllium deposit (Fig. 29, 30, 31; Meeves, 1966; see Appendix 7).
- This fault zone resulted in the uplift of the andesite of Monticello Box against rhyolite tuffs and Quaternary sedimentary rocks, which formed the Monticello Box (Fig. 29, 30, 31).
- A portion of the fault at the mouth of Monticello Box is altered similar to rocks found in Red Paint Canyon, suggesting altering fluids moved along the fault zone (Fig. 29).

- Brecciation, typical of fault zones, is common in the andesite and rhyolite along the fault zone at Monticello Box.
- Red, white, and gray banded, advanced argillic-altered rock fragments are found within exposed, unaltered sediments of the Santa Fe Group in drainages north and south of Cañada Alamosa. The presence of these rock fragments indicate the alteration was larger in extent than that exposed today and was subsequently eroded.
- Drilling in Red Paint Canyon strongly suggests complex fracturing and faulting (Meeves, 1966).
- A Quaternary basalt flow is truncated by a north-south fault near Spring Canyon well, north of Ojo Caliente spring (Fig. 31).

The major Red Paint Canyon fault zone continues northward from Red Paint Canyon where it is offset by a northeast-trending fault near Monticello Box. A portion of the Red Paint Canyon fault at the mouth of Monticello Box is altered similar to Red Paint Canyon. The Spring Canyon windmill is along the northern extension of the north-trending Red Paint Canyon fault zone. Alum Spring, south of the beryllium deposit, is in altered rhyolite within the southern Red Paint Canyon fault zone. Ojo Caliente (elevation 6230 ft), Willow Springs (elevation 6200 ft), and other warm springs west of the Ojo Caliente spring (Fig. 4) are along or near subparallel, north-south-trending faults that form the Red Paint Canyon fault zone, although these springs are not necessarily along specific faults. Alum Spring is along this same fault zone in altered rhyolite tuff (Tas). The Red Paint Canyon fault displaces a Quaternary basalt flow, east of the Spring Canyon well and indicates movement along the fault during Quaternary times. Outcrops in drainages north of Cañada Alamosa include a small exposure of rhyolite, and sandstones and conglomerates of the Santa Fe Group. Sediments of the Santa Fe Group also are faulted (Fig. 30).

Cañada Alamosa fault

The north-trending straight portion of Cañada Alamosa in the middle of the Montoya Butte quadrangle is the result of a north-trending fault exposed in the Cañada Alamosa (Fig. 7, 32). Cañada Alamosa curves near the junction with San Mateo Canyon, where the rhyolite of Cañada Alamosa is exposed (Figs.7; 10; McLemore, 2011). Part of the Cañada Alamosa fault could turn northwest and be concealed beneath the rhyolite of Alamosa Canyon. Several field observations and other evidence indicate that the Cañada Alamosa fault zone is another major fault system:

- Abundant slickenslides and brecciation along the fault.
- Acid-sulfate alteration along the fault in Christmas Canyon and elsewhere (Fig. 10; McLemore, 2011).
- Separates latite of Montoya Butte from Quaternary sediments.
- Thick lavas of the rhyolite of Alamosa Canyon are found along this fault, specifically forming the lower box in the southern portion of the quadrangle and north of Kelly Canyon in the north-central portion of the quadrangle.
- Cañada Alamosa bends at the northern portion of the fault (north of Kelly Canyon) and flows along it, until it reaches the north-south trend of the fault until the lower box.

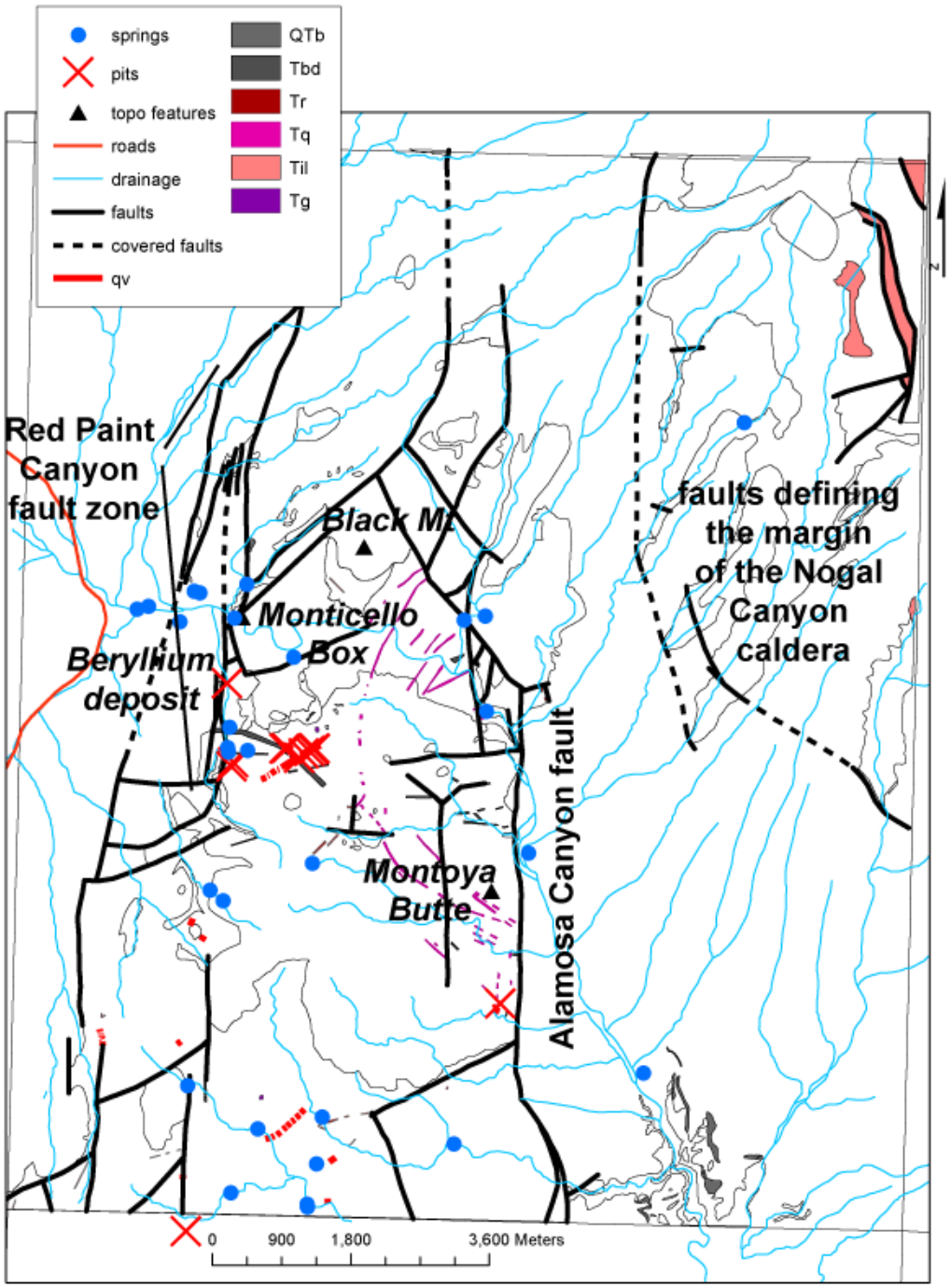

FIGURE 26. Structure map of Montoya Butte quadrangle. Blue circles are springs, red lines are veins, gray lines are basalt dikes and flows, black lines are faults and X are prospect pits. Light gray lines are outlines of geologic units shown in Figure 10.

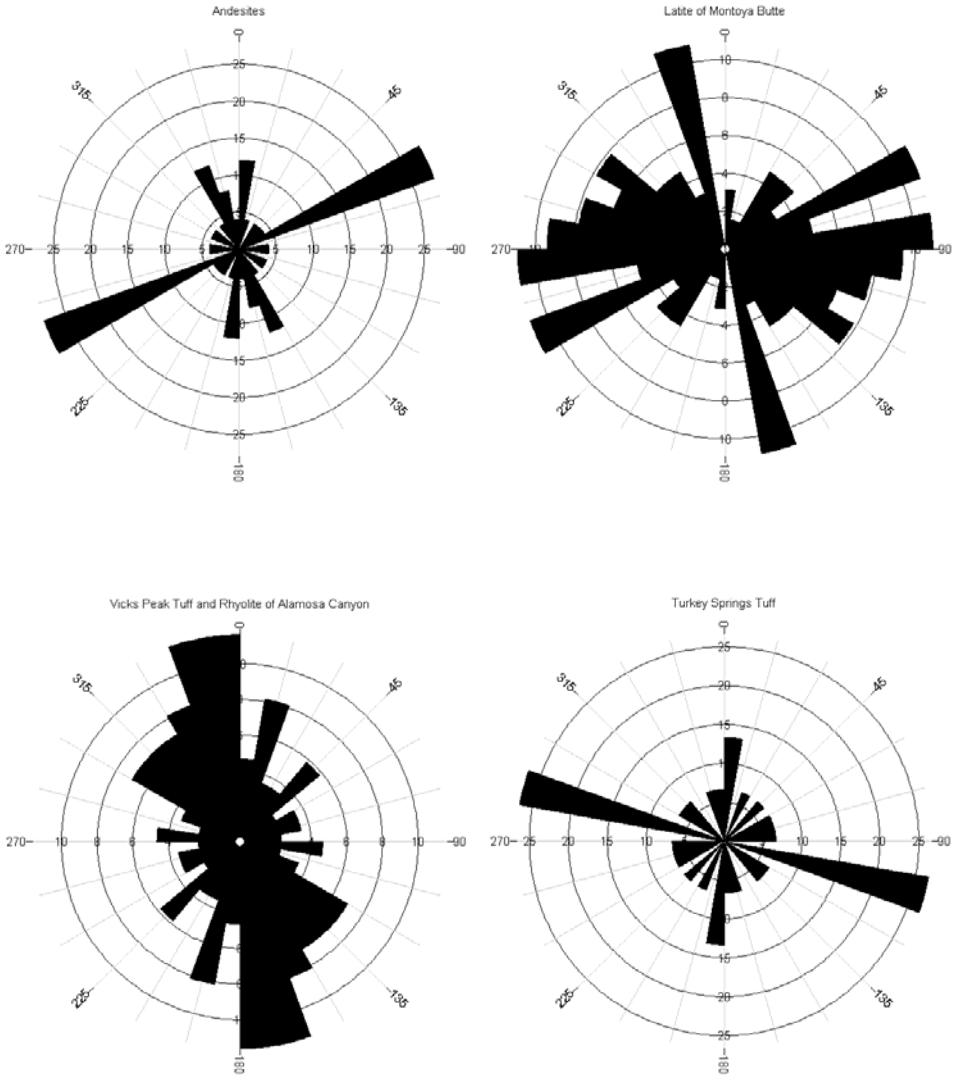

FIGURE 27. Rose diagram showing strike of foliations of andesite of Monticello Box, latite of Montoya Butte, Vicks Peak Tuff/Rhyolite of Alamosa Canyon, and Turkey Springs Tuff. Measurements are in Appendix 4. Note the foliation of the andesite trends northeast; the foliation of the latite trends north-northwest and east-northeast, the foliation of the Vicks Peak Tuff and rhyolite of Alamosa Canyon trends north-northeast, and the Turkey Springs Tuff trends east-southeast.

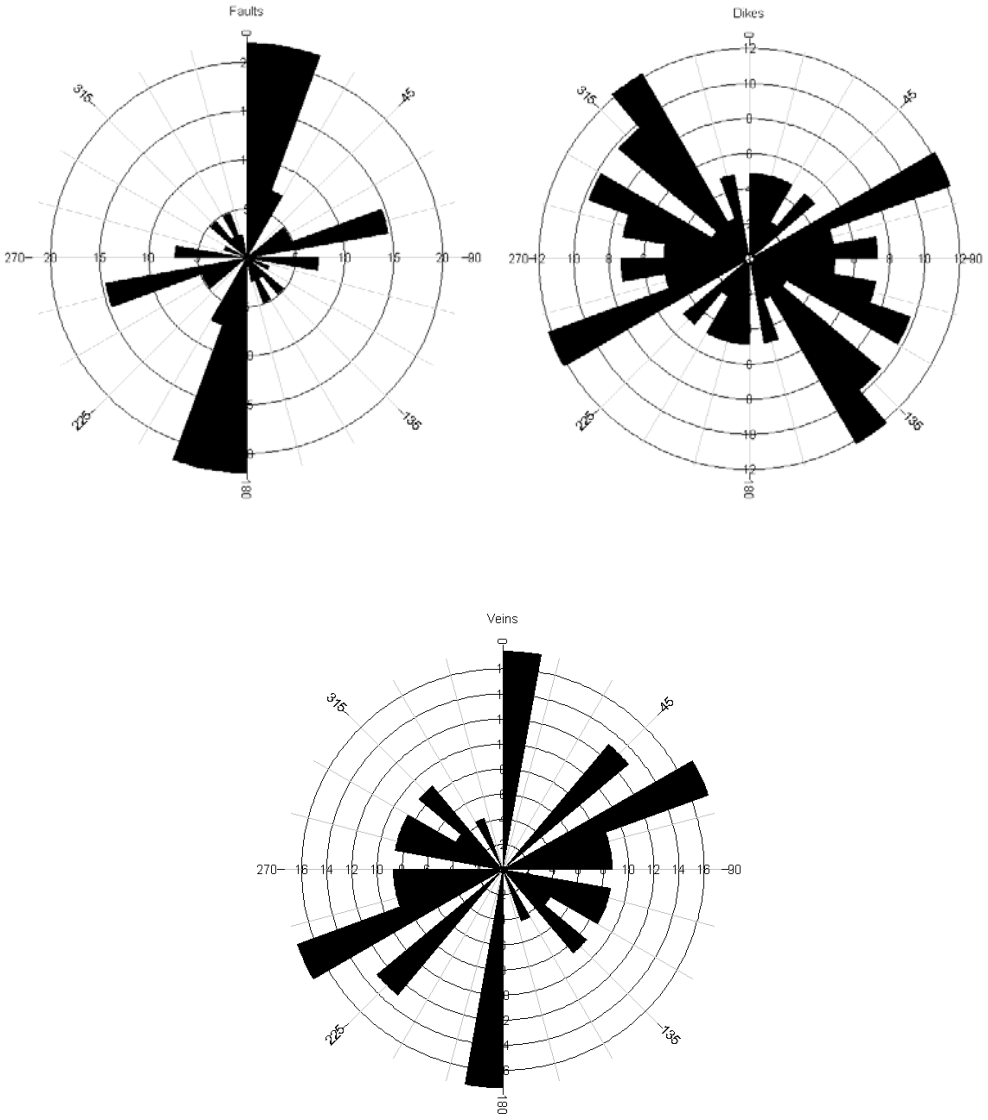

FIGURE 28. Rose diagram showing direction of strike of faults, dikes, and veins in the Montoya Butte quadrangle. Measurements are in Appendix 4. Note the faults trend north-northeast, the dikes trend northwest and northeast, and the veins trend north and northeast.

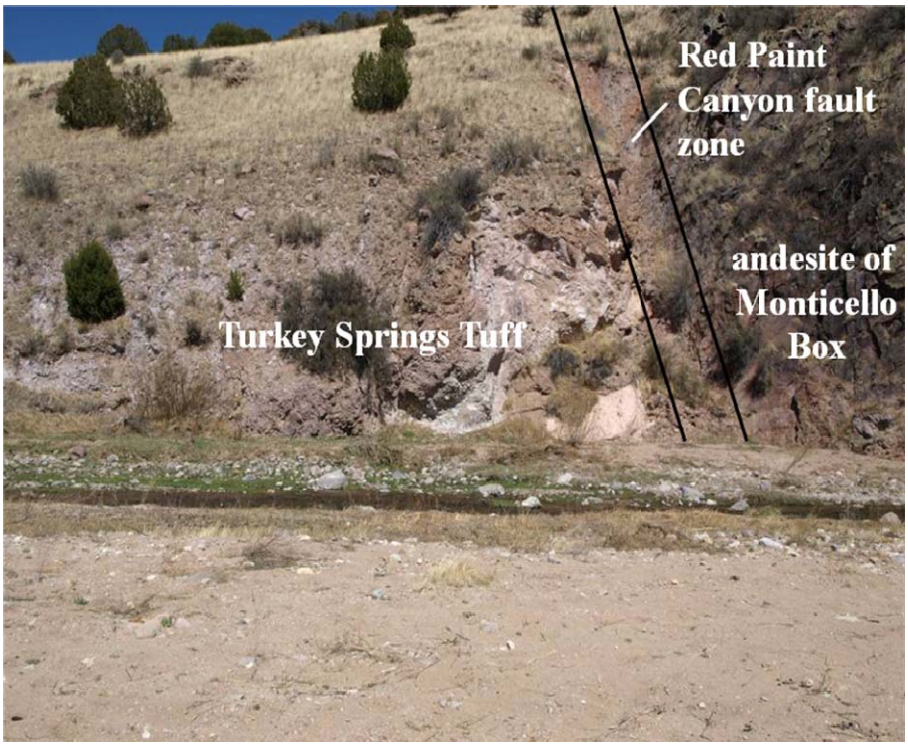

FIGURE 29. Red Paint Canyon fault separating andesite on the right from Turkey Springs Tuff on the left, at the entrance to Monticello Box. Note the hematitic argillic alteration along the fault. A sample collected from the Red Paint Canyon fault zone contained smectite, mixed layered clays, kaolinite, illite, chlorite, quartz, and hematite (Mont-8, Appendix 5).

FIGURE 30. Northern extent of a fault within the Red Paint Canyon fault zone between Quaternary sedimentary rocks and Turkey Springs Tuff (Bull Canyon, SE section 30). Walking stick is 1 m long.

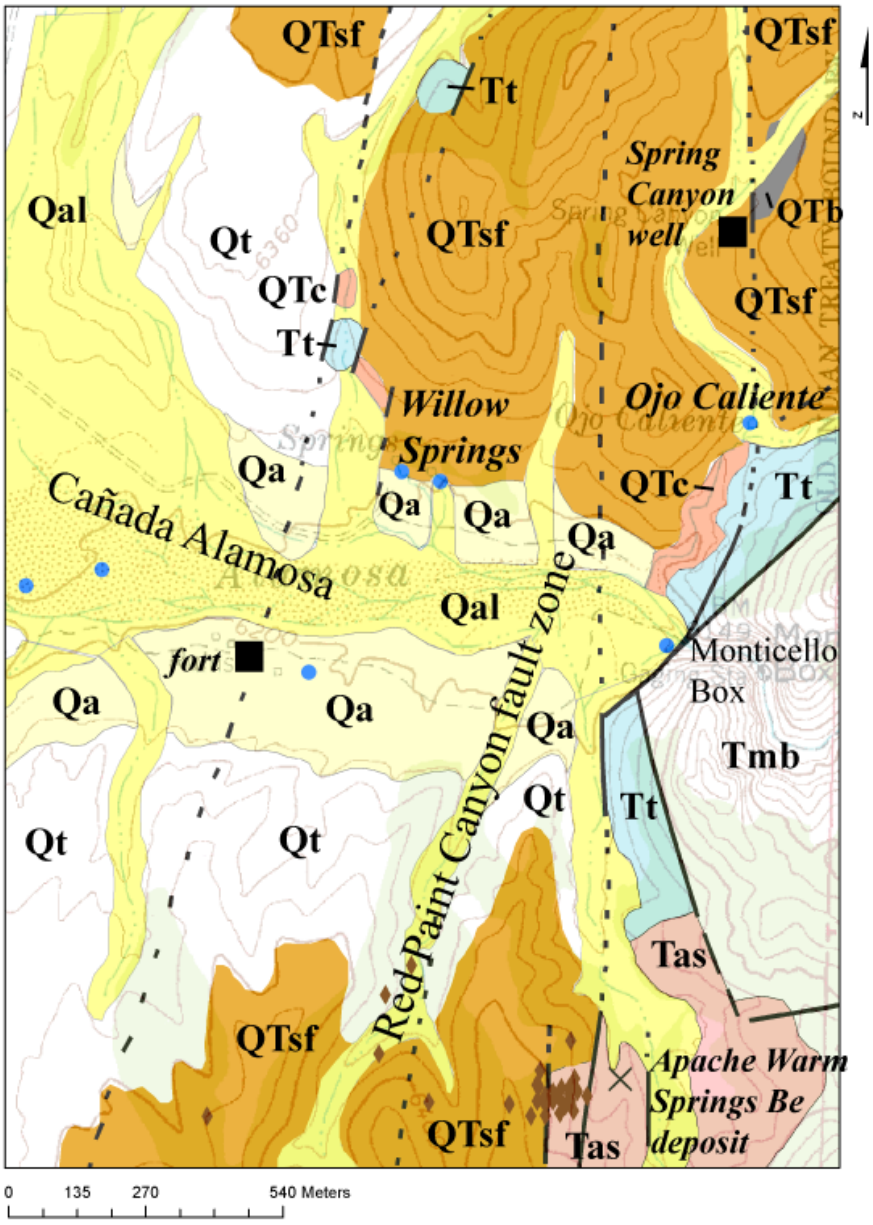

FIGURE 31. Detailed geologic map of the Monticello Box area, upper Cañada Alamosa, Montoya Butte topographic quadrangle, Socorro County, New Mexico (T9S, R7W). Modified by V.T. McLemore (McLemore, 2011, geologic mapping June 2005-October 2009) from Hillard (1969) and Maldonado (1980). Units explained in Figures 33, 40, and Table 3. Blue circles are springs (Appendix 2) and brown diamonds are exploration drill holes (Appendix 7). Most faults are approximate and are identified by geologic mapping (Fig. 29; McLemore, 2011), projection of faults mapped at the surface north and south of this area (McLemore, 2011), and from interpretations of the drill data (Fig. 36; Appendix 7).

Heyl et al. (1983) suggest that the northwest-trending straight valley of Cañada Alamosa in the Priest Tank quadrangle, south of the Montoya Butte quadrangle could be related to an unconcealed northwest-trending fault there, connecting to the Cañada Alamosa fault in the Montoya Butte quadrangle. If this fault forms Cañada Alamosa, it could be a ring fracture surrounding the Nogal Canyon caldera.

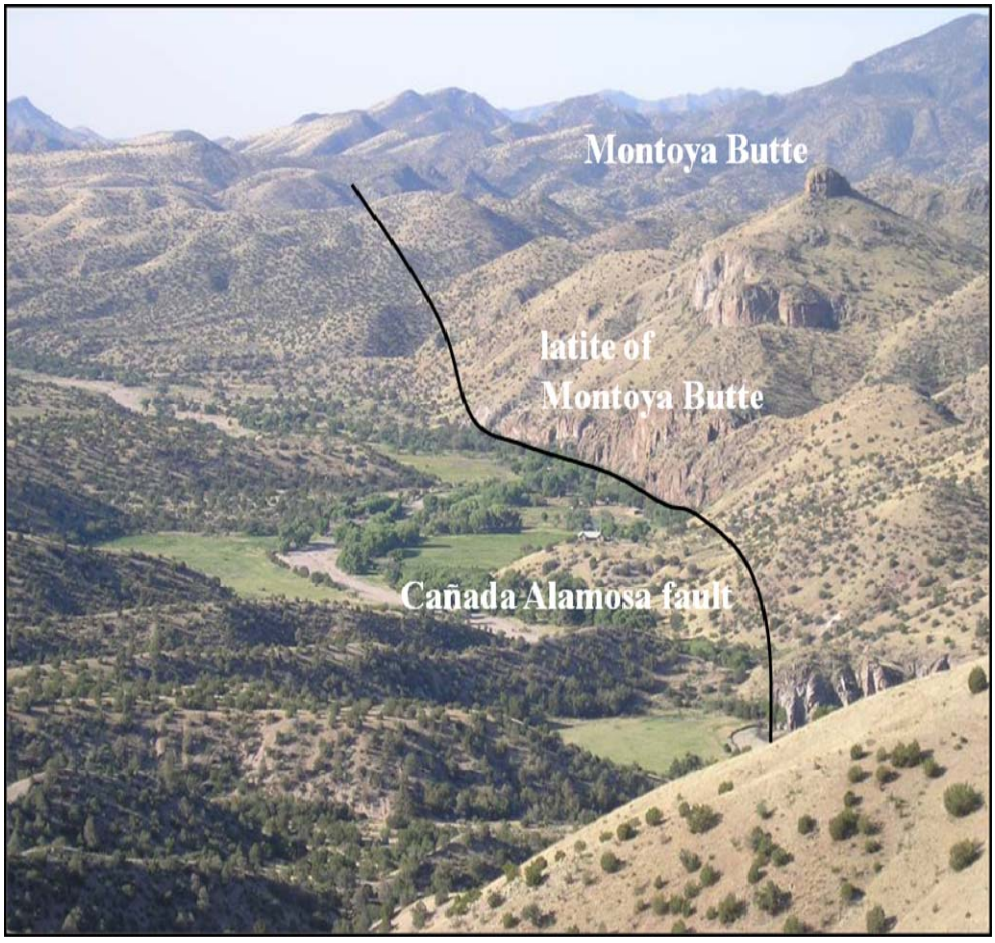

FIGURE 32. Looking south along Cañada Alamosa fault. Montoya Butte (latite of Montoya Butte) is above the fault.

Joints, fractures, and shear zones

The volcanic rocks are strongly fractured and jointed. Many drainages are controlled in part by the joints and fracture in the volcanic rocks; similar relationships are found throughout the San Mateo Mountains (Farkas, 1969).

Nogal Canyon caldera

The Nogal Canyon caldera (28.4 Ma) is in the southern San Mateo Mountains and is a resurgent caldera, although many of the structures related to the caldera are buried by the post-caldera rhyolite flows and domes (Deal, 1973; Deal and Rhodes, 1976; Lynch,

2003). However, the western margin of the caldera is exposed in Kelly and San Mateo Canyons (Fig. 10; McLemore, 2011). The Cañada Alamosa fault could be a ring fracture related to the Nogal Canyon caldera.

Monticello graben

Alamosa Creek drains through the Monticello graben, which forms the valley separating the southern San Mateo Mountains and the Sierra Cuchillo ~30 km long, ~4 km wide, and has a minimum of ~1 km of stratigraphic separation. The Monticello graben has similar structural, depositional, and geomorphic characteristics as the Winston graben to the west (Machette, 1987; Harrison, 1992; Machette et al., 1998), except that the Monticello graben is not a closed basin and drains into both the Palomas Basin and Rio Grande. The Monticello graben is cut off to the south by the Chise lineament of Harrison (1992), where the northern Palomas basin begins. To the north, the Monticello graben is bordered by the San Mateo Mountains and Alamosa Creek basin. Predominantly north- to northeast-trending normal faults along the Sierra Cuchillo form the western flank of the Monticello graben, including the Cañada Alamosa fault. Several normal faults along the San Mateo Mountains, including the Dark Canyon fault, form the eastern flanks of the Monticello graben. The deflection in the southern Monticello graben (i.e., Cañada Alamosa) corresponds with the Chise lineament of Harrison (1992). The Monticello graben is indicated by a low aeromagnetic anomaly (blue to green color in Fig. 34) surrounded by magnetic high anomalies (red color). The Winston and Monticello grabens were likely formed during the Miocene and little or no extension has occurred since (Chapin, 1978; Machette, 1987; Harrison, 1992).

Aeromagnetic map

The Ojo Caliente No. 2 mining district lies on the northern edge of an aeromagnetic high anomaly (red color in Fig. 34) that could be indicative of a rhyolite dome or monzonitic intrusion in the subsurface (Fig. 34). The Iron Mountain beryllium deposit is found in the northern Sierra Cuchillo, south of the Ojo Caliente No. 2 district and also is characterized by a high aeromagnetic anomaly (red color in Fig. 34). Drilling at Iron Mountain encountered a monzonitic intrusion at depth (Davis, 1986a; Robertson, 1986). The Monticello graben and upstream portion of the Alamosa Creek basin is indicated by an aeromagnetic low anomaly (green to blue color in Fig. 34).

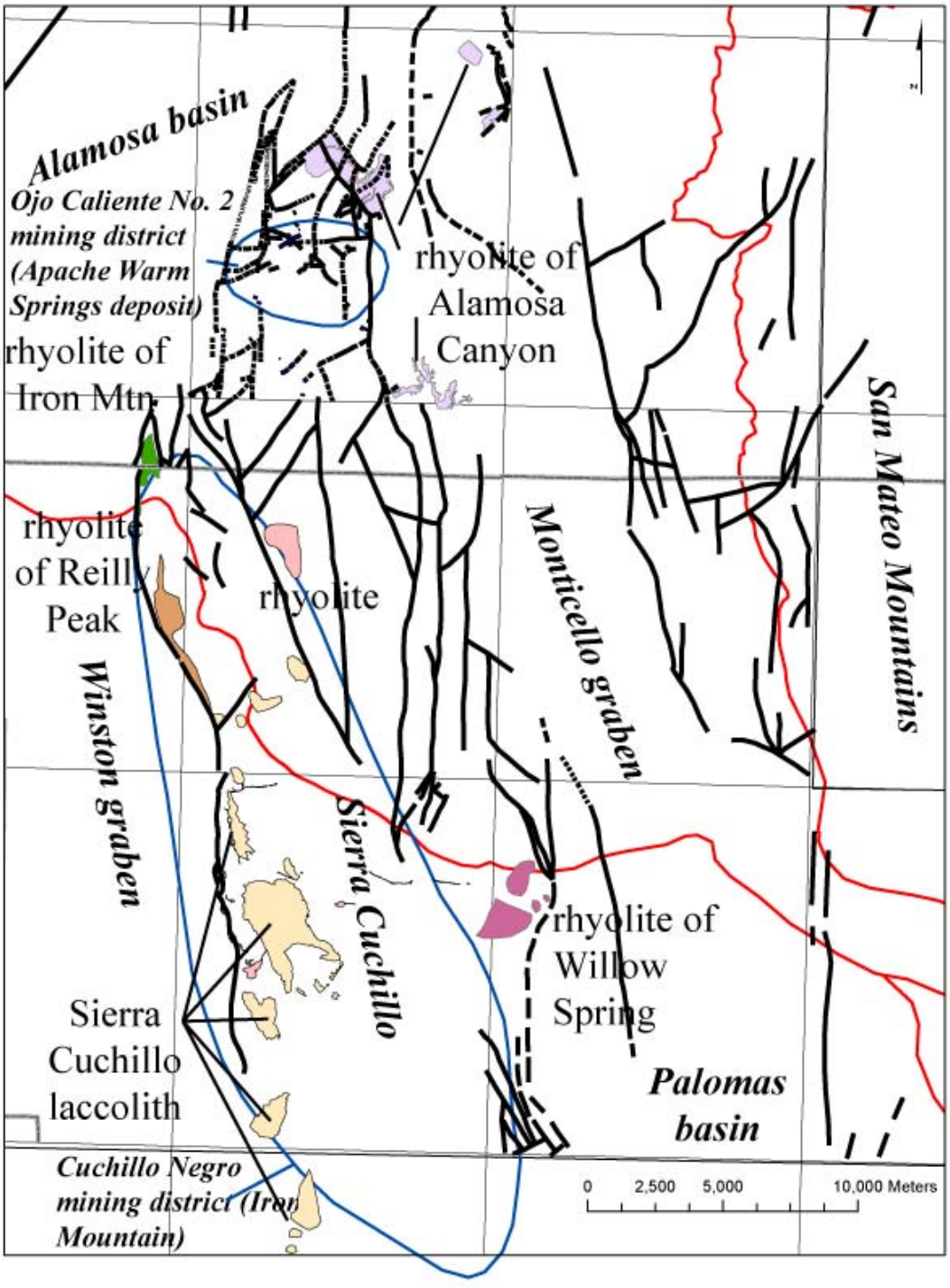

FIGURE 33. Regional structure map of the Sierra Cuchillo-San Mateo area showing Monticello and Winston grabens and Palomas and Alamosa basins. Red line is boundary of Alamosa basin. Mining districts are blue polygons. Major granitic-rhyolite intrusions are shown in colored polygons and discussed in text. Not all rhyolite intrusions in the San

Mateo Mountains are shown. Black lines are faults from this report, Osburn (1984), Harrison (1992), Jahns et al., (2006), and Ferguson et al. (2007).

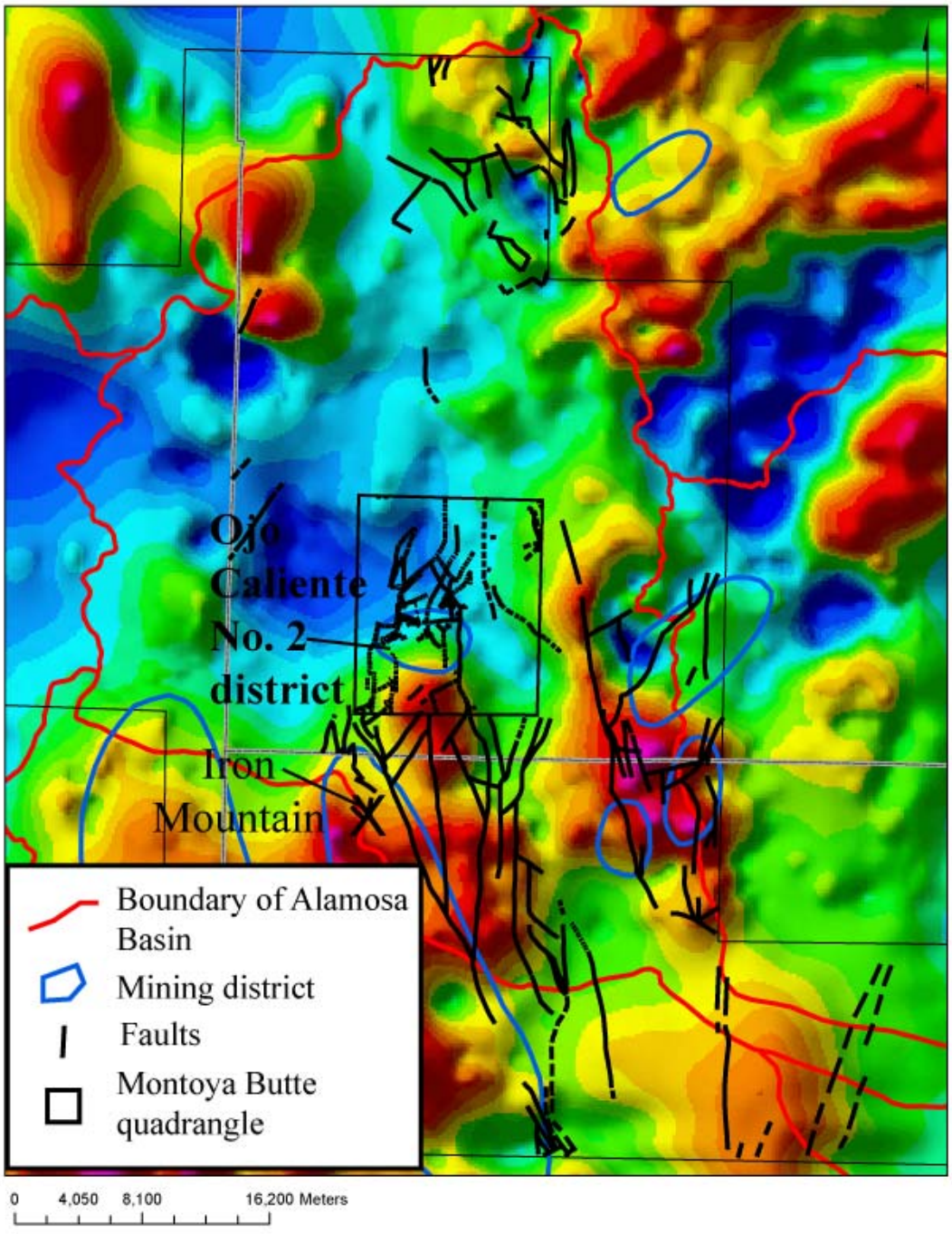

FIGURE 34. Aeromagnetic map of Alamosa Creek basin, from Kucks et al. (2001). Note the aeromagnetic high (red) south of the Ojo Caliente No. 2 mining district, which could be indicative of a rhyolite dome or monzonitic intrusion in the subsurface. Names of mining districts (blue polygons) are in Figure 8. The scale of this map is not sufficient resolution to indicate any correlation, if any, to areas of alteration.

EVALUATION OF THE NURE DATA FOR ALAMOSA CREEK BASIN

The NURE data for New Mexico were downloaded from Smith (1997). Samples from the Alamosa Creek basin were extracted from the data and analyzed for this study (methods and problems with the data are described in Appendix 9). The samples from the Alamosa Creek basin were collected and analyzed by the same procedures and same laboratories over a period of 1-2 yrs. Distribution of NURE stream-sediment samples in Alamosa Creek basin is shown in Figure 35. Table 6 is a summary of descriptive statistics for selected elements. Descriptive statistics, correlation coefficients, factor analyses, statistical plots, and geochemical anomaly maps for selected elements are in Appendix 9.

The NURE geochemical data reflects the major rock types and mineralogy of the regional area, as demonstrated by the correlation coefficients and factor analysis. Uranium has a strong correlation with La, Ce, and Y (i.e., Factor 4), which suggests that these elements are in the same minerals. Factor 1 represents concentrations of heavy and resistant minerals, such as magnetite and zircon, among others (i.e., strong correlations among Cr, V, Fe, Co, Ti, Ni, Sc, Cu, P, Mg, and Zr). Factor 2 represents rock-forming minerals, such as feldspars and clays (i.e., strong correlations among Mg, Zr, Nb, K, U, Ba, Ca, and Th). Factor 3 represents a correlation among Be, Zn, Mn, and Pb. Factor 4 represents minerals containing REE (La, Ce, Y). A strong correlation among Cu, Pb, and Zn would be expected in areas of significant precious- and base-metal deposits and the lack of the correlation among Cu, Pb, and Zn in the Alamosa Creek basin is consistent with the lack of significant deposits in this area.

The geochemical anomaly maps also provide information on the lithology, mineralogy, and mineral deposits in the Alamosa Creek basin. There are no geochemical anomalies of Be, Co, Cr, Mo, Ag, and Zr found in the Montoya Butte quadrangle (Appendix 9), although some anomalies are found elsewhere in the Alamosa Creek basin. The largest Be anomaly in New Mexico is associated with the Iron Mountain Fe-Be-W-Sn skarn deposits in the northern Cuchillo Negro district (McLemore, 2010b). Several anomalies of Cu, Pb, and Zn are found at the southern margin of the Montoya Butte quadrangle and adjacent Jarolasa quadrangle. A prospect pit exposing quartz veins is found in the area, but no sulfides were found (Appendix 1). This anomaly is likely insignificant, because there have been no significant mineralized veins found in the area. However, several anomalies (i.e., Cu, Pb, Zn, Ag, Mo, U, V, La, Ce) are found associated with the mining districts in the southern San Mateo Mountains (i.e., San Mateo Mountains and San Jose districts), which are consistent with mineral deposits found in those districts (Table 1). Geochemical anomalies of REE (La, Ce, Y), Sr, and Zr are found in areas draining where the Turkey Springs Tuff, rhyolite of Alamosa Canyon, and Vicks Peak Tuff outcrop, which is consistent with the known geochemistry of these high silica, peraluminous to slightly peralkaline rhyolites.

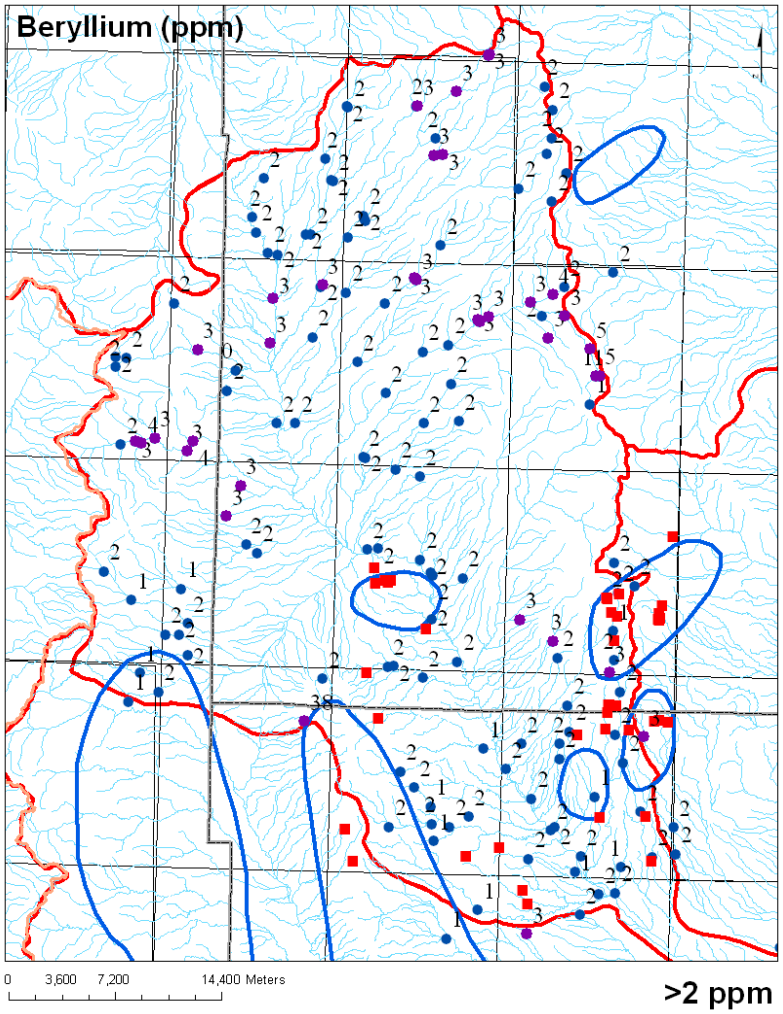

FIGURE 35. Distribution of NURE stream sediment samples and samples with anomalously high beryllium in Alamosa Creek basin, New Mexico (Smith, 1997). Names of mining districts are in Figure 8. Red squares are mines and prospects. Purple circles are samples with >2 ppm Be.

TABLE 6. Descriptive statistics of selected elements of processed NURE data for Alamosa Creek basin, New Mexico. Data are in parts per million (ppm). Upper crustal abundance is from Rudnick and Gao (2005). Threshold value is the value above which is determined to be a geochemical anomaly, as described in Appendix 9.

Method	U	Th	La	Ce	Y	Cu	Pb	Zn	Be	Li	Nb	Cr
Upper crustal abundance	2.7	10.5	31	63	21	28	17	67	2.1	24	12	92
Mean	3.7	11.0	42.8	87.9	28.9	19.0	24.1	85.4	2.4	25.8	20.0	38.6
Median Basin	3.6	10.0	42.0	85.0	26.0	17.0	22.0	70.0	2.0	26.0	19.0	33.0
Maximum	15.2	25	112	187	280	88	102	1246	38	50	39	142
Minimum	1.6	2	17	45	11	7	11	40	1	16	8	16
Threshold value	4	14	47	99	32	22	28	88	2	28	24	44

MINERAL RESOURCES

Volcanic-epithermal vein deposits

Description

The oldest mineral deposits in the Montoya Butte quadrangle are found in the Ojo Caliente No. 2 mining district, and consist of small volcanic-epithermal vein deposits that occur exclusively along faults and fractures within fault zones (Fig. 36). The term "epithermal" includes a broad range of deposits that formed by ascending waters at shallow to moderate depths (<1,500 m), moderate temperatures (50°-300°C), and relatively low pressures (few hundred bars). Work by White (1955, 1981) established the now-recognized association between epithermal-mineral deposits and active geothermal (or hot springs) systems. Subsequent work by Henley (1985) and associates (Henley and Brown, 1985) in New Zealand confirmed this association.

Three types of veins are found in the Ojo Caliente No. 2 mining district, copper-silver veins (<4.5 m wide), calcite veins (<2 m wide), and quartz veins (<2 m wide). The Taylor mine is the only vein developed by a shaft (Fig. 37); only a few small prospect pits are found along some of the other veins in the quadrangle (Fig. 5; Appendix 1, Fig. A1-1). Detailed descriptions of individual prospects are in Appendix 1.

The copper-silver veins are found at the Taylor mine, east of the Red Paint Canyon fault zone. The shaft is estimated to be 38 m deep with 29 m of drifts at the bottom (Lasky, 1932), and is above the water table. Quartz veins with copper minerals strike N65-75°E and dips 80°NW to vertical and cuts altered andesite. The andesite is altered to epidote and chlorite and silicified. The main vein at the Taylor mine is approximately 4.5 m wide, 300 m long and contains various amounts of malachite, azurite, chrysocolla, and cerusite with iron and manganese oxides. A reported assay contained 61.7% Pb, 1.2% Cu, 433 ppm Ag, and 0.65 ppm Au (Lasky, 1932). A sample collected from the dump for this study contained 1.29% Pb, 0.99% Cu, and 1.65% Zn (Appendix 3, MONT-6).

A second type of vein deposit is simple fissure-filling or fracture-coating of white calcite with minor colorless to green fluorite and colorless to white quartz (Fig. 38; Appendix 1). The calcite is typically coarse-grained, with white calcite crystals as large as several centimeters. Complex vein textures, such as complex banding, multiple brecciation and rhythmic layering typical of most volcanic-epithermal districts (McLemore, 1996), are generally absent. These calcite veins are variable in size, rarely exceeding 1 m wide and less than 30 meters long. Chloritization, epidotization, and locally silicification are found adjacent to the calcite veins. Coarse-grained calcite also is locally found filling fractures, amygdule-fillings, and cavities within the andesite flows. No visible pyrite or any other sulfides are found. Fluorite rarely exceeds a few percent.

A third type of vein consists of mainly quartz that is brecciated, bifurcating, sinuous, and pinch and swell along strike, and locally contains calcite, epidote, chlorite and clay minerals. These veins exhibit one or two stages of brecciation cemented by quartz. Complex vein textures, such as multiple brecciation and rhythmic layering, are typically absent. These veins are variable in size, rarely exceeding 2 m wide and less than 50 meters long. A few veins are banded with calcite cores surrounded by quartz-epidote, but there is no visible pyrite or other sulfides. Typically silicification, chloritization, epidotization, and clay alteration are found along and between the veins.

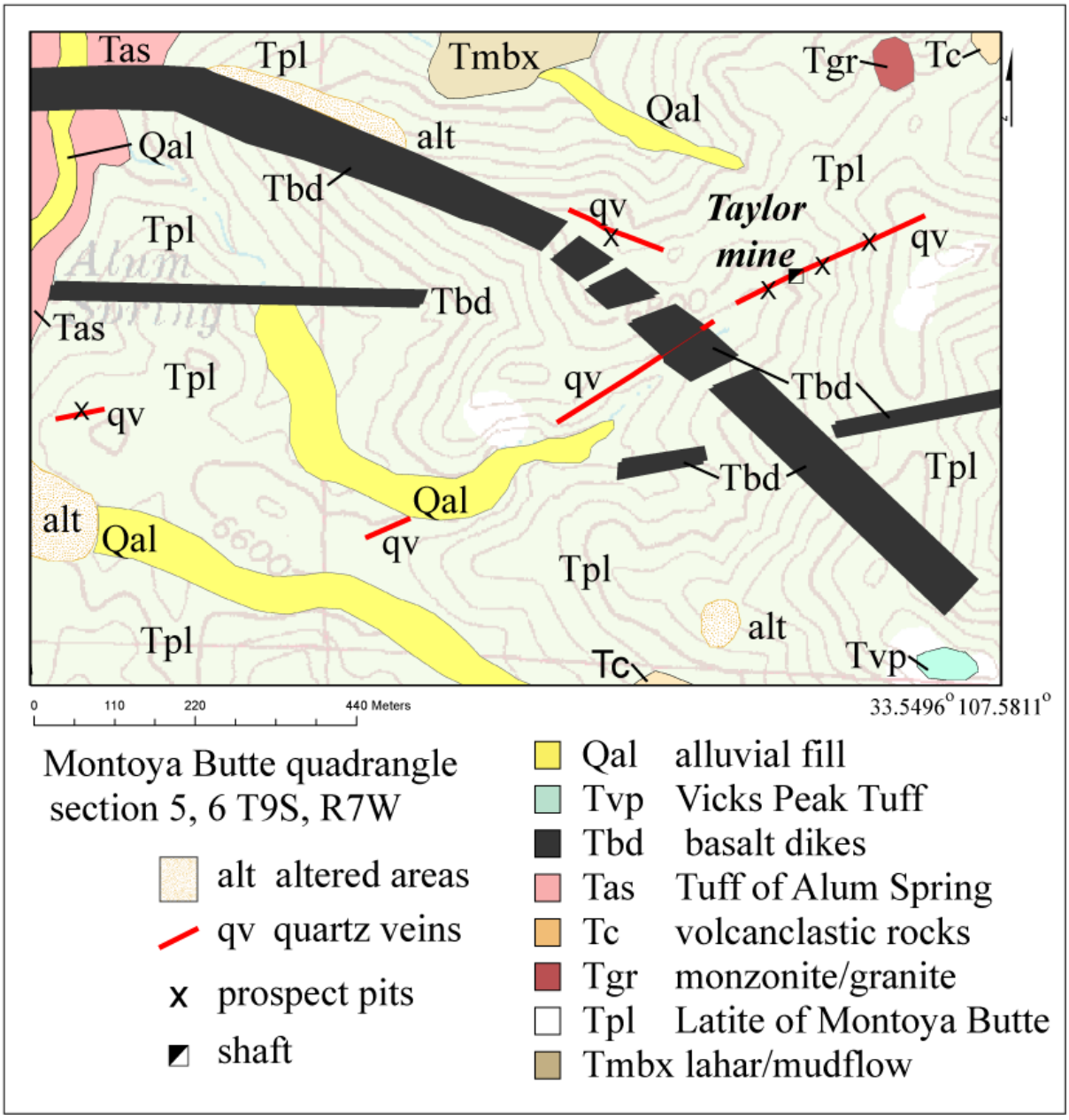

FIGURE 36. Detailed geologic map of the Taylor mine area, Ojo Caliente No. 2 mining district, Socorro County, New Mexico (McLemore, 2011).

FIGURE 37. Taylor shaft, looking east.

FIGURE 38. Brecciated quartz veins, eastern Montoya Butte quadrangle.

The most extensive alteration adjacent to and along faults in the district is silicification. Silicified zones vary in width along strike and some zones reach widths of several tens of meters. Locally parallel or bifurcating faults or veins occur that are separated by silicified and locally brecciated host rock. Quartz and calcite occurs as amygdule-fillings, fracture coatings, thin quartz veins, breccia cements, and as replacements of primary minerals near the faults. Locally, chloritization, argillization, and sericitization occur in a halo surrounding mineralized faults. Epidote locally occurs within this halo and indicates temperatures of formation >200°C (McLemore, 1993).

Discussion

The volcanic-epithermal veins in the Montoya Butte quadrangle are simple quartz-calcite veins and one copper-silver vein that indicates warm to hot hydrothermal waters circulating through the area along faults and fractures.

Mineral-resource potential

The procedure for evaluating the mineral-resource potential of an area is summarized in Appendix 11. The lack of any significant sulfides or other base-metal minerals or any mineral zoning (such as a pyrite halo) suggests that a major volcanic-epithermal system containing precious or base metals either never formed in this area or if one did occur, it is at depth. The low chemical analyses and lack of significant geochemical anomalies in the NURE data and the survey by Griffitts and Alminas (1968) also indicate that these deposits are not economically significant. Therefore, the mineral-resource potential for volcanic-epithermal precious and base metals vein deposits in the Montoya Butte quadrangle, including the Ojo Caliente No. 2 mining district, is low with a moderate to high degree of certainty.

Apache Warm Springs beryllium deposit

Description

The most significant mineral deposit in the Ojo Caliente No. 2 district is the Apache Warm Springs beryllium deposit (Fig. 39, 40; mine identification number NMSO0152), which consists of volcanogenic Be deposits (volcanic-hosted replacement, volcanic-epithermal, Spor Mountain Be-F-U deposits; Lindsey and Shawe, 1986; Foley et al., 2010). A detailed geologic map and cross section as interpreted by the author is in Figure 36. Bertrandite ($Be_4Si_2O_7(OH)_2$) is found in small quartz veins and stringers, along fractures with clay minerals, and disseminated with the rhyolite and rhyolite ash-flow tuff. Summary of drilling is in Appendix 7. Meeves (1966) reports assays as high as 2.05% BeO in drilling during the U.S. Bureau of Mines drilling program, additional chemical analyses for Be are in Appendix 7 (Table A7-1). Only one hole in the recent drilling, BE18A, contained beryllium analyses higher than 50 ppm, with the highest analysis of 2600 ppm Be (Fig. 36; Appendix 7; P and E Mining Consultants, Inc., 2009). It is possible that the beryllium deposit could continue south of the known extent in Red Paint Canyon (Fig. 34), as indicated by the magnetic anomalies (Fig. 34). The Beryllium Group, LLC controlled the property in 2001-2002, drilled 14 holes, and reported a resource of 39,063 metric tones (43,060 short tons, not NI 43-101 compliant, as reported by Mining Engineering, 2002). For comparison, the Spor Mountain, Utah rhyolite-hosted Be deposit has reported proven reserves amounting to 6,425,000 metric tons of 0.266%

Be and currently produces approximately 40,000-60,000 metric tons Be/year (Brush Engineered Materials, Inc., 2009).

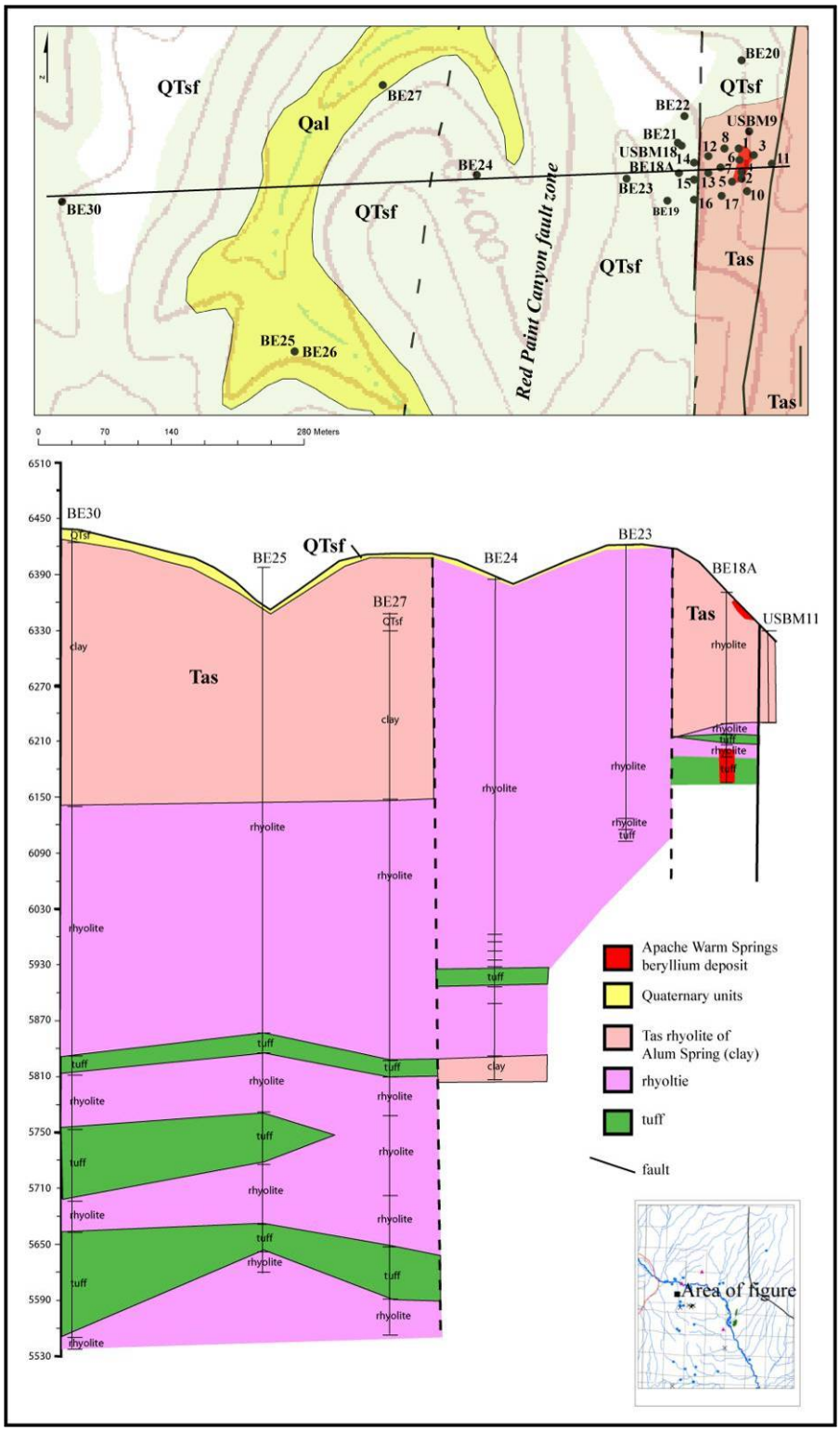

FIGURE 39. Detailed geologic map and cross section of the Apache Warm Springs beryllium deposit and adjacent area (N section 6, T9S, R7W; McLemore, 2011).

Interpretations are by the author from examination of drill cuttings, using available drill data (Appendix 7), and surface mapping.

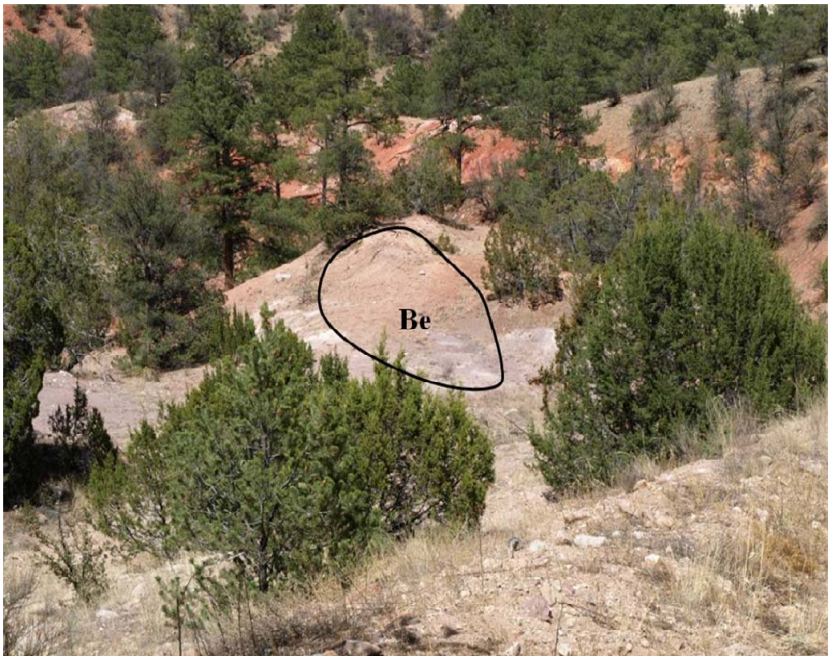

FIGURE 40. Apache Warm Springs beryllium deposit (Be), as delineated by P and E Mining Consultants, Inc. (2009) as determined from trenching and drilling, looking northeast (N section 6, T9S, R7W).

The depth to water at the Apache Warm Springs deposit varies from 16 to 152 m, as determined by drilling (Appendix 7). Drilling indicates that several perched water tables and/or water-bearing zones in the rhyolite are present and the perched water zones and the rhyolite lavas are offset by faulting (Fig. 39; Meeves, 1966; see Appendix 7). At least one of the recent drill holes was converted to a stock well for the rancher who owns the area.

Alteration

The Apache Warm Springs beryllium deposit is characterized by intense acid-sulfate alteration (also known as advanced argillic alteration), which produces the multiple shades of white, red, yellow, orange, purple, green, brown, and black that gives Red Paint Canyon its name. Alteration is a general term describing the mineralogical, textural, and chemical changes of a rock as a result of a change in the physical, thermal, and chemical environment in the presence of water, steam, or gas (Henley and Ellis, 1983). This type of alteration typically forms a zoned halo surrounding the mineral deposit and is an attractive target for prospecting, especially for volcanic-epithermal gold-silver veins, porphyry copper and molybdenum deposits, and volcanogenic Be deposits, to name a few types of associated mineral deposits. A modern analog for the formation of this alteration and beryllium mineralization would be a geothermal system, such as the Norris Geyser Basin in Yellowstone National Park (Muffler et al., 1971; Henley and Ellis, 1983; Kharaka et al., 2000; Rodgers et al., 2002).

The alteration at the Apache Warm Springs beryllium deposit can be differentiated into two zones on the basis of mineralogy, texture, and inferred temperatures as (1) clay zone (Fig. 41) and (2) silicified zone (Fig. 42). Boundaries between the zones are typically gradational and are distinguished by quartz content and texture. The altered areas are characterized by the leaching and replacement of the matrix and primary minerals in the original host rock by kaolinite, illite, quartz, hematite, and locally illite/smectite, pyrite, anatase, alunite, bertrandite, and possibly pyrophyllite. The texture of the original lithologies (Tas) is typically destroyed and replaced by clay minerals. The largest of these areas are mapped on Figure 40. Stratigraphic position and relict textures suggest that original lithologies were volcaniclastic rocks and rhyolite ash-flow tuffs (rhyolite of Alum Spring, Tas), possibly part of a rhyolite dome structure. The intensity of alteration varies and some primary minerals such as quartz, titanite, zircon, and apatite are locally preserved. The alteration is older than the Quaternary-Tertiary sedimentary rocks, which are unaltered and contain boulders and clasts of the altered tuff (Tas).

FIGURE 41. Clay zone with red hematite-kaolinite and white kaolinite surrounding the Apache Warm Springs beryllium deposit (N section 6, T9S, R7W). A sample collected from the site shown on the left contains kaolinite, quartz, and hematite (Mont-35, Appendix 5). A sample collected from the white clay shown in the photograph on the right contains quartz, kaolinite, illite, smectite and mixed layered clays (Mont-61, Appendix 5).

FIGURE 42. Silicified zone, looking southwest. The Apache Warm Springs beryllium deposit is to the right (N section 6, T9S, R7W).

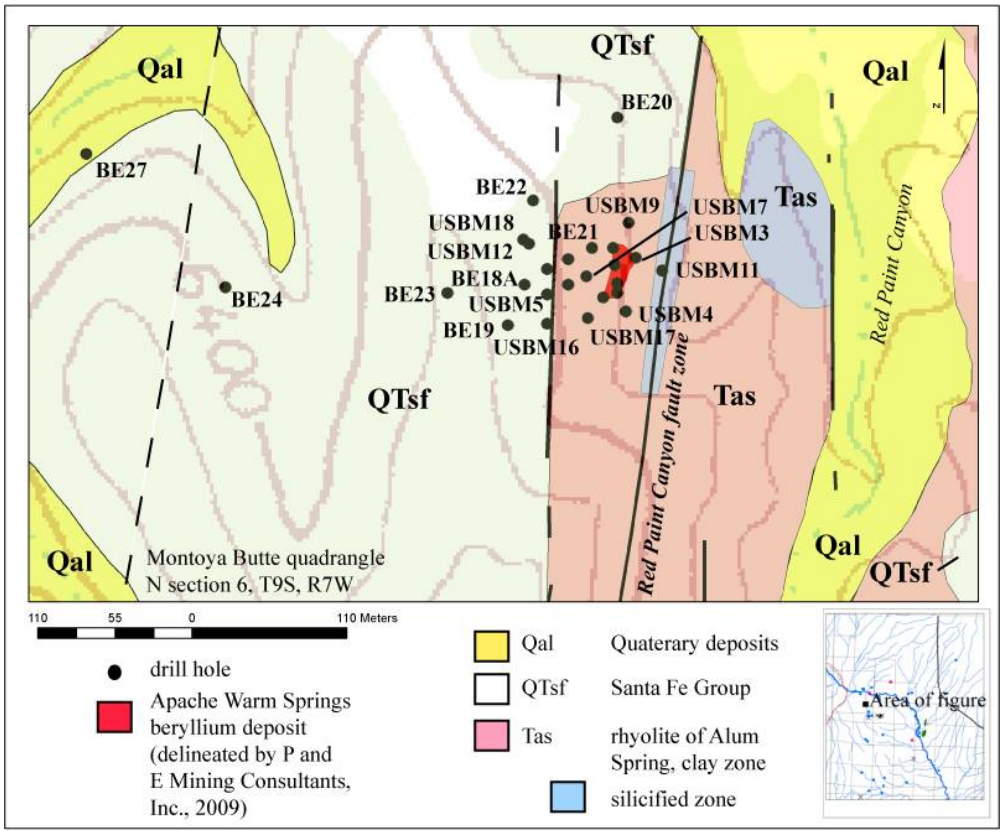

FIGURE 43. Alteration map of the Apache Warm Springs beryllium deposit. The western fault (between BE27 and BE24) is identified from drilling data (Fig. 37; Appendix 7).

The outermost altered zone in Apache Warm Springs beryllium deposit is designated the clay zone, which is characterized by the alteration and replacement of the matrix and primary minerals in the host rock by kaolinite, illite, quartz, hematite, and locally illite/smectite, pyrite, anatase, tridymite, diaspore, alunite, despujolsite(?), and rare pyrophyllite. This mineral assemblage results in bleached and iron-stained rocks that occur in multiple shades of white, red, yellow, orange, purple, green, brown, and black. The intensity of alteration varies and locally some primary minerals such as quartz, titanite, zircon, and apatite are locally preserved. Some areas within the clay zone are soft and friable and consist only of clay minerals. This alteration represents the outermost altered zone typical of many acid-sulfate altered areas in many districts, where this alteration forms a halo surrounding precious- and base-metal vein deposits (McLemore, 1993, 1996).

The silicified zone is typically the most extensive zone in most acid-sulfate altered areas in the district, but in the Apache Warm Springs beryllium deposit it is found only along faults at the beryllium deposit. The silicified zone is characterized by alteration and replacement of primary minerals by quartz, kaolinite, illite, and locally pyrite, diaspore, pyrophyllite, alunite, jarosite, anatase and other iron and titanium oxides. The intensity of alteration varies, but is typically higher than in the clay zone. Quartz content is typically high (>60%) and decreases toward the clay zone. These rocks are usually bleached, iron stained, and found as multiple shades of white, red, yellow, orange, purple, green, brown, and black. Textures vary from fine to medium grained, massive to brecciated and vuggy to sugary. Silica deposition and replacement are common. In some thin sections, thin quartz veins cut the altered rock. Quartz also locally replaces primary minerals such as feldspar, pyroxenes, and amphiboles.

Faults could occur in the altered areas; but, the alteration is typically too intense to accurately map them. Only a few exposed faults in the altered zone are therefore mapped in Figure 43, based upon visible silicification and brecciation. Additional altered areas are in the vicinity of faults and on ridges east of the known deposit (Fig. 10; McLemore, 2011).

Discussion

The Apache Warm Springs beryllium deposit is similar in geology and grade to the Spor Mountain beryllium deposit in Utah (Fig. 44), which is the world's most important source of beryllium (Barton and Young, 2002; Cunningham, 2003; Jaskala, 2007). The Spor Mountain deposit is currently in production and has reserves at the end of 2009 amounting to 6.425 million metric tons with an average grade of 0.266% Be, or 15,800 metric tons of contained Be, which is sufficient for 100 years at the current production rate (McLemore, 2010b). The Apache Warm Springs deposit contains an estimated 39,063 metric tones (43,060 short tons) of 0.05-2.5% Be (Fig. 44; Mining Engineering, 2002). The Apache Warm Springs deposit is hosted by rhyolite that could be part of a rhyolite dome similar to the dome found at the junction of Cañada Alamosa and San Mateo Canyon (Fig. 10; McLemore, 2011) and elsewhere in the San Mateo Mountains (Lynch, 2003; Ferguson et al., 2007). Red Paint Canyon fault zone controlled the emplacement of the rhyolite dome, alteration, and beryllium mineralization.

Mineral-resource potential

The mineral-resource potential of the Apache Warm Springs beryllium deposit is low to moderate with a moderate to high degree of certainty, because the known extent of the beryllium deposit at the surface and in the subsurface where drilled is low grade and too small for economic development in the current market. The NURE data also indicate that the stream sediment samples in the area are low in Be concentrations. However, additional exploration drilling could locate additional beryllium in the subsurface. Spor Mountain, Utah produces most of the beryllium used in the U.S. today and the known reserves at Spor Mountain are sufficient to meet projected beryllium demand in the U.S. in the near future (McLemore, 2010b, c). Any potential exploration or subsequent mining would have to plan for environmental issues, especially the effect of mining on Ojo Caliente and adjacent warm and cold springs (McLemore, 2008). Ojo Caliente, the adjacent warm and cold springs and Alum Spring lie along Red Paint Canyon fault zone where the Apache Warm Springs beryllium deposit is located. Future hydrologic studies are underway that will characterize the ground water conditions in this area.

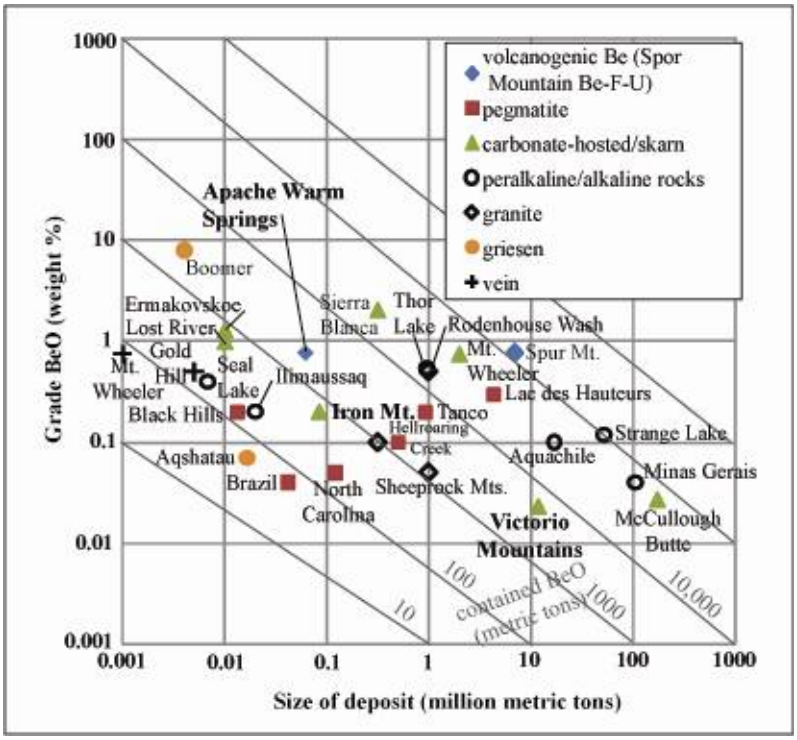

FIGURE 44. Grade and tonnage of selected beryllium deposits, including the Apache Warm Springs deposit (modified from Barton and Young, 2002 using references in McLemore, 2010b). Deposits in bold are located in New Mexico. Note that size of deposits includes production and reserves/resources and are not always NI 43-101 compliant and subject to change.

Geothermal resource potential

The area surrounding the warm springs at Ojo Caliente (Fig. 31, 46) along the northern edge of Cañada Alamosa west of Monticello Box was examined for the potential of geothermal resources (Summers, 1965, 1976, 1979; Stone and Mizell, 1977; Swanberg, 1980; U.S. Geological Survey and New Mexico Bureau of Mines and Mineral

Resources**,** 1981; Witcher, 1995). Ojo Caliente is approximately 27.5°C with a pH of 7.9 (Myers et al., 1994); Summers (1965, 1976) report a temperature of 28.1°C in 1965. Alum Spring is approximately 16°C with a pH of 7.9 (Myers et al., 1994). Subsequent measurements of these and Willow Springs have similar temperatures and pH. Chemical analyses of Ojo Caliente and Willow Springs are in Myers et al. (1994). Additional hydrologic studies are underway by NMBGMR personnel.

Most of the length of the Rio Grande rift system in New Mexico is characterized by high heat flow and conductive thermal gradients (Reiter et al., 1975; Seager, 1975; U.S. Geological Survey and New Mexico Bureau of Mines and Mineral Resources**,** 1981; Witcher, 1995). Reiter et al. (1975) defined regional geothermal trends associated with the Rio Grande rift based on heat flow measurements greater than 2.5 HFU (heat-flow unit, μcal/cm2-sec) and the Monticello Box area is north of this zone, with an average HFU of 2.0 (U.S. Geological Survey and New Mexico Bureau of Mines and Mineral Resources**,** 1981). The deep sedimentary basins, complex basement faults, and bedrock constrictions along the Rio Grande rift system create geohydrologic conditions that can sustain local or basin-scale forced convective systems that bring thermal water to the surface in the form of thermal springs, such as found at Monticello Box (Morgan and Daggett, 1981; Witcher, 2002).

Three potential geothermal models are consistent with the geothermal springs found at Monticello Box and elsewhere in New Mexico: 1) discharge of regional heated ground-water flow driven by topographic hydraulic gradient, 2) deep, upward-flowing thermal waters along a fault near a constriction of the underlying aquifer, and 3) constriction caused by thinning of the aquifer over a buried horst (Fig. 46; Morgan and Daggett, 1981, fig. 21). Most geothermal systems along the Rio Grande rift generally involve deep circulation and heating of ground water. The heating by deep convection (models 2 and 3) at Monticello Box are supported by Myers et al. (1994), who state "*water containing a small dissolved-solids concentration probably represents heating of the local waters by the underlying warm bedrock…*" and "*warm water having large concentrations of dissolved solids from some wells probably represents deep, circulating water in the bedrock or along faults in the bedrock.*" Recharge in the San Mateo Mountains can easily provide the hydrologic head required for forcing thermal waters heated by deep convection upwards along the Red Paint Canyon fault zone. Similar models are proposed for most of the geothermal systems in New Mexico, including those at Socorro (Stone, 1977; Gross and Wilcox, 1983; Anderholm, 1987; Barroll, 1989; Barroll and Reiter, 1990), T or C (Lund and Witcher, 2002), Gila Hot Springs (Witcher and Lund, 2002), McGregor (O'Donnell et al., 2001), and New Mexico State University in Las Cruces (Witcher et al., 2002). Geothermal systems in general, including the warm springs at Monticello Box, are structurally and geologically complex as demonstrated in the Gila Hot Springs area (Witcher and Lund, 2002). Morgan and Daggett (1981) concluded that "*geothermal resources in southwestern New Mexico are not directly related to recent magmatism or active faulting*", but faults can provide some structural control on ground-water flow. The Cañada Alamosa area is not seismically active, as would be expected if a near-surface magma body existed similar to that found in the Socorro area (Finnegan and Pritchard, 2009; Majkowski, 2009), and there is no indication of such a magma body in examination of the regional gravity and magnetic geophysical maps by the author.

Hot and warm springs systems are complex geologic phenomena that are not always well understood, even with abundant geologic and geophysical data. For example, Lund and Witcher (2002) describe an incident in the T or C hot springs area where the system is fairly well modeled. But, a few years ago, dredging of the Rio Grande upstream of the T or C commercial hot springs resulted in a drop of artesian head and temperature at several commercial wells in T or C. The owners of the commercial operations notified the authorities and the situation was immediately remediated (see Lund and Witcher, 2002 for more details). This example illustrates the hydrologic complexity of the connection between the Rio Grande surface water coming from the north and hot ground water, thought to originate in the Palomas basin to the west of T or C, and the hot springs in T or C (Lund and Witcher, 2002).

Although once examined for potential for geothermal resources, the Monticello Box area currently is not designated a Known Geothermal Resource Area (Summers, 1972; Stone and Mizell, 1977; U.S. Geological Survey and New Mexico Bureau of Mines and Mineral Resources**,** 1981) and has low geothermal potential because the water temperature of the springs is too low for commercial purposes. Therefore, the geothermal resource potential is low with a high degree of certainty. However, on-going hydrologic studies of the Alamosa Creek Basin by NMBGMR will add to the knowledge of the area and likely provide better hydrologic models. It is recommended that any deep drill holes be measured for precision temperature logging to assess the geothermal potential and the ground water patterns (Reiter et al., 1975; Reiter, 2005).

FIGURE 45. Ojo Caliente, looking south.

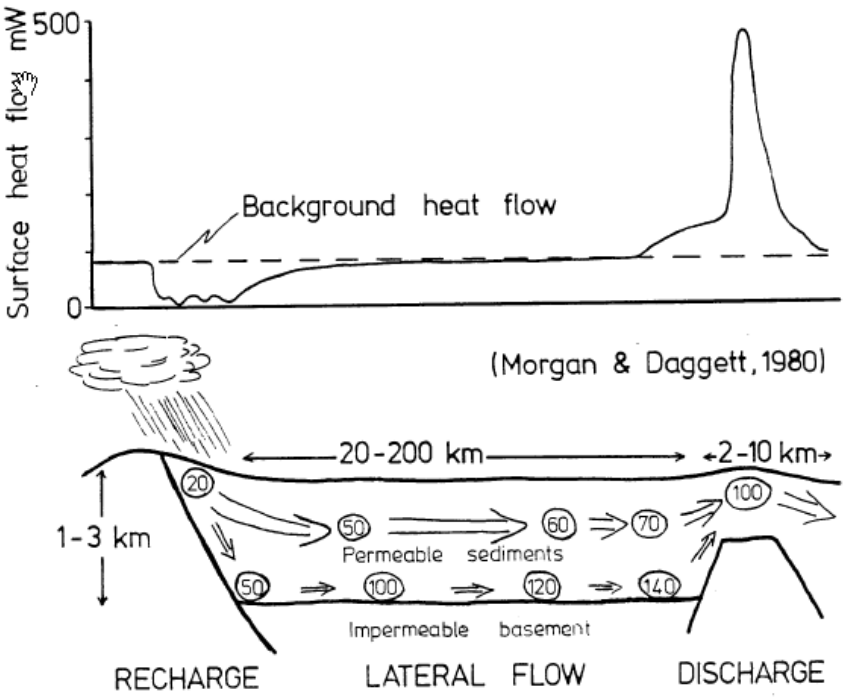

FIGURE 46. Diagrammatic section of hypothetical Rio Grande geothermal system by forced ground-water convection (modified from Morgan and Daggett, 1981, figure 21) Arrows denote ground-water flow direction and the size of the arrows indicate relative volumes of flow. Flow is through permeable rocks or along fractures. The expected surface heat flow profile is shown in the upper portion of the diagram. A similar model is envisioned to explain the thermal springs at Monticello Box, upper Alamosa Canyon.

Mineral-resource potential of other commodities

Only four other potential commodities are found in the Montoya Butte quadrangle; clay, aggregate, fluorite, and uranium. Clay is found in the Quaternary units, the floodplain deposits and in the altered area adjacent to the Apache Warm Springs beryllium deposit (Appendix 5). Three possible clay pits have been found near two Pueblo sites, as discussed below, but these sites have no additional resource potential. The mineral-resource potential for clay is low with a high degree of certainty because of low grade and small size. Fluorite veins are found in several areas in the Ojo Caliente No. 2 mining district, but these veins are small (less than 1 m wide) and very low grade. Therefore the mineral-resource potential for fluorite is low with a high degree of certainty. Although it is reported that uranium was produced from the Apache Warm Springs beryllium deposit, the resource potential for uranium is low with a high degree of certainty because of low grade and small size. The mineral-resource potential for aggregate for local use is high with a high degree of certainty in the active alluvial and floodplain deposits, but the deposits require adequate testing to determine the quality before use as aggregate. There is no resource potential for any other commodities in the quadrangle.

DISCUSSION

Stratigraphic correlations

The correlation of the rocks defined in the Montoya Butte quadrangle with previous stratigraphy defined by various workers throughout the San Mateo Mountains and Sierra Cuchillo range is summarized in Table 7. These correlations are based upon new age dates (Table 2), local stratigraphic correlations of units (Table 7), and chemical analyses of volcanic and intrusive rocks. In addition, similarities in geochemical composition of the various units aid in regional correlations as described in the Petrochemistry section, and in the description of units, above.

Two periods of granitic-rhyolitic rocks have intruded the Paleozoic sedimentary section in the Sierra Cuchillo and San Mateo Mountains, which are separated by andesite to latite flows and breccias; the older event is >38-36 Ma and the younger is 27-29 Ma (Table 7; Fig. 33). Similar age relationships are found in the Black Range (Harrison, 1992). The oldest intrusion is the Sierra Cuchillo porphyritic granodiorite to quartz monzonite laccolith in the southern portion of the Sierra Cuchillo (Fig. 33), and is 38.2±0.9 Ma (U-Pb on zircon, Michelfelder, 2009). The Reilly Peak rhyolite is 36.0±1.4 Ma (K-Ar, Davis, 1986a, b) and could be related to the Sierra Cuchillo laccolith because of similar major- and trace-element composition (Fig. 25, Appendix 3; Davis, 1986a, b; Michelfelder, 2009) and the imprecise K-Ar age date. The Reilly Peak rhyolite was originally called monzonite porphyry by Jahns (1944) and is intruded by younger rhyolite dikes and stocks. However, the monzonite plugs intruding the latite of Montoya Butte (36 Ma, Appendix 6) and andesite of Monticello Box also are similar in geochemical composition to the Sierra Cuchillo laccolith and Reilly Peak rhyolite, which suggests intrusive activity could span for ~2 Ma. More age determinations are required. These older intrusions could be related to the Emory caldera (34.9 Ma) in the Black Range to the southwest because of similar age and chemical composition to the Kneeling Nun Tuff that erupted from that caldera (Fig. 1).

The youngest granitic-rhyolitic rocks are found throughout the Sierra Cuchillo and San Mateo Mountains as dikes, stocks, and lavas. In the Sierra Cuchillo, porphyritic rhyolite and rhyolite aplite intruded the Paleozoic rocks and older granitic-rhyolitic rocks; the rhyolite aplite intrudes the porphyritic rhyolite (Fig. 33; Jahns, 1944; Robertson, 1986). K-Ar dating of these rhyolites is imprecise and ranges from 29.2±1.1 Ma at Iron Mountain to 22.6±0.8 Ma at Reilly Peak (Table 7; Fig. 33). The Iron Mountain rhyolite porphyry is pinkish gray and contains 40-50% phenocrysts of orthoclase and quartz in a fine-grained groundmass of orthoclase, quartz, and oligoclase with minor biotite, apatite, magnetite, zircon, and fluorite. The Iron Mountain rhyolitic aplite is light pink, equigranular, and consists of orthoclase phenocrysts in a fine-grained matrix of quartz, orthoclase, and oligoclase with minor biotite, apatite, fluorite, and topaz. The Reilly Peak rhyolite is white to gray, fine-grained, and consists of albite, quartz, and minor biotite, titanite, epidote, muscovite, hematite, amphibole, apatite, and magnetite (Davis, 1986a, b). The Reilly Peak rhyolite is 36.0±1.4 Ma (K/Ar, Davis, 1986a, b). The porphrytic rhyolite at Reilly Peak is 22.6±0.8 Ma (K/Ar, Davis, 1986a, b) and the Iron Mountain rhyolitic aplite is 29.2±1.1 Ma (K/Ar; Chapin et al., 1978; Robertson, 1986). Better age determinations exist for the rhyolite of Willow Spring in the eastern Sierra Cuchillo and in the San Mateo Mountains. The rhyolite of Willow Springs (or Willow Springs dome)

is 28.2±0.5 Ma (U-Pb on zircon, Michelfelder, 2009) to 27.8±1.0 Ma (fission track, Heyl et al., 1983).

In the San Mateo Mountains, Lynch (2003) determined that the Vicks Peak Tuff, granite porphyry, and overlying rhyolite lava (i.e., rhyolite of Alamosa Canyon) erupted between 28.58 and 28.16 Ma, which is consistent with the age of the rhyolite of Alamosa Canyon as determined in this study (Appendix 4). Although, rhyolite dikes found elsewhere in the San Mateo Mountains have not been dated, they are likely of a similar age. Note that the Taylor Creek rhyolite domes in the northern Black Range erupted during this younger event at approximately 27.9 Ma (Dalrymple and Duffield, 1988; Duffield et al., 1990; Duffield and Dalrymple, 1990); tin deposits are associated with these rhyolite domes (Harrison, 1992).

TABLE 7. Stratigraphic correlations of units in the Montoya Butte quadrangle with units elsewhere in the San Mateo Mountains and Sierra Cuchillo range (excluding Quaternary-Tertiary sedimentary units). Ages of ignimbrites from McIntosh et al. (1992a, b), Lynch (2003) and references cited. Thickness of units in parenthesis from the references cited. *Field relationships (Jahns et al., 1978; Robertson, 1986; Davis, 1986a, b; Michelfelder, 2009) indicate that the rhyolite aplite in the Sierra Cuchillo is younger than the porphyritic rhyolite, but K-Ar age determinations suggest that some of the porphyritic rhyolite could be younger. More age determinations are required on the rhyolites in the Sierra Cuchillo. Yellow highlighted column is the preferred stratigraphic section for the Montoya Butte quadrangle. Age determinations of three samples in this area are in Appendix 6. Crossections are in McLemore (2011).

Sierra Cuchillo, West Side Chise (Jahns et al., 2006)	Sierra Cuchillo, East side Willow Springs (Jahns et al., 2006; Michelfelder, 2009)	Iron Mountain, Sierra Cuchillo (Jahns et al., 1978; Davis, 1986a, b; Robertson, 1986; Michelfelder, 2009)	Sierra Cuchillo, southwestern San Mateo Mountains (this report, modified from Hillard, 1967, 1969; Maldonado 1974, 1980)	San Mateo Mountains (Lynch, 2003)	Southern San Mateo Mountains (Hermann, 1986)	Western San Mateo Mountains (Ferguson et al., 2007)	Central San Mateo Mountains (Ferguson, 1986)
Olivine basalt (30 m)		Olivine basalt	Olivine basalt (0-10 m)				
			Volcaniclastic rocks (0-7 m)	Volcaniclastic rocks	Upper volcaniclastic unit	Volcaniclastic rocks	
						Beartrap Canyon Formation	
		Andesite dikes	Andesite flows (0-7 m)			Andesite lava	
			Turkey Springs Tuff (24.5 Ma) (0-60 m)	Turkey Springs Tuff (24.4 Ma) (70-105 m)	Turkey Springs Tuff (24.4 Ma)	Turkey Springs Tuff (24.4 Ma)	Turkey Springs Tuff (24.4 Ma)
						Andesite lava	Rhyolite lavas
				Volcaniclastic rocks (5-60 m)	Lower volcaniclastic rocks	Unit of East Red Canyon	Unit of East Red Canyon
						Rhyolite	Rhyolite lavas
						South Canyon Tuff (27.4 Ma)	South Canyon Tuff (27.4 Ma)
						Rhyolite lavas	Rhyolite

Sierra Cuchillo, West Side Chise (Jahns et al., 2006)	Sierra Cuchillo, East side Willow Springs (Jahns et al., 2006; Michelfelder, 2009)	Iron Mountain, Sierra Cuchillo (Jahns et al., 1978; Davis, 1986a, b; Robertson, 1986; Michelfelder, 2009)	Sierra Cuchillo, southwestern San Mateo Mountains (this report, modified from Hillard, 1967, 1969; Maldonado 1974, 1980)	San Mateo Mountains (Lynch, 2003)	Southern San Mateo Mountains (Hermann, 1986)	Western San Mateo Mountains (Ferguson et al., 2007)	Central San Mateo Mountains (Ferguson, 1986)
							lavas
			Rhyolite of Alum Spring (0-100? m)		Ash-fall tuff		
							Lemitar Tuff (29.0 Ma)
		Rhyolite aplite (29.2 Ma)*				Rhyolite of Welty Hill	
			Granite of Kelly ; Canyon	Granite		Granite	
	Rhyolite of Willow Springs (28.2 Ma)	Porphyritic rhyolite (22.6 Ma)*, Rhyolite of Willow Springs (28.2 Ma), Iron Mountain rhyolite	Rhyolite of Alamosa Canyon (28.4 Ma) (0-400 m)	Rhyolite lava (28.4 Ma) (550 m)	Alamosa Creek rhyolite (28.4 Ma)	Rhyolite lavas	Rhyolite lavas
			Vicks Peak Tuff (28.4 Ma) (0-400 m)	Vicks Peak Tuff (28.4 Ma) (690 m)	Vicks Peak Tuff (28.4 Ma)	Vicks Peak Tuff (28.4 Ma)	Vicks Peak Tuff (28.4 Ma)
					La Jencia Tuff (28.8 Ma)		La Jencia Tuff (28.8 Ma)
Upper andesite sequence (152 m)		Upper andesite sequence (152 m)			Rock Spring Formation andesites and volcaniclastics		
Rhyolite-trachyte sequence (213 m)	Rhyolite-trachyte sequence (411+ m)	Rhyolite-trachyte sequence (411+ m)					
					Hells Mesa Tuff (32.0 Ma)		
Lower andesite sequence (168 m)	Lower andesite sequence (76 m)	Lower andesite sequence (76 m)			Pre-Hells Mesa Tuff rocks		Basaltic andesite lava
		Reilly Peak rhyolite (36 Ma)	Monzonite plugs				
Dacite-rhyolite sequence (122 m)	Dacite-rhyolite sequence (192+m)	Dacite-rhyolite sequence (192+m) (36.6 Ma)					
Latite-andesite sequence (183+ m)	Latite-andesite sequence (244+ m)	Latite-andesite sequence (244+ m) (36.2 Ma)	latite of Montoya Butte (0-90 m) (35.7 Ma), lahar (0-220 m), andesite of Monticello Box (0-120 m)		Red Rock Ranch Formation andesites and volcaniclastics		
Sierra Cuchillo laccolith		Sierra Cuchillo laccolith, monzonite to granite to rhyolite (38.6 Ma)					
		Andesite (41.0					

Sierra Cuchillo, West Side Chise (Jahns et al., 2006)	Sierra Cuchillo, East side Willow Springs (Jahns et al., 2006; Michelfelder, 2009)	Iron Mountain, Sierra Cuchillo (Jahns et al., 1978; Davis, 1986a, b; Robertson, 1986; Michelfelder, 2009)	Sierra Cuchillo, southwestern San Mateo Mountains (this report, modified from Hillard, 1967, 1969; Maldonado 1974, 1980)	San Mateo Mountains (Lynch, 2003)	Southern San Mateo Mountains (Hermann, 1986)	Western San Mateo Mountains (Ferguson et al., 2007)	Central San Mateo Mountains (Ferguson, 1986)
		Ma)					
Cambrian-Cretaceous sedimentary rocks	Cambrian-Cretaceous sedimentary rocks	Cambrian-Permian sedimentary rocks	Permian sedimentary rocks				

Petrochemistry

Igneous petrologists commonly compare geochemical data to various studies that relate chemical compositions of igneous rocks from throughout the world to plate tectonic settings. A study by Pearce et al. (1984) establishes that igneous rocks formed in various tectonic settings have different chemical signatures. Pearce et al. (1984) refers to these settings as ocean ridge, volcanic arc, syn-collusion (formed by collusion of two plates), and within-plate fields. Rocks formed in these tectonic settings are characterized by well-defined fields on chemical variation plots. Most andesites from the area plot within the volcanic arc or within-plate fields. Most of the rhyolites and ash-flow tuffs from the area plot in the tectonic fields of volcanic arc and within-plate granites (Fig. 25). The similarity in chemical composition of rocks in the quadrangle to the composition of rocks formed in volcanic arc and within-plate tectonic settings infers that the rocks were formed in complex tectonic settings related to the subduction of lithospheric crust (i.e., volcanic arc) and formation of the Rio Grande rift (i.e., extensional tectonic setting). These chemical trends are consistent with current theories of the tectonic evolution of the area (McMillan, 2004).

Formation and age of mineralization and alteration

The Apache Warm Springs deposit and the quartz veins are volcanic-epithermal deposits. A modern analog for the formation of this beryllium mineralization, quartz veins, and associated alteration and would be a geothermal system, such as the Norris Geyser Basin in Yellowstone National Park (Muffler et al., 1971; Henley and Ellis, 1983; Kharaka et al., 2000; Rodgers et al., 2002). The Apache Warm Springs deposit is hosted by rhyolite that could be part of a rhyolite dome similar to the dome found at the junction of Cañada Alamosa and San Mateo Canyon (Fig. 10; McLemore, 2011) and elsewhere in the Sierra Cuchillo and San Mateo Mountains. Red Paint Canyon fault zone likely controlled the emplacement of the rhyolite dome, alteration, and beryllium mineralization. Deposits at Iron Mountain and Reilly Peak in the northern Cuchillo Negro district (south of the Ojo Caliente No. 2 district), contain Fe-Be-W-Sn skarn deposits that are related to chemically-similar rhyolites (Fig. 25; Appendix 3). The rhyolites in the Sierra Cuchillo are 29-22 Ma (Table 7) and adularia from a scheelite skarn at Reilly Peak was dated as 27.3±0.6 Ma (Davis, 1986a). The Iron Mountain deposit formed from boiling saline fluids rich in Na-K-Ca-Cl salts at temperatures between 300-385°C (as determined by fluid inclusion studies by Nkambule, 1988). The Apache Warms Springs deposits likely formed at the same time by similar fluids and temperatures.

Although, the age of the mineral deposits in the Montoya Butte quadrangle cannot be directly determined because of lack of suitable dateable minerals, the age of the mineral deposits can be estimated by stratigraphic position, age of faults, analogy to other deposits, and other geologic evidence. The difference in mineralogy, trace-element chemistry (Appendix 3), associated alteration, and host rocks between the two types of mineral deposits (volcanic-epithermal veins, volcanogenic Be deposits) as described above, suggests that they are not related and formed at different times by two separate hydrothermal (or geothermal) systems.

The volcanic-epithermal veins cut the latite of Montoya Butte, but are not found in the Vicks Peak Tuff, rhyolite of Alamosa Canyon, or Turkey Springs Tuff. Furthermore, these younger rhyolites are not significantly altered by hydrothermal fluids. The veins trend north and northeast, similar to the orientations of some of the faults (Fig. 28), suggesting that the veins and faults are of similar age. These northeast-trending faults appear to be some of the oldest faults, probably older than the caldera, because they have a different orientation than the caldera ring fractures and these faults do not cut the Vicks Peak Tuff. Therefore, the volcanic-epithermal veins likely are at least 36 Ma, but possibly younger than the formation of the Nogal Canyon caldera (28 Ma).

The Apache Warm Springs beryllium deposit and associated alteration is hosted by the rhyolite of Alum Spring, which overlies the latite of Montoya Butte (36 Ma) and likely overlies the Vicks Peak Tuff, and is overlain by the Turkey Springs Tuff (24.4 Ma). Small areas of acid-sulfate alteration, similar to that at the beryllium deposit, are found in rhyolite tuffs and volcaniclastic rocks within the latite of Montoya Butte, especially along faults. The Quaternary sedimentary rocks exposed along Cañada Alamosa west of Monticello Box contain rock fragments and cobbles of altered rhyolite of Alum Spring, indicating that the alteration occurred before deposition of these units. Therefore, the beryllium deposit and associated alteration is older than the Turkey Springs Tuff (24.4 Ma), but is younger than the latite of Montoya Butte, and likely younger than the Vicks Peak Tuff (28 Ma). Similar relationships are found further south in the Cuchillo Negro district, where the Ag-Cu-Pb-Zn veins and skarns are associated with the older 36-38 Ma granitic-rhyolitic rocks and the Fe-Be-W-Sn skarns are associated with the younger 29-27 Ma rhyolites (Jahns, 1944; Davis, 1986a).

The geothermal system represented by the modern warm springs formed recently and is not related to either of these older systems. Most modern geothermal systems have durations of episodic activity of less than 3 million years, and most are less than a few hundred thousand years (P. L. R. Browne, unpublished report, Spring 1992; McLemore, 1993, table 6.5; Silberman, 1985). Therefore, at least three separate geothermal systems were/are present in the Ojo Caliente No. 2 mining district: 1) the oldest system forming the volcanic-epithermal veins (~28-36 Ma), 2) the system forming the Apache Warm Springs beryllium deposit and associated alteration (24.4-28 Ma), and 3) the current, modern system related to Ojo Caliente, Willow Springs, and other warm springs feeding Cañada Alamosa.

Relationship to other altered/mineralized areas in central New Mexico

The rhyolite of Alamosa Canyon, rhyolite of Alum Spring, and rhyolite of Spring Canyon are similar in composition to the tin-bearing Taylor Creek Rhyolite; these rhyolites are metaluminous to weakly peraluminous, high-silica, topaz rhyolites. At

Taylor Creek, 20 vents were active with pyroclastic flows, falls, and surges. The first stage of eruption was followed by extrusion of rhyolite flows forming domes (Duffield et al., 1990). The tin was in the rhyolite magma and as the lava cools and devitrifies, the tin differentiates or is transported by residual fluids into the outer rind of the lava. Subsequent low-temperature convection mobilizes them along faults and within permeable tuffs and rhyolites (Burt and Sheridan, 1981; Duffield et al., 1990). A similar origin is proposed for the beryllium deposits at Spor Mountain, except that the rhyolites were erupted through carbonate sedimentary rocks, which appears to aid in concentration of the beryllium.

The Taylor Creek rhyolite, west of the Montoya Butte quadrangle (Fig. 1), also is a topaz-bearing rhyolite. Topaz-bearing rhyolites are compositionally distinct, rare high-silica rhyolites that are enriched in F, Li, Rb, Cs, U, Th, and Be, and are associated with volcanogenic and epithermal deposits of Be, Sn, U, and F (Burt and Sheridan, 1981; Christiansen et al., 1983). The rhyolites at Spor Mountain also are topaz-bearing, high-fluorine rhyolite lava flows forming domes that are interbedded with tuffs, tuffaceous breccias, and associated fault breccias (Bikum, 1980; Lindsey, 1981; Lindsey and Shawe, 1986). The rhyolite of Alamosa Canyon, rhyolite of Alum Springs, and porphyritic rhyolite and rhyolite aplite at Iron Mountain and Reilly Peak are similar in chemistry to topaz rhyolites; topaz was found in the Iron Mountain rhyolite aplite (Robertson, 1986), but topaz has not been found in the other rhyolites in the Sierra Cuchillo or San Mateo Mountains. Topaz rhyolites appear to be evolved from partial melts of Proterozoic lower crust in an extensional tectonic setting, which is consistent with the formation of the younger 27-29 Ma rhyolites in the Sierra Cuchillo and San Mateo Mountains. The older Reilly Peak rhyolite, Sierra Cuchillo laccolith, and monzonite plugs in the Montoya Butte quadrangle are more similar to other calc-alkaline rhyolites, not topaz rhyolites, and could represent a transition between older arc-related Laramide volcanism and younger extensional Rio Grande volcanism (McMillan et al., 2000).

GEOARCHAEOLOGY

Geoarchaeology is the study of geological processes that effect archaeological sites, or how the geology relates to the mineral resources and archaeologic features. Geoarchaeology uses geologic concepts, methods, and principles for solving archeological problems. The questions addressed in this report include:

- What geomorphic surfaces are the Pueblo sites found?
- What mineral resources were used?

Major Pueblo sites in the Montoya Butte quadrangle

Four major Pueblo sites are found in the Montoya Butte area, which are currently under study (Fig. 7; Laumbach and Laumbach, 2009): Montoya site (Mimbres phase, A.D. 1000-1130, and Socorro phase, A.D. 1100-1200), Victorio site (Tularosa phase, A.D. 1175-1275, with earlier Pueblo components), Pinnacle ruin (Magdalena Phase, A.D. 1250-1400+), and Kelly Canyon site (Socorro Phase, A.D. 1100-1200). Most Pueblo sites are found along the Victorio and Montoya (Qtv and Qtm) terraces, especially at and downstream of the intersection of Kelly Canyon with Cañada Alamosa (Fig. 20, 21). Several pit houses are found on the Montoya terraces (Qtm), and there was likely farming in the floodplains as well as along the terraces near the Pueblo sites. More detailed

information on the Pueblo sites is in Laumbach and Laumbach (2009) and earlier reports. Additional work is underway.

Lithics

A visual analysis of a representative selection of lithic artifacts from the four sites was performed by the author and compared to known lithologies in the quadrangle. The majority of the lithic artifacts, including stone tools, hammer stones, and projectile points found at the Pueblo sites (Laumbach and Laumbach, 2009), are made from local rhyolite and tuff (Vicks Peak tuff, rhyolite of Alamosa Canyon, and rhyolite dikes), and siltstone from the latite of Montoya Butte. Andesite (typically recorded as basalt) was rarely used as tools. Rare manos and matates are rhyolite and vesicular basalt, both of which are found locally. Alkali basalt from local flows was used as grinding stones and could have been traded (Fig. 18). Some of the lithic artifacts, including obsidian, chert, quartzite, and silicified wood, are not found in the immediate area. The chalcedony artifacts could be local or imported from outside Cañada Alamosa. Malachite and azurite are found in several sites that likely came from the Taylor mine or other mines in the San Mateo Mountains. Rare turquoise and beads were imported from outside the canyon. Numerous quartz crystals are found in all sites that came from both locally and elsewhere.

Obsidian arrowheads and flakes are found at the four Pueblo sites and more than 500 samples were analyzed by X-ray fluorescence analysis (XRF; Ferguson et al., 2009a, b). Obsidian from different regions from throughout New Mexico and Arizona have established distinctive geochemical trends, especially in Zr, Nb, Rb, and Sr concentrations (possibly related to geologic source and geologic age; Shackley, 2005), which can be used to determine the sources of obsidian artifacts. Most, if not all, of the obsidian artifacts are from elsewhere in New Mexico and not the Cañada Alamosa area (Ferguson et al., 2009a, b), as determined from comparing chemical analyses of the artifacts with known and suspected sources of obsidian throughout New Mexico (Shackley, 2005). Approximately 31% of the archaeological obsidian from Cañada Alamosa originates from the Mule Creek area in Catron County; approximately 25% of the obsidian originates from the Mt. Taylor volcanic field in Cibola County. Other sources are from Gwynn Canyon and Red Hill, north of Mule Creek, the Jemez Mountains in northern New Mexico (10%) and approximately 13% of the obsidian artifacts originate from a newly identified source in the Magdalena Mountains (Ferguson et al., 2009b; LeTourneau et al., 2010).

Vitrophyre is found in several areas in the Montoya Butte quadrangle where the Vicks Peak Tuff and rhyolite of Alamosa Canyon are exposed, but none of the vitrophyre outcrops found thus far is of significant quality for obsidian artifacts and the chemical composition differs from the chemical composition of the obsidian artifacts.

Clays used in pottery

Hundreds of pottery sherds were collected from the Pueblo sites in Cañada Alamosa area by the archaeologists and nearly 500 pottery samples were analyzed by Instrumental Neutron Activation Analysis (INAA) to determine the chemical composition of the pottery samples (Ferguson and Glascock, 2008; Ferguson et al., 2009a). Local clays were collected by the author and also were analyzed by INAA to determine chemical composition and by clay mineral analysis to determine clay

mineralogy. Possible clay pits have been identified near the Victorio site, Kelly Canyon site, and on a mesa south of the Victorio site (Fig. 47). Another of the local clay sites in the floodplain is shown in Figure 48. A pot was made from this clay by some of the archaeologists to show that the clay could be used in making pottery (Fig. 49). The clays are predominantly illite, smectite, and mixed layered clays (Appendix 5).

Eight compositional groups of pottery samples and clays have been identified (Ferguson and Glascock, 2008; Ferguson et al., 2009a). The local clays correlate with two compositional groups, consisting of common pottery sherds. Some of earliest decorated ceramics appear to be made locally (Mogollon Red/Black and perhaps Mimbres Boldface Black/White), as were the latest (Magdalena Black/White). Most other decorated types are apparently made elsewhere, presumably to the north or the south. The full sequence of Mimbres whitewares was imported from the south while the sequence of San Marcial Black/White, Kiatuthlana Black/White, Socorro Black/White, Tularosa Black/White, and St. Johns Polychrome all appear to be coming from the same general area, suggesting long term contact with a particular northern population. This suggests that local clays were likely used in the production of common pottery, but much of the other pottery samples were made elsewhere and imported into the canyon.

White kaolinite and red kaolinite mixed with hematite are found in Red Paint Canyon (Fig. 40) and could have been a local source of clay for slip for pottery and even perhaps for paints. The Apache people used this source for their red paint.

a b

FIGURE 47. Possible clay pit at the Victorio (a) and Kelly Canyon (b) sites.

FIGURE 48. Clay suitable for pottery, blue-gray clay (sample MONT-54, contains illite and smectite, Appendix 5).

FIGURE 49. Pot made with clay from sample MONT-76.

Building materials

The Pueblo people utilized boulders from the immediate terraces for construction of walls. At the Pinnacle site, the latite of Montoya Butte was used. At the other sites, predominantly rhyolite boulders (Fig. 50, 51; Vicks Peak tuff, rhyolite of Alamosa Canyon, rhyolite dikes), latite of Montoya Butte, and andesite found in the terrace (Qtm,

Qtv) and alluvial (QTsf) deposits were used. Rare basalt boulders from local sources also were used in some walls. Adobe walls made from the local soil were locally utilized as well.

FIGURE 50. Walls of a room block at the Victorio site made of rhyolite boulders with mortar made from local clay.

FIGURE 51. Walls of a room made of latite of Montoya Butte near the top of Montoya Butte.

CONCLUSIONS

Geology of the quadrangle

The Montoya Butte quadrangle includes portions of the Sierra Cuchillo and San Mateo Mountains. Permian sedimentary rocks are exposed in the southwestern portion of the quadrangle and likely underlie much of the area at depth. Volcanic rocks include an

older sequence of andesite, lahar, and latite (around >38-36 Ma) followed by a younger sequence of ash flow tuffs and rhyolite lavas (around 22-29 Ma) associated with the formation of the Nogal Canyon (28.4 Ma) and Bear Trap Canyon (24.4 Ma) calderas in the San Mateo Mountains. Local alkaline basalt flows cut the older Quaternary-Tertiary sedimentary rocks and are similar in composition to basalt flows in central New Mexico that are 2-4 Ma. Local and regional faulting formed the Monticello graben where Alamosa Creek flows, between the San Mateo Mountains and Sierra Cuchillo. Quaternary sedimentary rocks eroded from the San Mateo Mountains and Sierra Cuchillo filled the Monticello graben and formed a series of alluvial fans, pediments and stream terraces. Alamosa Creek cut through the Quaternary sedimentary rocks and the 2-4 Ma basalt flows.

Regional correlations of the rocks

Table 7 summarizes the regional correlations between the rocks in the Montoya Butte quadrangle with rocks in the San Mateo Mountains and Sierra Cuchillo. Since the volcanic flows and rhyolite domes are grossly similar, but erupted over a long period of time (i.e., 22 to >38 Ma), they represent a series of small, but discrete magma pulses: 1) pre-caldera volcanic rocks around >38-36 Ma (possibly related in part to the eruption of the Emery caldera at 34.9 Ma), 2) Nogal Canyon caldera-related rhyolites at 27-29 Ma, 3) rocks related to the Bear Trap caldera (24 Ma), 4) post-caldera rhyolites and andesites (20-24 Ma), and 5) alkali basalts (around 2-4 Ma). The younger 27-29 Ma rhyolites in the Sierra Cuchillo and San Mateo Mountains appear to be evolved from partial melts of Proterozoic lower crust in an extensional tectonic setting. The older Reilly Peak rhyolite, Sierra Cuchillo laccolith, and monzonite plugs in the Montoya Butte quadrangle are more similar to other calc-alkaline rhyolites, not topaz rhyolites, and could represent a transition between older arc-related Laramide volcanism and younger extensional Rio Grande volcanism (McMillan et al., 2000). The formation of the rhyolites is consistent with predominantly fractional crystallization (Bobrow, 1984; Rye et al., 1990). The differences in incompatible trace elements between the different granitic to rhyolite rocks are likely related to either differences in the crustal rocks that were assimilated during magmatic differentiation (McMillan, 2004; Chapin et al., 2004; Michelfelder, 2009) or by minor potential contamination from crustal sources and/or magma mixing (Bobrow, 1984).

Mineral deposits in the Ojo Caliente No. 2 mining district

At least three separate geothermal systems were/are present in the Ojo Caliente No. 2 mining district in the Montoya Butte quadrangle: 1) the oldest system forming the volcanic-epithermal veins (~28-36 Ma), 2) the system forming the Apache Warm Springs beryllium deposit and associated alteration (24.4-28 Ma), and 3) the current, modern system related to Ojo Caliente, Willow Springs, and other warm springs feeding Cañada Alamosa. Copper-silver production has been insignificant from the volcanic-epithermal veins and a small quantity of uranium ore reportedly was produced from the beryllium deposit. The resource potential of the volcanic-epithermal veins is low with a moderate to high degree of certainty because the vein deposits exposed at the surface are low grade and too small for economic development in the current market. The resource potential of the Apache Warm Springs beryllium deposit is low to moderate with a moderate to high

degree of certainty, because the known extent of the beryllium deposit at the surface and in the subsurface where drilled is low grade and too small for economic development in the current market. But, additional exploration drilling could locate additional beryllium. Any potential exploration or subsequent mining would have to plan for environmental issues, especially the affects of mining on the Ojo Caliente and adjacent warm and cold springs feeding the Cañada Alamosa (McLemore, 2008). The mineral-resource potential for geothermal resources, clay, fluorite, and uranium is low with a high degree of certainty. The mineral-resource potential for aggregate is high in the active alluvial and floodplain deposits, but testing would have to be completed to determine the quality of the aggregate resources. There is no resource potential for any other commodities in the quadrangle.

Relationship of the geology to the archaeology

Four major Pueblo sites are found in the Montoya Butte area, which are currently under study: Montoya site (Mimbres phase, A.D. 1000-1130, and Socorro phase, A.D. 1100-1200), Victorio site (Tularosa phase, A.D. 1175-1275, with earlier Pueblo components), Pinnacle ruin (Magdalena Phase, A.D. 1250-1400+), and Kelly Canyon site (Socorro Phase, A.D. 1100-1200). Most Pueblo sites are found along the Victorio and Montoya (Qtv and Qtm) terraces, downstream of the intersection of Kelly Canyon with Cañada Alamosa. Several pit houses are found on the Montoya terraces (Qtm). The majority of the lithic artifacts, including stone tools, hammer stones, and projectile points (Laumbach and Laumbach, 2009), found at the Pueblo sites are made from local rhyolite and tuff (Vicks Peak Tuff, rhyolite of Alamosa Canyon, and rhyolite dikes) and siltstone from the latite of Montoya Butte. Some of the lithic artifacts, including obsidian, chert, quartzite, and silicified wood, are not found in the immediate area and were imported into the canyon. Local clays were likely used in the production of common pottery, but some of the pottery was made elsewhere and imported into the canyon. The Pueblo people utilized boulders from the immediate sites for construction of walls. At the Pinnacle site, the latite of Montoya Butte was used. At the other sites, predominantly rhyolite boulders (Vicks Peak tuff, rhyolite of Alamosa Canyon, rhyolite dikes, latite of Montoya Butte) found in the terrace and alluvial deposits were used. Adobe walls made from the local soil were locally utilized as well.

RECOMMENDATIONS

It is recommended that any deep drill holes be measured for precision temperature logging to assess the geothermal potential and the ground water patterns (Reiter et al., 1975; Reiter, 2005).

REFERENCES

Anderson, E. C., 1957, The metal resources of New Mexico and their economic feature through 1954: New Mexico Bureau of Mines and Mineral Resources, Bulletin 39, 183 p.

Anderholm, S.K., 1987, Hydrogeology of the Socorro and La Jencia basins, Socorro County, New Mexico: U.S. Geological Survey, Water-Resources Investigation Report 84-4342, 62 p.

Anthony, E.Y., Hoffer, J.M., Waggoner, W.K., and Chen, W., 1992, Compositional diversity in late Cenozoic mafic lavas in the Rio Grande rift and Basin and Range province, southern New Mexico: Geological Society of America Bulletin, v. 104, p. 973–979.

Aredt, J.W., Butz, T.R., Cagle, G.W., Kane, V.E. and Nicols, C.E., 1979, Hydrogeochemical and stream sediment reconnaissance procedures of the National Uranium Resource Evaluation project: Oak Ridge Gaseous Diffusion Plant, Report GJBX-32(80), 56 p.

Atwood, G.W., 1982, Geology of the San Juan Peak area, San Mateo Mountains, Socorro County, New Mexico; with special reference to the geochemistry, mineralogy, and petrogenesis of an occurrence of riebeckite-bearing rhyolite: M.S. thesis, University of New Mexico, Albuquerque, 168 p.

Bachman, G.O. and Mehnert, H.H., 1978, New K-Ar dates and the late Pliocene to Holocene geomorphic history of the central Rio Grande region, New Mexico: Geological Society of America, Bulletin, v. 89, p. 283-292.

Bailey, C.E., 2006, A case study of land and water distribution in Canada Alamosa: Individual and community agency in the territorial frontier of southwestern New Mexico: B.A. thesis, College of William and Mary, Williamsburg, VA., 101 p.

Barroll, M.W., 1989, Analysis of the Socorro hydro-geothermal system, central New Mexico: Ph.D. dissertation, New Mexico Institute of Mining and Technology, 247 p.

Barroll, M.W. and Reiter, M., 1990, Analysis of the Socorro hydrogeothermal system: central New Mexico: Journal of Geophysical Research, v. 95, no. B13, p. 21949-21963.

Bartsch-Winkler, S.B. and Donatich, A.J., ed., 1995, Mineral and Energy Resources of the Roswell Resource Area, East-Central New Mexico: U.S. Geological Survey, Bulletin 2063, 145 p.

Barton, M.D. and Young, S., 2002, Non-pegmatitic deposits of beryllium: mineralogy, geology, phase equilibria and origin; *in* E.S. Grew, ed., Beryllium—mineralogy, petrology, and geochemistry: Reviews in Mineralogy and Geochemistry, v. 50, p. 591-691.

Basabilvazo, G.T., 1996, Ground-water resources of Catron County, New Mexico: U.S. Geological Survey, Water Resources Investigations Report 96-4258, 148 p.

Bikum, J.V., 1980, Fluorine and lithophile element mineralization at Spor Mountain, Utah; *in* Burt, D.M. and Sheridan, M.F., Uranium mineralization in fluorine-enriched volcanic rocks: U.S. Department of Energy, Report GJBX-225(80), p. 167-414.

Bisetty, K., 2009, Rare mineral fuelling nuclear ambitions for local investors: Business in Vancouver, p. 3, http://www.ibcadvancedalloys.com/i/pdf/BusinessinVancouver2009-06.pdf (accessed on Feb. 3, 2010).

Blodgett, D.D., 1973, Hydrogeology of the San Augustin Plains, New Mexico: M.S. thesis, New Mexico Institute of Mining and Technology, Socorro, 55 p.

Blodgett, D.D. and Titus, F.B., 1973, Hydrogeology of the San Agustin Plains, New Mexico: New Mexico Bureau of Mines and Mineral Resources, Open-file Report

51, 54 p., http://geoinfo.nmt.edu/publications/openfile/downloads/OFR014-99/51-75/51/ofr_51.pdf.

Bobrow, D.J., 1984, Geochemistry and petrology of Miocene silicic lavas in the Socorro-Magdalena area of New Mexico: M.S. thesis, New Mexico Institute of Mining and Technology, Socorro, 458 p.

Bornhorst, T.J., 1980, Major- and trace-element geochemistry and mineralogy of upper Eocene to Quaternary volcanic rocks of the Mogollon-Datil volcanic field, southwestern New Mexico: Ph.D. dissertation, University of New Mexico, Albuquerque, 1108 p.

Bornhorst, T.J., 1986, Granophile elements in mid-Cenozoic calc-alkalic rhyolitic volcanic rocks, Mogollon-Datil volcanic field, Southwestern New Mexico; *in* Taylor, R.P. and Strong, D.F., eds., Recent advances in the geology of granite-related mineral deposits: The Canadian Institute of Mining and Metallurgy, Special Volume 39, p. 331-341.

Bornhorst, T.J., 1988, Character of mid-Cenozoic andesites, basaltic andesites and related volcanic rocks, Mogollon-Datil volcanic field, southwestern New Mexico; *in* Drexler, J.W., and Larson, E.E., Cenozoic volcanism in the Southern Rocky Mountains updated: A tribute to Rudy C. Epis-Part 2: Colorado School of Mines Quarterly, v. 83, p. 1-13.

Bounessah, M. and Atkin, B.P., 2003, An application of exploratory data analysis (EDA) as a robust non-parametric technique for geochemical mapping in a semi-arid climate: Applied Geochemistry, v. 18, p. 1185-1195.

Brush Engineered Materials, Inc., 2009, Transforming our world and yours: Annual report, 122 p., http://files.shareholder.com/downloads/BW/925738805x0x368575/A9F177AF-D3E5-4546-8707-73F26F14E146/bw2009ar.pdf

Burt, D.M. and Sheridan, M.F., 1981, Model for the formation of uranium/lithophile element deposits in fluorine-rich volcanic rocks; *in* P.C. Goodell and A.C. Waters, Uranium in volcanic and volcaniclastic rocks: American Association of Petroleum Geologists, Studies in Geology No. 13, p. 99-109.

Cagle, G.W., 1977, The Oak Ridge analytical program; in Symposium on hydrogeochemical and stream sediment reconnaissance for uranium in the United States: U.S. Department of Energy, Report GJBX-77(77), p. 133-156.

Carlton, K.R., 1992, Warm Springs special resource study, Socorro County, New Mexico: National Resource Reconnaissance Report, unpublished report, 75 p.

Cather, S.M., McIntosh, W.C., and Chapin, C.E., 1987, Stratigraphy, age, and rates of deposition of the Datil Group (Upper Eocene-Lower Oligocene), west-central New Mexico: New Mexico Geology, v. 9, p. 50-54.

Chapin, C.E., 1978, Overview of Cenozoic features, San Marcial basin; *in* J.W. Hawley, compiler, Guidebook to Rio Grande rift in New Mexico and Colorado: New Mexico Bureau of Mines and Mineral Resources, Circular 163, p. 96-97.

Chapin, C.E., 1989, Volcanism along the Socorro accommodation zone, Rio Grande rift, New Mexico, *in* Chapin, C.E., and Zidek, J., eds., Field excursions to volcanic terranes in the western United States, Vol. I: Southern Rocky Mountain region: New Mexico Bureau of Mines and Mineral Resources, Memoir 46, p. 46–57.

Chapin, C.E., Siemers, W.T., and Osburn, G.R., 1975, Summary of radiometric ages of New Mexico rocks: New Mexico Bureau of Mines and Mineral Resources, Open-file Report 60.

Chapin, C.E., Jahns, R.H., Chamberlin, R.M., and Osburn, G.R., 1978, First day road log from Socorro to Truth or Consequences via Magdalena and Winston; in Field Guild to selected caldrons and mining districts of the Datil-Mogollon volcanic field, New Mexico: New Mexico Geological Society, Special Publication no. 7, p. 17-19.

Chapin, C.E., Wilks, M., and McIntosh, W.C., 2004, Space-time patterns of Late Cretaceous to present magmatism in New Mexico; comparison with Andean volcanism and potential for future volcanism; in Tectonics, geochronology and volcanism in the southern Rocky Mountains and Rio Grande rift: New Mexico Bureau of Geology and Minerals Resources, Bulletin 160, p. 13-40.

Chamberlin, R.M, 2009, Rare-earth geochemical anomaly at Sierra Larga, New Mexico: NURE stream-sediment data suggest a monazite placer deposit in the Permian Gloria Sandstone: New Mexico Geological Society Guidebook 60, p. 71-73.

Cheeney, R.F., 1983, Statistical methods in geology for field and lab decisions: George Allen and Unwin, London, 169 p.

Christiansen, E.H., Burt, D.M., Sheridan, M.F., and Wilson, R.T., 1983, The petrogenesis of topaz rhyolites from the western United States: Contributions Mineralogy and Petrology, v. 83, p. 16-30.

Committee on Beryllium Alloy Exposures, 2007, Health effects of beryllium exposure: a literature review: Committee on Toxicology, National Research Council, 109 p., http://www.nap.edu/catalog/12007.html

Correa, B.P., 1980, Fluorine and lithophile element mineralization in the Black Range and Sierra Cuchillo, New Mexico; *in* Burt, D.M. and Sheridan, M.F., Uranium mineralization in fluorine-enriched volcanic rocks: U.S. Department of Energy, Report GJBX-225(80), p. 459-494.

Correa, B.P.**,** 1981, The Taylor Creek rhyolite and associated tin deposits, southwestern New Mexico: M.S. thesis, Arizona State University, Tempe, 105 p.

Cox, D.P., and Singer, D.A., 1986, Mineral deposit models, U.S. Geological Survey, Bulletin 1693, 379 p.

Cox, E.W., 1985, Geology and gold-silver deposits in the San Jose mining district, southern San Mateo Mountains, Socorro County, New Mexico: M.S. thesis, New Mexico Institute of Mining and Technology, Socorro, 115 p. http://ees.nmt.edu/alumni/papers/1986i_cox%20ii_ew.pdf.

Cunningham, L.D., 2003, Beryllium: U.S. Geological Survey, Minerals Yearbook, 7 p., http://minerals.usgs.gov/minerals/pubs/commodity/beryllium/berylmyb03.pdf.

Cunningham, L.D., 2004, Beryllium recycling in the United States in 2000: U.S. Geologic Survey, Circular 1196-P, 15 p.

Dalrymple, G.B. and Duffield, W.A., 1988, High-precision $^{40}Ar/^{39}Ar$ dating of Oligocene rhyolites from the Mogollon-Datil volcanic field using a continuous laser system: Geophysical Research Letters, v. 15, no. 5, p. 463-466.

Davis, J.M. and Hawkesworth, C.J., 1995, Geochemical and tectonic transitions in the evolution of the Mogollon-Datil volcanic field, New Mexico, USA: Chemical Geology, v. 119, p. 31–53.

Davis, L.L., 1986a, The petrology and geochemistry of the intrusive rocks and associated iron-rich polymetallic skarn at Reilly Peak, New Mexico: M.S. thesis, University of Georgia, Athens, 108 p.

Davis, L.L., 1986b, The Reilly Peak Tertiary (?) Intrusive—A High-Silica Rhyolite: The New Mexico Geological Society, Guidebook 37th Field Conference, p. 167-171.

Deal, E.G., 1973, Geology of the northern part of the San Mateo Mountains, Socorro County, New Mexico: Ph.D. dissertation, University of New Mexico, Albuquerque, 268 p.

Deal, E.G. and Rhodes, R.C., 1976, Volcano-tectonic structures in the San Mateo Mountains, Socorro County, New Mexico: New Mexico Geological Society, Special Publication no. 5, p. 51-56.

De la Roche, H., Leterrier, J., Grandclaude, P. and Marchal, M., 1980, A classification of volcanic and plutonic rocks using R1,R2-diagrams and major element analysis—its relationships with current nomenclature: Chemical Geology, v. 29, p. 183-210.

Duffield, W.A., and Dalrymple, G.B., 1990, The Taylor Creek Rhyolite of New Mexico: a rapidly emplaced field of lava domes and flows: Bulletin of Volcanology, v. 52, p. 475-487.

Duffield, W.A., Reed, B.L., and Richter, D.H., 1990, Origin of rhyolite-hosted tin mineralization: evidence from the Taylor Creek Rhyolite, New Mexico: Economic Geology, v. 85, p. 392-398.

Ellinger, S.T., 1988, A stream sediment geochemical survey of the eastern half of the Capitan Mountains, Lincoln County, New Mexico: M.S. thesis, West Texas State University, Canyon, TX, 108 p.

Ellinger, S.T. and Cepeda, J.C.**,** 1991, A geochemical survey of ferrous and selected base metals in the eastern half of the Capitan Mountains, Lincoln County, New Mexico: New Mexico Geological Society, Guidebook, 42, p. 299-304.

Elston, W.E., Bikerman, M. and Damon, P.E., 1968, Significance of new K-Ar dates from southeastern New Mexico; in Correlation and chronology of ore deposits and volcanic rocks: U.S. Atomic Energy Commission, Annual Program COO-689-100, AT(11-1)-689, Geochronology Labs, University of Arizona, p. AIV-1-AIV-20.

Farkas, S.E., 1969, Geology of the southern San Mateo Mountains, Socorro and Sierra Counties, New Mexico: PhD. Dissertation, University of New Mexico, Albuquerque, 181 p.

Ferguson, C.A., 1986, Geology of the central San Mateo Mountains, Socorro County, New Mexico: New Mexico Bureau of Mines and Mineral Resources, Open-file Report 252, 135 p., http://geoinfo.nmt.edu/publications/openfile/downloads/OFR200-299/251-275/252/ofr_252.pdf.

Ferguson, C.A., Osburn, G.R., and McCraw, D.J., 2007, Preliminary geologic map of the Welty Hill quadrangle, Socorro County, New Mexico: New Mexico Bureau of Geology and Mineral Resources, Map 148, scale 1:24,000, http://geoinfo.nmt.edu/publications/maps/geologic/ofgm/downloads/148/Welty_Hill_v1p-01.pdf.

Ferguson, J.R. and Glascock, M.D., 2008, Instrumental neutron activation analysis pottery from Rio Alamosa and Rio Salado, southwestern New Mexico: unpublished report, 38 p.

Ferguson, J.R., Laumbach, K.W., Lekson, S.H., Laumbach, T.S., and McLemore, V.T., 2009a, The "Ins and Outs" of Cañada Alamosa archaeology: compositional analysis of obsidians, ceramics, and clays from the Cañada Alamosa, Socorro County, New Mexico: abstract and poster presented at the 24th annual meeting of the Society for American Archaeology.

Ferguson, J.R., McLemore, V.T., and Laumbach, K.W., 2009b, Use of compositional analyses of obsidian artifacts in understanding the occupation history of Pueblo Indians in the Canada Alamosa area, Socorro County, New Mexico, *in:* New Mexico Geological Society, 2009 Annual Spring Meeting, Abstracts with Programs, New Mexico Institute Mining and Technology, Socorro, New Mexico, New Mexico Geology, v. 31, no. 2, 51 p.

File, L., and Northrop, S.A., 1966, County, township, and range locations of New Mexico's Mining Districts: New Mexico Bureau of Mines and Mineral Resources Circular 84, 66 p.

Finnegan, N. J. and Pritchard, M. E., 2009, Magnitude and duration of surface uplift above the Socorro magma body, Geology, v. 37, no. 3, pp. 231-234.

Fodor, R.V., 1975, Petrology of basalt and andesite of the Black Range, New Mexico: Geological Society of America Bulletin, v. 86, p. 295-304.

Fodor, R.V., 1978, Ultramafic and mafic inclusions and megacrysts in Pliocene basalt, Black Range, New Mexico: Geological Society of America Bulletin, v. 89, p. 451-459.

Foley, N.K., Seal, R.R., II, Piatak, N.M., and Hetland, B.R., 2010, An occurrence model for the national assessment of volcanogenic beryllium deposits: U.S. Geological Survey Open-File Report 2010-1195, 4 p., http://pubs.usgs.gov/of/2010/1195/, accessed September 5, 2010.

Foruria, J., 1984, Geology, alteration and precious metal reconnaissance of the Nogal Canyon area, San Mateo Mountains, New Mexico: M.S. thesis, Colorado State University, Fort Collins, 178 p.

Frost, B.D., Barnes, C.G., Collins, W.J., Arculus, R.J., Ellis, D.J., and Frost, C.D., 2001, A geochemical classification for granitic rocks: Journal of Petrology, v. 42, no. 11, p. 2033-2048.

Furlow, J.W., 1965, Geology of the San Mateo Peak area, Socorro County, New Mexico: M.S. thesis, University of New Mexico, Albuquerque.

Goudarzi, G. H., 1984, Guide to preparation of mineral survey reports on public lands, U. S. Geological Survey, Open-file Report 84-787, 50 p.

Grew, E.S., 2002, Mineralogy, petrology and geochemistry of beryllium: an introduction and list of beryllium minerals; *in* E.S. Grew, ed., Beryllium—mineralogy, petrology, and geochemistry: Reviews in Mineralogy and Geochemistry, v. 50, p. 1-76.

Griffitts, W.R. and Alminas, H.V., 1968, Geochemical evidence for possible concealed mineral deposits near the Monticello Box, northern Sierra Cuchillo, Socorro County, New Mexico: U.S. Geological Survey, Circular 600, 13 p., http://pubs.er.usgs.gov/usgspubs/cir/cir600.

Gross, G.W. and Wilcox, R., 1983, Groundwater circulation in the Socorro geothermal area: New Mexico Geological Society, Guidebook 34, p. 311-318.

Grunsky, E.C., 2010, The interpretation of geochemical survey data: Geochemistry: Exploration, Environment, Analysis, v. 10, p. 27-74.

Haag, D.M., 1991, Late Oligocene to Early Pleistocene basalts of southwestern New Mexico: M.S. thesis, New Mexico State University, Las Cruces, 77 p.

Hawkes, H.E. and Webb, J.S., 1962, Geochemistry in mineral exploration: Harper, New York.

Hall, J.S., 2004, New Mexico Bureau of Mines and Mineral Resource's Clay Laboratory Manual: Unpublished New Mexico Bureau of Geology and Mineral Resources report.

Hansel, J.M. and Martell, C.J., 1977, Automated energy-dispersive X-ray determination of trace elements in streams: U.S. Department of Energy Report GJBX-52(77), 8 p.

Harley, G.T., 1934, The geology and mineral resources of Sierra County, New Mexico; New Mexico Bureau of Mines and Mineral Resources, Bulletin 10, 220 p.

Harrison, R.W., 1989, Geology of Winston 7 ½' quadrangle, Sierra County, New Mexico: New Mexico Bureau of Mines and Mineral Resources, Open-file Report OF-358, 19 p., http://geoinfo.nmt.edu/publications/openfile/downloads/OFR300-399/351-375/358/ofr_358.pdf.

Harrison, R.W., 1992, Cenozoic stratigraphy, structure, and epithermal mineralization of north-central Black Range, New Mexico in the regional geologic framework of south-central New Mexico: Ph.D. Dissertation, New Mexico Institute of Mining and Technology, Socorro, 444 p., http://ees.nmt.edu/alumni/papers/1992d_harrison_rw.pdf.

Harrison, R.W., 1994, Winston graben: Stratigraphy, structure, and tectonic setting: in Keller, G.R. and Cather, S.M., eds., Basins of the Rio Grande rift: Structure, Stratigraphy, and tectonic setting: Geological Society of America, Special Paper 291, p. 227-240.

Haxel, G.B., 2002, Geochemical evaluation of the NURE data for the southwest United States (abstr.): Geological Society of America, Abstracts with Programs, v. 34, no. 6, p. 340.

Hawley, J.W. and Kottolowski, F.E, 1969, Quaternary geology of the south-central New Mexico; in F.E. Kottlowski and D. LeMone, eds., Border stratigraphy symposium: New Mexico Bureau of Mines and Mineral Resources, Circular 104, p. 89-104.

Henley, R. W., 1985, The geothermal framework for epithermal deposits; *in* Burger, B. R. and Bethke, P. M., eds., Geology and geochemistry of epithermal systems: Reviews in Economic Geology, v. 2, p. 1-24.

Henley, R. W. and Brown, K. L., 1985, A practical guide to the thermodynamics of geothermal fluids and hydrothermal ore deposits; *in* Berger, B. R. and Bethke, P. M., eds., Geology and geochemistry of epithermal systems: Reviews in Economic Geology, v. 2, p. 25-44.

Henley, R.W., and Ellis, A.J., 1983, Geothermal systems, ancient and modern: a geochemical review: Earth Science Reviews, v. 19, p. 1–50.

Hermann, M.L., 1986, Geology of the southwestern San Mateo Mountains, Socorro County, New Mexico: M.S. thesis, New Mexico Institute of Mining and Technology, Socorro, 202 p., http://ees.nmt.edu/alumni/papers/1986t_hermann_ml.pdf.

Heyl, A.V., Maxwell, C.H., and Davis, L.L., 1983, Geology and mineral deposits of the Priest Tank quadrangle, Sierra County, New Mexico: U.S. Geological Survey Miscellaneous Field Studies Map MF-1665, map scale 1:24,000.

Hillard, P.D., 1967, General geology and beryllium mineralization near Apache Warm Springs, Socorro County, New Mexico: M.S. thesis, New Mexico Institute of Mining and Technology, Socorro, 58 p., http://ees.nmt.edu/alumni/papers/1967t_hillard_pd.pdf.

Hillard, P.D., 1969, Geology and beryllium mineralization near Apache Warm Springs, Socorro County, New Mexico: Socorro, New Mexico Bureau of Mines and Mineral Resources Circular 103, 16 p.

Hunt, C.B., 1978, Surficial geology of southwest New Mexico: New Mexico Bureau of Mines and Mineral Resources, Geologic Map 42, scale 1:500,000.

Irvine, T.N., and Baragar, W.R.A., 1971, A guide to the chemical classification of the common volcanic rocks: Canadian Journal of Earth Sciences, v. 8, p. 523-548.

Jahns, R.H., 1943, Tactite rocks of the Iron Mountain district, Sierra and Socorro Counties, New Mexico: Ph.D. dissertation, California Institute of Technology, Pasadena, 153 p.

Jahns, R.H., 1944a, Beryllium and tungsten deposits of the Iron Mountain district, Sierra and Socorro Counties, New Mexico: U.S. Geological Survey, Bulletin 945-C, p. 45-79.

Jahns, R.H., 1944b, "Ribbon rock," an unusual beryllium-bearing tactite: Economic Geology, v. 39, p. 175-205.

Jahns, R.H., 1955, Geology of the Sierra Cuchillo, New Mexico: New Mexico Geological Society Guidebook, 6th Field Conference, p. 158-174.

Jahns, R.H., McMillan, D.K., and O'Brient, J.D., 2006, Preliminary geologic map of the Chise quadrangle, Sierra County, New Mexico: New Mexico Bureau of Geology and Mineral Resources, Open-file Map Series OFGM-115, scale 1:24,000, http://geoinfo.nmt.edu/publications/maps/geologic/ofgm/details.cfml?Volume=115.

Jahns, R.H., McMillan, D.K., O'Brient, J.D., and Fisher, D.L., 1978, Geologic section in the Sierra Cuchillo and flanking areas, Sierra and Socorro Counties, New Mexico, in Chapin, C.E., and Elston, W.E., eds., Field guide to selected cauldrons and mining districts of the Datil-Mogollon volcanic field, New Mexico: New Mexico Geological Society Special Publication 7, p. 131-138.

Jaskula, B.W., 2009, Beryllium: U.S. Geological Survey, Mineral Commodity Reports, 7 p., http://minerals.usgs.gov/minerals/pubs/commodity/beryllium/myb1-2007-beryl.pdf

Johnson, D.M., Hooper, P.R., and Conrey, R.M., 1999, XRF analysis of rocks and minerals for major and trace elements on a single low dilution Li-tetraborate fused bead: JCPDS-International Centre for Diffraction Data, p. 843-867.

Julyan, R., 1998, The place names of New Mexico: University of New Mexico Press, Albuquerque, 2nd edition, 385 p.

Keith, S.B., Gest, D.E., DeWitt, E., Tull, N.W., and Everson, B.A., 1983, Metallic mineral districts and production in Arizona: Arizona Bureau of Geology and Mineral Technology, Bulletin 194, 58 p.

Kharaka, Y.K., Sorey, M.L., and Thordsen, J.J., 2000, Large-scale hydrothermal fluid discharges in the Norris-Mammoth corridor, Yellowstone National Park, USA: Journal of Geochemical Exploration, v. 69-70, p. 201-205.

Kucks, R.P., Hill, P.L., and Heywood, C.E., 2001, New Mexico magnetic and gravity maps and data; a web site for distribution of data: U.S. Geological Survey, Open-file Report 01-0061, http://greenwood.cr.usgs.gov/pub/open-file-reports/ofr-01-0061/ (January 2009).

Lasky, S.G., 1932, The ore deposits of Socorro County, New Mexico: New Mexico Bureau of Mines and Mineral Resources, Bulletin, 8, 139 p.

Laughlin, A.W., Cole, G.L., Freeman, S.H., Aldrich, M.J., and Maassen, L.W., 1985, A computer assisted mineral resource assessment of Socorro and Catron Counties, New Mexico: Geology and Geochemistry Group, Earth and Space Sciences Division, Los Alamos National Laboratory, Los Alamos, New Mexico, unclassified report LA-UR-85-375.

Laumbach, K.W. and Laumbach, T.S., 2009, Cañada Alamosa project: A preliminary report on the 2005 research season: Human Systems Research report No. 2005-24, 295 p.

Le Bas, M.J., Le Martre, R.W., Streckusen, A., and Zanettin, B., 1986, A chemical classification of volcanic rocks based on the total alkali-silica diagram: Journal of Petrology, v. 27, p. 745-750.

LeMaitre, R. W., ed., 1989, A classification of igneous rocks and glossary of terms: Blackwell Scientific Publications, Oxford, Great Britain, 193 p.

LeTourneau, P.D., Ferguson, J.R., and McLemore, V.T., 2010, Alameda Springs, a newly characterized obsidian source in west-central New Mexico: Society for American Archaeology, annual meeting presentation, St. Lousi, MO, April 14-18, p. 149, http://www.saa.org/Portals/0/J_M.pdf, accessed on May 28, 2010.

Lindgren, W., Graton, L. C., and Gordon, C. H., 1910, The ore deposits of New Mexico: U.S. Geological Survey, Professional Paper 68, 361 p.

Lindsey, D.A., 1981, Volcanism and uranium mineralization at Spor Mountain, Utah; in P.C. Goodell and A.C. Waters, eds., Uranium in volcanic and volcaniclastic rocks: American Association of Petroleum Geologists, Studies in Geology No. 13, p. 89-98.

Lindsey, D.A. and Shawe, D.R., 1986, Spur Mountain Be-F-U deposits; *in* R.L. Erickson, Characteristics of mineral deposit occurrences: U.S. Geological Survey, Open-file Report 82-795, p. 67-69.

Lovering, T.G. and Heyl, A.V., 1989, Mineral belts in western Sierra County, New Mexico, suggested by mining districts, geology, and geochemical anomalies: U.S. Geological Survey, Bulletin 1876, 58 p., http://pubs.er.usgs.gov/usgspubs/b/b1876.

Lozinsky, R.P., 1986, Geology and late Cenozoic history of the Elephant Butte area, Sierra County, New Mexico: New Mexico Bureau of Mines and Mineral Resources, Circular 187, 40 p.

Lozinsky, R.P., 1987, Cross section across the Jornada del Muerto, Engle, and northern Palomas Basins, south-central New Mexico: New Mexico Geology, v. 9, no. 3, p. 55-57, 63.

Lund, J.W. and Witcher, J.C. 2002, Truth or Consequence, New Mexico—A spa city: Geo-Heat Center Quarterly Bulletin, v. 23, no. 4, December, p. 20-24.

Lynch, S.D., 2003, Geologic mapping and $^{40}Ar/^{39}Ar$ geochronology in the northern Nogal Canyon caldera, within and adjacent to the southwest corner of the Blue Mountain quadrangle, San Mateo Mountains, New Mexico: M.S. thesis, New Mexico Institute of Mining and Technology, 102 p., http://ees.nmt.edu/alumni/papers/2003t_lynch_sd.pdf.

Machette, M.N., 1987, Preliminary assessment of Quaternary faulting near Truth or Consequences, New Mexico: U.S. Geological Survey, Open-file Report 87-652, 41 p., http://pubs.er.usgs.gov/usgspubs/ofr/ofr87652.

Machette, M.N., Personius, S.F., Kelson, K.I., Dart, R.L., and Haller, K.M., 1998, Map and data for Quaternary faults and folds in New Mexico: U.S. Geological Survey, Open-file Report 98-521, 367 p., http://pubs.er.usgs.gov/usgspubs/ofr/ofr98521.

Majkowski, L.**,** 2009, Deflection of Rio Salado terraces due to uplift of the Socorro magma body, Socorro, New Mexico: M.S. thesis, New Mexico Institute of mining and Technology, Socorro, 78 p.

Maldonado, F., 1974, Geologic map of the northern part of the Sierra Cuchillo, Socorro and Sierra Counties, New Mexico: M.S. thesis, University of New Mexico, Albuquerque, 59 p.

Maldonado, F., 1980, Geologic map of the northern part of the Sierra Cuchillo, Socorro and Sierra Counties, New Mexico: U.S. Geological Survey, Open-File Report 80-230, map scale 1:24,000, http://pubs.er.usgs.gov/usgspubs/ofr/ofr80230.

Marvin, R.F., Mehnert, H.H., and Naeser, C.W., 1988, U.S. Geological Survey radiometric ages-compilation C: part 2: Arizona and New Mexico: Isochron/West, v. 51, p. 5-13.

Mason, G.T., Jr. and Arndt, R.E., 1996, Mineral resources data system (MRDS): U.S. Geological Survey, Digital Data Series DDS-20, CD-ROM.

Matschullat, J., Ottenstein, R., and Reimann, C., 2000, Geochemical background—can we calculate it?: Environmental Geology, v. 39, no. 9, p. 990-1000.

Maxwell, C.H. and Oakman, M.R., 1990, Geologic map of the Cuchillo quadrangle, Sierra County, New Mexico: U.S. Geological Survey, Geologic Quadrangle Map GQ-1686, scale 1:24,000, http://ngmdb.usgs.gov/Prodesc/proddesc_1197.htm.

McDowell, T.W., and Claubaugh, S.E., 1979, Ignimbrites of the Sierra Madre Occidental and their relation to the tectonic history of western Mexico: Geological Society of America, Special Paper 180, p. 113-124.

McGraw, D.J., 2003a, Quaternary geology of the Montoya Butte 7.5 minute quadrangle, Socorro County, New Mexico: New Mexico Bureau of Geology and Mineral Resources, Open-file Report OF-GM 69-Q, scale 1:24,000, http://geoinfo.nmt.edu/publications/maps/geologic/ofgm/details.cfml?Volume=69 accessed February 10, 2010.

McGraw, D.J., 2003b, Quaternary geology of the Dusty 7.5 minute quadrangle, Socorro County, New Mexico: New Mexico Bureau of Geology and Mineral Resources, Open-file Report OF-GM 66-Q, scale 1:24,000,

http://geoinfo.nmt.edu/publications/maps/geologic/ofgm/details.cfml?Volume=66 accessed February 10, 2010.

McGraw, D.J., 2003c, Quaternary geology of the Wahoo Ranch 7.5 minute quadrangle, Socorro County, New Mexico: New Mexico Bureau of Geology and Mineral Resources, Open-file Report OF-GM 68-Q, scale 1:24,000, http://geoinfo.nmt.edu/publications/maps/geologic/ofgm/details.cfml?Volume=68 accessed February 10, 2010.

McIntosh, W.C., Kedzie, L.L. and Sutter, J.F., 1991, Paleomagnetic and $^{40}Ar/^{39}Ar$ dating database for Mogollon-Datil ignimbrites, southwestern New Mexico: New Mexico Bureau of Mines and Mineral Resources, Bulletin 135, 79 p.

McIntosh, W.C., Chapin, C.E., Ratté, J.C. and Sutter, J.F., 1992a, Time-stratigraphic framework for the Eocene-Oligocene Mogollon-Datil volcanic field southwestern New Mexico: Geological Society of America Bulletin, v. 104, p. 851-871.

McIntosh, W.C., Geissman, J.W., Chapin, C.E., Kunk, M.J. and Henry, C.D., 1992b, Calibration of the latest Eocene-Oligocene geomagnetic polarity time sale using $^{40}Ar/^{39}Ar$ dated ignimbrites: Geology, v. 20, p. 459-463.

McLemore, V. T., 1985, Evaluation of mineral-resource potential in New Mexico: New Mexico Geology, v. 7, no. 2, p. 50-53.

McLemore, V.T., 1993, Geology and geochemistry of the mineralization and alteration in the Steeple Rock district, Grant County, New Mexico and Greenlee County, Arizona: Ph.D. dissertation, University of Texas at El Paso; also New Mexico Bureau of Mines and Mineral Resources, Open-File Report 397, 526 p., http://geoinfo.nmt.edu/publications/openfile/downloads/OFR300-399/376-399/397/ofr_397.pdf.

McLemore, V.T., 1996, Volcanic-epithermal precious-metal deposits in New Mexico; *in* Cyner, A. R. and Fahey, P. L., eds., Geology and ore deposits of the American Cordillera: Geological Society of Nevada Symposium Proceedings, Reno/Sparks, Nevada, April 1995, p. 951-969.

McLemore, V.T., 2001, Silver and gold resources in New Mexico: New Mexico Bureau of Mines and Mineral Resources, Resource Map 21, 60 p.

McLemore, V.T., 2008, Beryllium exploration and mining, upper Cañada Alamosa, Socorro County, New Mexico: unpublished preliminary report, 14 p.

McLemore, V.T., 2010a, Use of the New Mexico Mines Database and ArcMap in Uranium Reclamation Studies: Society of Mining, Metallurgy and Exploration Annual Convention, Phoenix, Feb 2010, Preprint 10-125, 10 p., http://geoinfo.nmt.edu/staff/mclemore/documents/10-125.pdf

McLemore, V.T., 2010b, Beryllium Deposits in New Mexico, including evaluation of The NURE Stream Sediment Data: New Mexico Bureau of Geology and Mineral Resources, Open file Report, http://geoinfo.nmt.edu/publications/openfile/details.cfml?Volume=533.

McLemore, V.T., 2010c, Beryllium deposits in New Mexico and adjacent areas: abstract and poster presentation, Society of Economic Geologists, October, 2010.

McLemore, V.T., 2011, Geologic map of the Montoya Butte quadrangle, Socorro County, New Mexico: New Mexico Bureau of Geology and Mineral Resources, Open-file Geologic Map, scale 1:12,000.

McLemore, V.T. and Chamberlin, R.M., 1986, National Uranium Resource Evaluation (NURE) data available through New Mexico Bureau of Mines and Mineral Resources: New Mexico Bureau of Mines and Mineral Resources, pamphlet, 11 p., http://geoinfo.nmt.edu/libraries/nure/NURE_data.pdf

McLemore, V.T., and Chenoweth, W.C., 1989, Uranium resources in New Mexico: New Mexico Bureau of Mines and Mineral Resources, Resource Map 18, 37 p.

McLemore, V. T., Donahue, K., Breese, M., Jackson, M. L., Arbuckle, J., and, Jones, G., 2001, Mineral-resource assessment of Luna County, New Mexico: New Mexico Bureau of Mines and Mineral Resources, Open file Report 459, 84 p., CD-ROM.

McLemore, V.T. and Frey, B.A., 2009, Appendix 8—Quality control and quality assurance report (Task B1); *in* McLemore, V.T., Dickens, A., Boakye, K., Campbell, A., Donahue, K., Dunbar, N., Gutierrez, L., Heizler, L., Lynn, R., Lueth, V., Osantowski, E., Phillips, E., Shannon, H., Smith, M., Tachie-Menson, S., van Dam, R., Viterbo, V.C., Walsh, P., and Wilson, G.W., Characterization of Goathill North Rock Pile: New Mexico Bureau of Geology and Mineral Resources, Open-file report 523, http://geoinfo.nmt.edu/publications/openfile/details.cfml?Volume=523.

McLemore, V. T., Hoffman, G., Smith, M, Mansell, M., and Wilks, M., 2005a, Mining districts of New Mexico: New Mexico Bureau of Geology and Mineral Resources, Open-file Report 494, CD-ROM.

McLemore, V. T., Krueger, C. B., Johnson, P., Raugust, J. S., Jones, G. E., Hoffman, G. K. and Wilks, M., 2005b, New Mexico Mines Database: Society of Mining, Exploration, and Metallurgy, Mining Engineering, February, p. 42-47.

McLemore, V.T., McIntosh, W.C., and Pease, T.C., 1995, $^{40}Ar/^{39}Ar$ age determinations of four plutons associated with mineral deposits in southwestern New Mexico: New Mexico Bureau of Mines and Mineral Resources, Open-file Report OF-410, 36 p., http://geoinfo.nmt.edu/publications/openfile/downloads/OFR400-499/400-425/410/ofr_410.pdf.

McMillan, D.K., 1979, Crystallization and metasomatism of the Cuchillo Mountain laccolith, Sierra County, New Mexico: Ph.D. dissertation, Sanford University, 307 p.

McMillan, N.J., Dickins, A.P., and Haag, D., 2000, Evolution of magma source regions in the Rio Grande rift, southern New Mexico: Geological Society of America, Bulletin, v. 112, p. 1582-1593.

Meeves, H.C., 1966, Nonpegmatitic beryllium occurrences in Arizona, Colorado, New Mexico, Utah and four adjacent states: U.S. Bureau of Mines, Report of Investigations 6828, 68 p.

Michelfelder, G.S., 2009, Petrology and geochemistry of the Upper Eocene Sierra Cuchillo laccolith, Sierra County, New Mexico: M.S. thesis, New Mexico State University, Las Cruces, 186 p.

Michelfelder, G.S. and McMillan, N.J., 2009, Geochemical and geochronological analysis of the Cuchillo Mountain laccolith, Sierra County, New Mexico (abstr.): New Mexico Geology, v. 31, no. 2, p. 44.

Mining Engineering, 2002, News briefs, The Beryllium Group: Mining Engineering, February, p. 14.

Morgan, P. and Daggett, P.H., 1981, Active and passive seismic studies of geothermal resources in New Mexico and investigations of earthquake hazards to geothermal development: New Mexico Energy Research and Development Program, Report EMD 77-2203, 61 p.

Muffler, L.J.P., White, D.E., and Truesdell, A.H., 1971, Hydrothermal explosion craters in Yellowstone National Park: Geological Society of America, Bulletin, v. 82, p. 723–740.

Myers, R.G., Everheart, J.T., and Wilson, C.A., 1994, Geohydrology of the San Agustin basin, Alamosa Creek basin upstream from Monticello Box, and upper Gila basin in parts of Catron, Socorro, and Sierra Counties, New Mexico: U.S. Geological Survey, Water Survey Investigations Report 94-4125, 75 p., http://pubs.er.usgs.gov/usgspubs/wri/wri944125.

Nkambule, M.V., 1988, Skarn mineralization at Iron Mountain, New Mexico, in light of fluid inclusion studies: M.S. thesis, New Mexico Institute of Mining and Technology, Socorro, 60 p.

New Mexico Bureau of Geology and Mineral Resources, 2003, Geologic map of New Mexico: New Mexico Bureau of Geology and Mineral Resources, scale 1:500,000.

New Mexico Bureau of Mines and Mineral Resources, New Mexico State University Southwest Technology Institute, and TRC Mariah Associates, Inc., 1998, Mineral and energy resource assessment of the McGregor Range (Fort Bliss), Otero County, New Mexico: New Mexico Bureau of Mines and Mineral Resources Open-file report 456, 543 p., http://geoinfo.nmt.edu/publications/openfile/downloads/OFR400-499/451-475/456/ofr-456.pdf

North, R.M., and McLemore, V.T., 1986, Silver and gold occurrences in New Mexico: New Mexico Bureau of Mines and Mineral Resources, Resource Map 15, 32 p., 1 map.

O'Donnell, Jr., T.M., Miller, K.C., and Witcher, J.C., 2001, A seismic and gravity study of the McGregor geothermal system, southern New Mexico: Geophysics, v. 66, no. 4., p. 1002-1014.

Osburn, G.R., compiler, 1984, Socorro County geologic map: New Mexico Bureau of Mines and Mineral Resources Open-File Report 238, 14 p., 1 sheet, http://geoinfo.nmt.edu/publications/openfile/downloads/OFR200-299/226-250/238/ofr_238.pdf.

P and E Mining Consultants Inc., 2009, Technical report on the Warm Springs beryllium property, Socorro, County, New Mexico USA: unpublished report for BE Resources Inc., 52 p.

Pazzaglia, F.J. and Hawley, J.W., 2004, Neogene (rift flank) and Quaternary geology and geomorphology: New Mexico Geological Society, Special Publication 11, p. 407-437.

Pearce, J.A., Harris, N.B.W. and Tindle, A.G., 1984, Trace element discrimination diagrams for the tectonic interpretation of granitic rocks: Journal of Petrology, v. 24, p. 956–983.

Ray, L.L. and Smith, J.F., 1940, Glacial chronology of southern Rocky Mountains: Geological Society of America, Bulletin, v. 51, no. 12, p. 1851-1917.

Renne, P.R., Swisher, C.C., Deino, A.L., Karner, D.B., Owens, T.L., and DePaolo, D.J., 1998, Intercalibration of standards, absolute ages and uncertainties in $^{40}Ar/^{39}Ar$ dating: Chemical Geology, v. 145, p. 117-152.

Reimann, C. and Filzmoser, P., 2000, Normal and lognormal data distribution in geochemistry: death of a myth. Consequences for the statistical treatment of geochemical and environmental data: Environmental Geology, v. 39, no. 9, p. 1001-1014.

Reimann, C., Filzmoser, P. and Garrett, R.G., 2005, Background and threshold: critical comparison of methods of determination: Science of the Total Environment, v. 346, p. 1-16.

Reimann, C., Filzmoser, P., and Garrett, R.G., 2002, Factor analysis applied to regional geochemical data: problems and possibilities: Applied Geochemistry, v. 17, p. 185-206.

Reiter, M, 2005, Potential ambiguities in sub-surface temperature logs-Consideration of groundwater flow and ground surface temperature change: Pure and Applied Geophysics, v. 162, p. 343-355.

Reiter, M., Edwards, C.L., Hartman, H., and Weidman, C. 1975, Terrestrial heat flow along the Rio Grande rift, New Mexico and southern Colorado: Geological Society of America, Bulletin, v. 86, p. 811-818.

Robertson, D.E., 1986, Skarn mineralization at Iron Mountain, New Mexico: M.S. thesis, Arizona State University, 76 p.

Rodgers, K.A., Cook, K.L., Browne, P.R.L., and Campbell, K.A., 2002, The mineralogy, texture and significance of silica derived from alteration by steam condensate in three New Zealand geothermal fields: Clay Minerals, v. 37, p. 299-322.

Rollinson, H., 1993, Using geochemical data: evaluation, presentation, interpretation: Pearson Education Ltd., Essex, England, 352 p.

Roybal, F.E., 1991, Ground-water resources of Socorro County, New Mexico: U.S. Geological Survey, Water Resources Investigations Report 89-4083, 108 p., http://pubs.er.usgs.gov/usgspubs/wri/wri894083.

Rudnick, R.L. and Gao, C., 2005, Composition of the continental crust; in R.L. Rudnick, ed., The Crust: Treatise on Geochemistry, v. 3, Elsevier, San Diego, California, p. 1-64.

Rye, R.O., Lufkin, J.L., and Wasserman, M.D., 1990, Genesis of the rhyolite-hosted tin occurrences in the Black Range, New Mexico, as indicated by stable isotope studies; in H.J. Stein and J.L, Hannah, Ore-bearing granite systems; Petrogenesis and mineralizing processes: Geological Society of America, Special Paper 246, p. 233-250.

Sabey, P., 2005, Beryllium minerals; *in* Kogel, J.E, Trivedi, N.C., Barker, J.M., and Krukowski, S.T., ed., Industrial Minerals volume, 7th edition: Society for Mining, Metallurgy, and Exploration, Littleton, Colorado, p. 263-274.

Sharp, R.R., Jr. and Aamodt, P.L., 1978, Field procedures for the uranium hydrogeochemical and stream sediment reconnaissance by the Los Alamos Scientific Laboratory: U.S. Department of energy, Report GJBZ-68(78), 64 p.

Shawe, D.R., 1966, Arizona-New Mexico and Nevada-Utah beryllium belts: U.S. Geological Survey, Professional Paper 550-C, p. C206-C213.

Seager, W.R., 1975, Cenozoic tectonic evolution of the Las Cruces area, New Mexico: New Mexico Geological Society, Guidebook 26, p. 241-250.
Seager, W.R., Shafiqullah, M., Hawley, J.W., and Marvin, R.F., 1984, New K-Ar dates from basalts and the evolution of the southern Rio Grande rift: Geological Society of America, Bulletin, v. 95, p. 87-99.
Shackley, M.S., 2005, Obsidian, geology and archaeology in the North American southwest: University of Arizona Press, Tucson, 246 p.
Shand, S.J., 1943, The eruptive rocks: 2nd edition, John Wiley, New York, 444 p.
Silberman, M.L., 1985, Geochronology of hydrothermal alteration and mineralization: Tertiary epithermal precious-metal deposits in the Great Basin; in E.W. Tooker, ed., Geologic characteristics of sediment-hosted disseminated gold deposits—Search for an occurrence model: U.S. Geological Survey, Bulletin 1646, p. 55-70.
Smith, S.M., 1997, National geochemical database: reformatted data from the National Uranium Resource Evaluation (NURE) Hydrogeochemical and Stream Sediment Reconnaissance (HSSR) Program, version 1.4 (2006): U.S. Geological Survey Open-file Report 97-492. http://pubs.usgs.gov/of/1997/ofr-97-0492/
Smith, W.R., 1992, Geology of the southwestern margin of the Nogal Canyon cauldron, San Mateo Mountains, Sierra and Socorro Counties, New Mexico: M.S. thesis, University of Texas of the Permian Basin, Odessa, 96 p.
Steiger, R.H., and Jäger, E., 1977, Subcommission on geochronology: Convention on the use of decay constants in geo- and cosmochronology: Earth and Planet. Sci. Lett., v. 36, p. 359-362.
Stone, W.J., 1977, Preliminary hydrologic maps of the Socorro Peak area: New Mexico Bureau of Mines and Mineral Resources, Open-file maps, 4 sheets.
Stone, W.J. and Mizell, N.H., 1977, Geothermal resources of New Mexico—A survey of work to date: New Mexico Bureau Mines Mineral Resources, Open-file Report, OF-73, 123 p.
Sullivan, J.B., 1994, A New Mexican family Tafoya-Sullivan and the origins of Sierra County: Burke Publishing Co., San Antonio, TX, 144 p.
Summers, W.K, 1965, A preliminary report on New Mexico's geothermal energy resources: New Mexico Bureau Mines Mineral Resources, Circular 80, 41 p.
Summers, W.K., 1972, Geothermal resources of New Mexico: New Mexico Bureau Mines Mineral Resources, Resource Map 1, scale 1:1,000,000.
Summers, W.K., 1976, Catalog of thermal waters in New Mexico: New Mexico Bureau of Mines and Mineral Resources, Hydrologic Report 4, 80 p.
Swanberg, C.A., compiler, 1980, Geothermal resources of New Mexico: New Mexico Energy Institute, New Mexico State University, 1:500,000 scale.
Taylor, J.R., 1982, An Introduction to Error Analysis: The Study of Uncertainties in Physical Measurements: Univ. Sci. Books, Mill Valley, Calif., 270 p.
Taylor, T.P., Ding, M., Ehler, D.S., Formena, T.M., Kaszuba, J.P., and Sauer, N.N., 2003, Beryllium in the environment: a review: Journal of Environmental Science and Health, Part A, Toxic/Hazardous substances and environmental engineering, v. A38, no. 2, p. 439-469.
Taylor, R.B., and Steven, T.A., 1983, Definition of mineral-resource potential: Economic Geology, v. 78, p. 1268-1270.
U.S. Bureau of Mines, 1927-1990, Mineral yearbook: Washington, D.C., U.S.

Government Printing Office, variously paginated.
U.S. Bureau of Mines, 1995, MAS/MILS CD-ROM: U.S. Bureau of Mines, Special Publication 12-95, CD-ROM.
U.S. Geological Survey, 1902-1927, Mineral resources of the United States (1901-1923): Washington, D.C., U.S. Government Printing Office, variously paginated.
U.S. Geological Survey and New Mexico Bureau of Mines and Mineral Resources**,** 1981, Energy resources map of New Mexico: U.S. Geological Survey, Miscellaneous Investigations Series Map I-1327, scale 1:500,000
Watrus, J.M., 1998, A regional geochemical atlas for part of Socorro County, New Mexico: M.S. thesis, New Mexico Institute of Mining and Technology, Socorro, NM, 176 p., also New Mexico Bureau of Geology and Mineral Resources, Open-file Report OF-445, http://geoinfo.nmt.edu/ publications/openfile/details.cfml?Volume=445
Wellmer, 1998, Statistical evaluations in exploration for mineral deposits: Springer, New York, 379 p.
Whalen, J.B., Currie, K.L., and Chappell, B.W., 1987, A-type granites: geochemical characteristics, discrimination and petrogenesis: Contributions to Mineralogy and Petrology, v. 95, p. 40-418.
White, D. E., 1979, Duration of hydrothermal activity at Steamboat Springs, Nevada from ages of spatially associated volcanic rocks: U.S. Geological Survey, Professional Paper 4580, 13 p.
White, D. E., 1981, Active geothermal systems and hydrothermal ore deposits: Economic Geology, 75th anniv. volume, p. 392-423.
Willard, M.E., 1957, Reconnaissance geologic map of Lucera Spring thirty-minute quadrangle: New Mexico Bureau of Mines and Mineral Resources, Geologic Map 2.
Wilson, J.P., 1985, Between the river and the mountains: A history of early settlement in Sierra County, New Mexico: copyright John P. Wilson, report no. 40, 148 p.
Winchester, J.A. and Floyd, P.A., 1977, Geochemical discrimination of different magma series and their differentiation products using immobile elements: Chemical Geology, v. 20, p. 325-343.
Witcher, J.C., 1995, Geothermal resource data base, New Mexico: Southwest Technology Development Institute, report, New Mexico State University, 38 p.
Witcher, J.C., 2002, Geothermal energy in New Mexico: Geo-Heat Center Quarterly Bulletin, v. 23, no. 4, December, p. 2-5.
Witcher, J.C. and Lund, J.W., 2002, Gila Hot Springs: Geo-Heat Center Quarterly Bulletin, v. 23, no. 4, December, p. 25-29.
Witcher, J.C., Schoenmackers, R., Polka, R., and Cunniff, R.A., 2002, Geothermal energy at New Mexico State University in Las Cruces: Geo-Heat Center Quarterly Bulletin, v. 23, no. 4, December, p. 30-36.
Zumlot, T.Y., 2006, Environmental evaluation of New Mexico stream sediment chemistry using the National Uranium Resource evaluation (NURE) program: Ph.D. dissertation, University of Texas at El Paso, El Paso, 252 p.
Zumlot, T., Goodell, P., and Howari, F., 2009, Geochemical mapping of New Mexico, USA, using stream sediment data: Environmental Geology, v. 58, p. 1479-1497.